SLOVENIAN CRYSTALLOGRAPHIC SOCIETY
CROATIAN CRYSTALLOGRAPHIC ASSOCIATION

ENAINTRIDESETO SLOVENSKO-HRVAŠKO KRISTALOGRAFSKO SREČANJE

THIRTY-FIRST SLOVENIAN-CROATIAN CRYSTALLOGRAPHIC MEETING

18–22 June, 2025
Hotel Rogla
Rogla, Slovenia

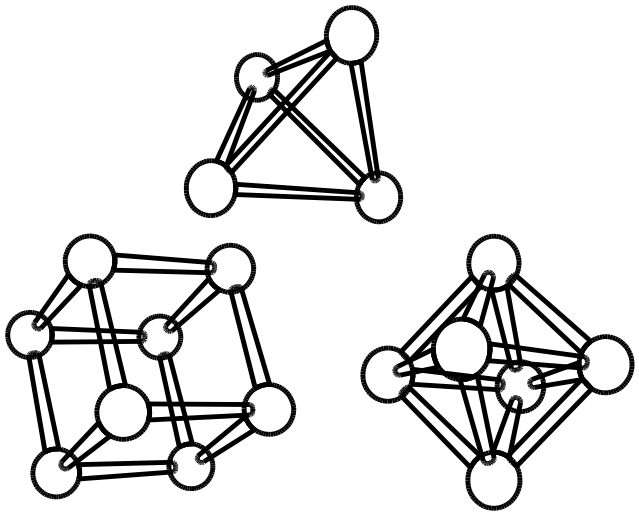

BOOK OF ABSTRACTS
PROGRAMME

THIRTY-FIRST SLOVENIAN-CROATIAN CRYSTALLOGRAPHIC MEETING

Rogla, Slovenia
18–22 June 2025

The Thirty-first Slovenian-Croatian Crystallographic Meeting will be held in the Hotel Rogla, Rogla, Slovenia, from Wednesday to Sunday, June 18–22, 2025.

The registration of the participants will take place on Wednesday, 18th June 2025 between 18:45 and 19:30. The opening of the Meeting is scheduled on Thursday, 19th June at 9:00.

The Meeting is being organized jointly by the Slovenian Crystallographic Society and by the Croatian Crystallographic Association under the auspices of the Faculty of Chemistry and Chemical Technology, University of Ljubljana, and promoted by the Slovenian Chemical Society.

ORGANIZING COMMITTEE:

Honorary Chairman	Ivan Leban, Ljubljana Dubravka Matković-Čalogović, Zagreb
Chairmen	Anton Meden, Ljubljana Marijana Đaković, Zagreb
Members	Lea Čolakić, Zagreb Ivica Đilović, Zagreb Gerald Giester, Vienna Amalija Golobič, Ljubljana Jakob Kljun, Ljubljana Matic Lozinšek, Ljubljana Valentina Milašinović, Zagreb Marta Počkaj, Ljubljana Nina Podjed, Ljubljana Željko Skoko, Zagreb

There will be five plenary lectures of 1 hour (45+15 minutes), a keynote lecture (30 minutes) and short oral presentations (10, 15 or 20 minutes).

The meeting is open for the contributions dealing with all aspects of crystallography and its application.

The official language of the meeting, written and spoken, will be English.

THIRTY-FIRST SLOVENIAN-CROATIAN CRYSTALLOGRAPHIC MEETING

is financially supported by:

Official representative of

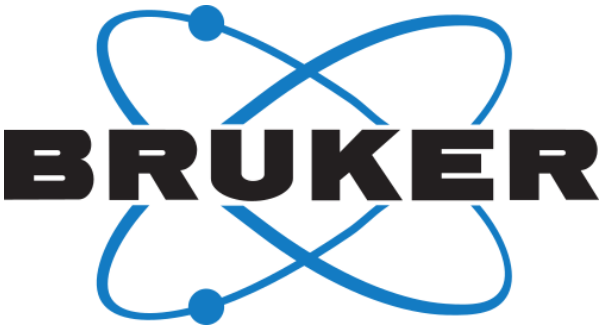
BRUKER


Aparatura
ANALYTICAL EQUIPMENT AND SYSTEMS


scan
VODILNI TEHNIČNO
USPOSOBLJENI SPECIALISTI
vakuum
kriotehnika
elektronska mikroskopija


JEOL
Solutions for Innovation


ITRLAB
JUST FOCUS


lek
član skupine Sandoz

PROGRAMME

WEDNESDAY, June 18, 2025

18^{45}–19^{30} **REGISTRATION OF PARTICIPANTS**

19^{30} **WELCOME RECEPTION**

THURSDAY, June 19, 2025

9^{00} **OPENING REMARKS** Chairpersons: A. Meden, M. Đaković

MORNING SESSION

9^{15} **PLENARY LECTURE** Chairperson: M. Đaković

ANDREA ČOBIĆ
Complete recrystallization of metamict allanite matrices under hydrothermal conditions

10^{15} **COFFEE BREAK**

ORAL PRESENTATIONS Chairpersons: A. Golobič, K. Molčanov

10^{45} **Izabela Đurasović**, Goran Štefanić, Marijan Marciuš, Robert Peter, Rafael Anelić, Fabio Faraguna, Marijan Gotić
The impact of supports on the Pt/SnO_2 catalytic reduction of 4-nitrophenol to 4-aminophenol

11^{00} **Uroš Rapuš**, Jakob Kljun, Iztok Turel
Rhenium and pyrithione: the gift that keeps on giving

11^{10} Blaženka Foretić, Zoran Štefanić, Juraj Ovčar, Dijana Žilić, Jasminka Popović, **Igor Picek**
The reversible electron transfer within supramolecular hexacyanoferrate-based charge-transfer complex

11^{20} **Mihails Arhangelskis**, Ivana Brekalo, Katarina Lisac, Joseph R. Ramirez, Petra Pongrac, Yizhi Xu, Michael Ferguson, Joseph M. Marrett, Tomislav Friščić, K. Travis Holman
Determination of highly complex structures of zeolitic imidazolate frameworks by powder X-ray diffraction

11^{40} **Nico Giordano**, Suchismita Guha, Beverly Stewart, Jakob Kjelstrup-Hansen, Matti Knaapila
High-pressure structure and phase behaviour of a naphthyl end-capped oligothiophene

11^{50} **Felix Hennersdorf**
Advancing Structural Science: Innovations in Rigaku Oxford Diffraction Instrumentation

12^{05} **LUNCH BREAK**

AFTERNOON SESSION

15^{00} **PLENARY LECTURE** Chairperson: M. Počkaj

EMMA E. MCCABE
Designing functional materials: mechanisms and consequences of broken inversion symmetry

16^{00} **COFFEE BREAK**

ORAL PRESENTATIONS

Chairpersons: M. Dragomir
V. Stilinović

16^{30} **Andreas Ertl**, Federico Pezzotta, Hans-Peter Meyer, Thomas Ludwig, Gerald Giester
Complex zoned tourmaline with darrellhenryite and fluor-rossmanite components from San Piero in Campo, Island of Elba, Italy

16^{40} **Žan Zakošek**, Evgeny Goreshnik, Janez Kovač
From order to disorder or from Pnma to Pbam

16^{50} **Krešimir Molčanov,** Petra Stanić, Lidija Androš Dubraja, Lidija Molčanov
Reversible single crystal-to-single crystal phase transformation and quantum crystallographic study of a charge-transfer system

17^{10} **Ana Siljanovska Virant**, Olha Sanko, Erik Uran, Matic Lozinšek
Crystal structure of O-protonated 2-fluoroacetamide

17^{20} **Jure Jakoš**, Elisabeth M. Huf, Jakob Kljun
A new metal complex with a natural asymmetric bipyridine

17^{35} **BREAK**

17^{55} **Olha Sanko**, Matic Lozinšek
Structural Characterization of XeF^+ Adducts with Fluoronitriles: $[CH_2FCN{-}XeF][AsF_6]$ *and* $[CHF_2CN{-}XeF][AsF_6]$

18^{05} **Mario Cetina**, Silvija Maračić, Silvana Raić Malić
Supramolecular structures of two N-heterocyclic hybrids based on quinoline and 1,2,3-triazole moieties

18^{15} **Marta Počkaj**
Cobalt(II) complexes with 4-(hydroxymethyl)pyridine and sulfato ligands

18^{25} **Andrii Hultiaiev**, Evgeny Goreshnik
Coordination of Cu(I) with guanazole and N-methyl guanazole derivatives

18^{40} **Kristian Radan**, Boris Žemva, Matic Lozinšek
Aggregation and anion formation in polyfluoridotitanates(IV): From monomers to extended frameworks

18^{55} **Bogdan Kotur**, Volodymyr Babizhetskyy, Oksana Myakush, Volodymyr Smetana, Anja-Verena Mudring
New ternary gallide $Zr_7Ru_{6+x}Ga_{17-x}$ ($0 \leq x \leq 2.0$): synthesis,crystal and electronic structures

FRIDAY, June 20, 2025

MORNING SESSION

9^{00} **PLENARY LECTURE** Chairperson: M. Lozinšek

REINHARD BOEHLER
The power of the laser-heated diamond cell combined with electron microscopy

10^{00} **COFFEE BREAK**

ORAL PRESENTATIONS Chairpersons: J. Jakoš
N. Tomašić

10^{30} **Mišel Hozjan**, Franc Perdih, Zvonko Jagličić
Copper coordination compounds with aminopyridine derivatives of picolinic acid

10^{40} **Ivana Kekez**, Darko Vušak, David Kučera-Čavara, Biserka Prugovečki
Interaction of DNA with copper(II)–homoserine coordination polymers: structural insights and biological relevance

11^{00} **Benjamin Poljanc**, Jakob Kljun, Iztok Turel
Exploring the Chemistry of Pyrithione and Copper

11^{10} **Ivana Veljković**, Danijela Kretić, Dragan Ninković, Dušan Veljković
Understanding the sensitivity of high-energy materials using crystallographic data

11^{25} **Amalija Golobič**, Filip Kóša, Miha Bukleski
Structure of two morpholinium iodidoantimonates and one iodidobismuthate

11^{35} Teodoro Klaser, **Željko Skoko**
Crystal Dynamics of Oxitropium Bromide: Thermal Expansion Anisotropy Preceding Explosive Phase Transition

11^{45} **Jernej Žižek**
Presentation of SCAN d.o.o.

12^{00} **LUNCH BREAK**

14^{00} **Conference trip to the Noordung centre in Vitanje & wine tasting at Zlati grič (Slovenske Konjice).**

20^{00} **CONFERENCE DINNER**

SATURDAY, June 21, 2025

MORNING SESSION

9^{00} **PLENARY LECTURE** Chairperson: J. Kljun

MAURO GEMMI
Single crystal electron diffraction on hard and soft matter

10^{00} **COFFEE BREAK**

ORAL PRESENTATIONS Chairpersons: A. Siljanovska Virant
M. Cetina

10^{30} **Boštjan Kobe**, Max T. B. Clabbers, Yan Li, Laura C. Pacoste, Weixi Gu, Jeffrey D. Nanson, Thomas Ve, Hongyi Xu
Application of MicroED to determining new macromolecular structures: the structure of Toll-like receptor adaptor MyD88 TIR-domain signalosome

11^{00} **Blaž Antonin**, Uroš Rapuš, Jakob Kljun
Synthesis and Characterization of Copper(I) Complexes with Chelating 2-(Methylthio)pyrimidines

11^{10} **Vesna Zalar Serjun**, Anton Meden, Romana Cerc Korošec, Marta Počkaj, Primož Oprčkal
Evolution of Phase Composition in Recycled Materials During Hydration and Carbonation

11^{25} Jasminka Kontrec, Branka Njegić Džakula, Nives Matijaković Mlinarić, Marijan Marciuš, **Nenad Tomašić**
Vaterite-calcite transformation mediated by micro- and nanoplastics addition

11^{35} **Bojan Kozlevčar**, Andrej Pevec
Copper(II) compounds with short α,ω-dicarboxylates

11^{45} **Nadja Ziherl**, Srečo D. Škapin, Matjaž Spreitzer, Amalija Golobič
Characterization of the $LaTaTiO_6$–$La_{1/3}TaO_3$ tie line in the system La_2O_3–Ta_2O_5–TiO_2 by X-ray powder diffraction

12^{00} LUNCH BREAK

AFTERNOON SESSION

15^{00} **PLENARY LECTURE** Chairperson: A. Meden

MATJAŽ MAZAJ, Andraž Krajnc, Tia Tajnšek, Amalija Golobič, Anton Meden, Sebastijan Kovačič, Erik S. Grape, Nataša Zabukovec Logar
Exploring dynamics and interactions in metal organic frameworks

16^{00} **COFFEE BREAK**

ORAL PRESENTATIONS

Chairpersons: B. Kozlevčar
I. Kekez

16^{30} **Jakob Kljun**, Uroš Rapuš, Tamás. Pivarcsik, Éva A. Enyedy, Iztok Turel
Crystal Structures and Solution Speciation Studies of Rhenium(I)-Tricarbonyl Complexes of Bipyridine Analogs

16^{45} **Erik Uran**, Matic Lozinšek
Xenon difluoride as a hydrogen-bond acceptor

16^{55} **Matic Lozinšek**, Klemen Motaln, Kshitij Gurung, Petr Brázda, Erik Uran, Kristian Radan, Mirela Dragomir, Lukaš Palatinus
Crystal structure determination of reactive compounds by 3D electron diffraction

17^{10} **Marijana Đaković**
Elucidation of the mechanism of elastic banding in crystalline coordination polymers with atomic-level precision

17^{20} **Klemen Motaln**, Matic Lozinšek
Coordination of xenon(II) fluorides to alkali metal cations

17^{30} **BREAK**

17^{50} **Darko Vušak**, Suzana Mal, Zvonimira Lemaić, Marija Zora Mišković, Nataša Zabukovec Logar, Biserka Prugovečki
Fine-Tuning of Adsorption Properties of Three-Component MOFs: From Synthesis to Structure-Activity Relationship

18^{05} **Mirela Dragomir**, Lia Šibav, Matic Lozinšek, Andrej Zorko
Crystal growth and magnetic properties of the quantum spin liquid candidate $NdTa_7O_{19}$ and other rare-earth heptatantalates

18^{20} **Anton Meden**
Crystal structures of three dyes determined by electron diffraction

18^{30} **Miha Virant**, Matic Lozinšek
Software for automatic processing of high-pressure ruby fluorescence spectra

18^{45} **Vladimir Stilinović**
Alan Lindsay Mackay, and the (Pre)-History of Quasicrystals

19^{05} **Ivica Đilović**, Draginja Mrvoš-Sermek, Marina Tašner, Darko Vušak, Dubravka Matković-Čalogović
Can the robustness of the L-carnosine copper(II) dimer be utilized as a versatile building block?

19^{15} **CLOSING REMARKS**

Chairpersons: M. Đaković
A. Meden

SUNDAY, June 22, 2025

9^{00} **EVALUATION AND FAREWELL COFFEE**

CONTRIBUTIONS

PLENARY LECTURES

Complete recrystallization of metamict allanite matrices under hydrothermal conditions

Andrea Čobić

University of Zagreb, Faculty of Science, Department of Geology, Horvatovac 102b, 10000 Zagreb, Croatia

A mineral is an element or a chemical compound that is usually crystallized. A metamict mineral, on the other hand, is amorphous and already deviates from the strict definition of minerals in this basic condition. However, metamict minerals that were demonstrably crystalline before metamictization are considered to be minerals[1] and their discovery is therefore an interesting phenomenon in the world of minerals. The question arose as to why these minerals became metamict and whether and how it is possible to prevent or reverse this process.

More recently, metamict minerals have been a good basis for research into materials for the disposal of nuclear waste, as they are their natural analogues. In this way, it is easiest to see the effects of radioactive decay of elements on minerals with different crystallochemical properties and, by analogy, on various other artificial materials. As they contain radioactive elements, they are also suitable for dating using the Th-Pb and U-Pb methods.

Numerous metamict minerals have been well researched since their discovery, but mostly those with relatively simple crystallochemical properties[2]. The problem in research is metamict minerals with complex crystallochemical properties. An additional problem is metamict minerals that contain hydroxyl groups, which leave the crystal structure during classical recrystallisation by heating to temperatures well above 100°C, and it is not possible to restore them completely, but they decompose into new phases[3].

As allanite is a mineral with complex crystallochemical properties and also contains hydroxyl groups, conventional recrystallisation do not lead to complete recrystallisation (fig. 1). At higher temperatures, the crystal structure collapses due to two processes: oxidation of individual elements in the structure and loss of hydroxyl groups. For this reason, a new experimental method of recrystallisation under hydrothermal conditions is introduced[4].

In this talk I will show how the hydrothermal conditions during the recrystallisation of allanite lead to complete recrystallisation (fig.1), but in different ways for allanite with different degrees of amorphization (metamictization) of the crystal structure.

All processes were monitored by X-ray powder diffraction, high-resolution transmission electron microscopy coupled with selected area electron diffraction (HRTEM+SAED), infrared (IR), Raman and Mössbauer spectroscopy as well as thermal methods.

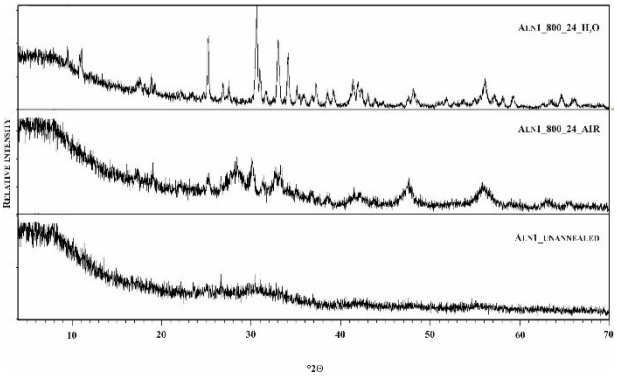

Figure 1: Comparative diffractograms of ALN1 sample (from bottom to top): unannealed (ALN_unannealed); annealed at 800°C for 24 h in air (ALN1_800_24) showing incomplete recrystallization; hydrothermally treated at 800°C for 24 h (ALN1_800_24_H2O) showing complete recrystallization

References:

1. Nickel, E.H., The definition of a mineral. *The Canadian Mineralogist.* **1995**, *33*, 689-690.
2. Tomašić, N.; Bermanec, V.; Gajović, A.; Rajić Linarić, M. R.: Metamict minerals: An insight into a relic crystal structure using XRD, Raman spectroscopy, SAED and HRTEM. *Croatica Chemica Acta,* **2008***, 81***,** 391-400.
3. Janeczek, J.; Eby, R. K.: Annealing of radiation damage in allanite and gadolinite. *Physics and Chemistry of Minerals.* **1993***, 19***,** 343-356.
4. Čobić, A.; Bermanec, V.; Tomašić, N.; Škoda, R.: The hydrothemal recrystallization of metamict allanite-(Ce). *The Canadian Mineralogist.* **2010***, 48***,** 513-521.

Funding information: grant nr. 119-0000000-1158, Ministry of Science, Education and Sports, Croatia

Designing functional materials: mechanisms and consequences of broken inversion symmetry

Emma E. McCabe *,[1]

[1] Department of Physics, Durham University, South Road, Durham, DH1 3LE, U. K.

Many properties of functional materials rely on structures with broken inversion symmetry (among other requirements).[1] As we seek to design materials with more challenging combinations of properties (for example polar semiconductors for photovoltaic applications, or chiral magnetic systems for spintronics), it's useful to consider strategies we might use to design next generation functional materials. This talk begins by discussing some of the properties associated with loss of inversion symmetry including enantiomorphism, piezoelectricity and pyroelectricity.[2]

I'll explore some traditional approaches and categories of materials including proper and improper ferroelectrics,[3] and materials with polar structures stabilized by geometric vs electronic driving forces. Electronic factors may only lower the symmetry of cation coordination environments without breaking crystal inversion symmetry, but this can still be advantageous for properties.[4]

The talk will then consider more diverse compositions for breaking inversion symmetry to design polar or chiral materials, including anion-ordering[5] and cation-ordering.[6] A key challenge that's common to several of these strategies is the length scale of symmetry breaking,[7] which presents challenges but also opportunities. before looking at strategies that allow us to use a wider range of compositions to design functional materials.

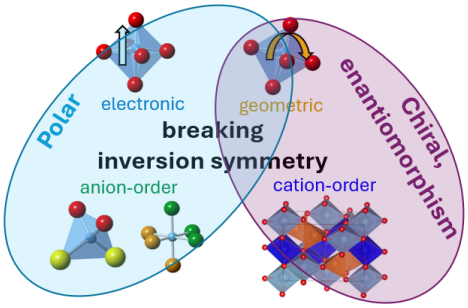

Figure/Scheme 1: Schematic highlighting some mechanisms to break inversion symmetry and some of the physical properties associated with non-centrosymmetry (alongside other requirements)

References:

1. Newnham, R. E. *Properties of materials: anisotropy, symmetry, structure*; Oxford University Press, 2005.
2. Ok, K. M.; Chi, E. O.; Halasyamani, P. S. *Chem. Soc. Rev.* **2006**, *35* (8), 710-717.
3. Benedek, N. A.; Rondinelli, J. M.; Djani, H.; Ghosez, P.; Lightfoot, P. *Dalton Trans.* **2015**, *44* (23), 10543-10558,
4. Al Bacha, S.; Saitzek, S.; Roussel, P.; Huvé, M.; McCabe, E. E.; Kabbour, H. *Chem. Mater.* **2023**, *35* (22), 9528-9541.
5. (a) Attfield, J. P. *Cryst. Growth & Design* **2013**, *13* (10), 4623-4629. (b) Fry, A. M.; Seibel, H. A.; Lokuhewa, I. N.; Woodward, P. M. *J. Am. Chem. Soc.* **2012**, *134* (5), 2621-2625. (c) Fry, A. M.; Woodward, P. M. *Cryst. Growth & Design* **2013**, *13* (12), 5404-5410. (d) Giddings, A. T.; Scott, E. A. S.; Stennett, M. C.; Apperley, D. C.; Greaves, C.; Hyatt, N. C.; McCabe, E. E. *Inorg. Chem.* **2021**, *60* (18), 14105-14115.
6. (a) Liu, J.; Wang, X.; Borkiewicz, O. J.; Hu, E.; Xiao, R.-J.; Chen, L.; Page, K. *Inorg. Chem.* **2019**, *58* (21), 14389-14402. (b) Oh, Y. S.; Artyukhin, S.; Yang, J. J.; Zapf, V.; Kim, J. W.; Vanderbilt, D.; Cheong, S.-W. *Nature Commun.* **2014**, *5* (1), 3201. (c) Li, M.-R.; McCabe, E. E.; Stephens, P. W.; Croft, M.; Collins, L.; Kalinin, S. V.; Deng, Z.; Retuerto, M.; Sen Gupta, A.; Padmanabhan, H.; et al. *Nature Commun.* **2017**, *8* (1), 2037.
7. (a) Katayama, T.; Chikamatsu, A.; Hirayama, M. *Advanced Functional Materials* **2025**. (b) Stone, G.; Ophus, C.; Birol, T.; Ciston, J.; Lee, C.-H.; Wang, K.; Fennie, C. J.; Schlom, D. G.; Alem, N.; Gopalan, V. *Nature Commun.* **2016**, *7* (1), 12572.

Funding information: We thank The Leverhulme Trust (RPG-2017-362), the Royal Society (equipment grant RG130844, international exchange scheme IES\R3\170112), the EU Cost Action "Towards oxide-based electronics", the RSC (research fund R23-4339620653).

The power of the laser-heated diamond cell combined with electron microscopy

Reinhard Boehler

University of Tennessee, Tennessee, USA

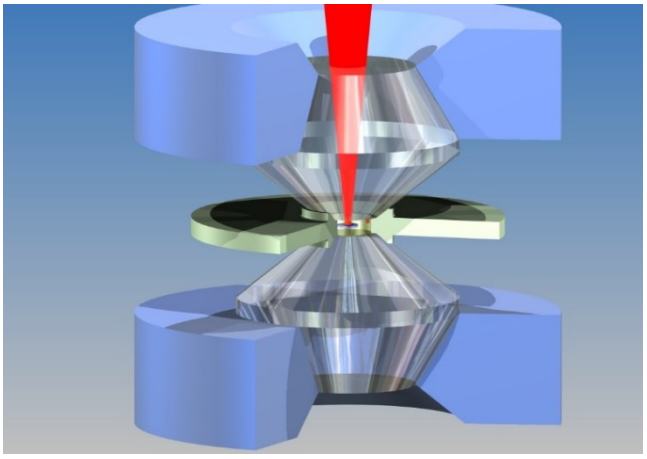

The laser-heated diamond anvil cell is the tool of choice for creating extreme pressure and temperature condition. The properties of diamond allow not only very high static pressures but are also provide an excellent window for *insitu* optical, spectroscopic, X-ray and neutron studies.

The unique thermal properties of diamond allow sample temperatures exceeding 5000 K and both pressures and temperatures are measured with unsurpassed accuracy.

I will show a variety of examples for measuring melting temperatures of metals at the conditions of the Earth's core, measuring phase equilibria of minerals at the conditions of the Earth's deep mantle, and how new materials with unique properties can be synthesized with ease. As a highlight, I will show the first measurement of the melting curve of diamond where melting is documented with electron microscopic studies. The results imply that the melt of diamond must be denser than diamond – similar to the observations on Si and Ge. This contradicts all theoretical work on the phase diagram of diamond.

Finally, I will show new developments on neutron diffraction in the diamond cell at the Oak Ridge National Laboratory.

Single crystal electron diffraction on hard and soft matter

Mauro Gemmi* [1]

[1] Electron Crystallography, Istituto Italiano di Tecnologia, Pontedera Italy.

Single crystal electron diffraction, usually known as 3D ED or MicroED, has undergone an impressive development in the last two decades becoming nowadays one of the most interesting novelties in crystallography[1]. 3D ED is performed by collecting ED patterns tilting the crystals around the goniometer axis of a TEM, a data collection that with the eyes of an x-ray crystallography we would call a phi scan. There are two effective ways to properly integrate the reflection in the reciprocal space: either the patterns are collected stepwise with the beam precessing on a cone or by collecting the patterns while the goniometer is rotating continuously. The first method is known as PEDT, the second as cRED which stand as Precession assisted Electron diffraction Tomography and continuous Rotation Electron Diffraction. Both methods are effective for structure solution and refinement. Advantages of both methods will be discussed and highlighted. PEDT is more suitable if the region of interest is small and we must be sure that the beam keep probing it during the entire rotation. cRED is more suitable if the crystal is beam sensitive and the experiment should be fast and low dose. Examples will be shown on structure solution problems solved with both methods. The application of 3D ED to fancy structural problem like the structure determination of 2D materials will be presented (see figure 1). The case of beam and vacuum sensitive samples will be discussed showing how the development of single electron hybrid detectors together with methods of crystal tracking during crystal rotation allows us to perform experiments under very low dose conditions, that guarantee good data collection on relatively beam sensitive samples, like organics[2], MOF and SOF. The quality of these data collections allows to perform very accurate refinement using the dynamical refinement software with the determination of hydrogen positions or the direct observation of the presence of the solvent in the MOF/SOF channels[3]. Finally, a possible future scenario will be discussed with examples on how a serial ED could be performed. Serial ED is a data collection in which the entire sample grid is scanned in diffraction mode collecting the maximum number of single ED patterns possible trying to reach an adequate completeness to solve a crystal structure. It is the only possibility in case the crystals amorphize after few seconds of exposure to the electron beam and it is the way to further extend the field of application of electron diffraction.

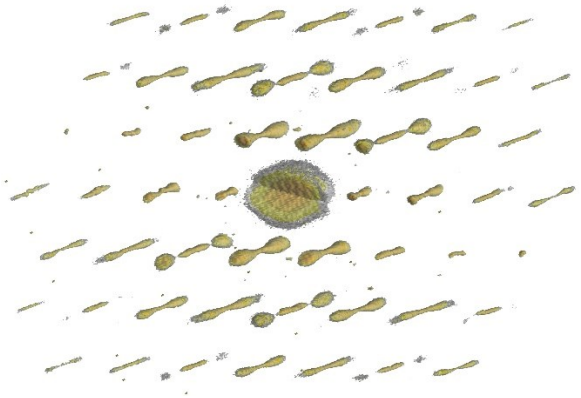

Figure1: Reconstruction of the reciprocal space of a single layer of WS_2 with 3D ED.

References:

1. Gemmi, M., Mugnaioli, E., Gorelik, T. E., Kolb, U., Palatinus, L., Boullay, P., Hovmöller, S., Abrahams, J. P., 3D Electron Diffraction: The Nanocrystallography Revolution. *ACS Cent. Sci.* **2019**, *5*, 1315–1329.
2. Anyfanti, G., Husanu, E., Andrusenko, I., Marchetti, D., Gemmi, M., Crystal Structure Determination of the Antipsychotic Drug of Olanzapine Form III. *IUCrJ* **2024**, *11*, 843–848.
3. Marchetti, D., Pedrini, A., Massera, C., Faye Diouf, M. D., Jandl, C., Steinfeld, G., Gemmi, M, 3D Electron Diffraction Analysis of a Novel, Mechanochemically Synthesized Supramolecular Organic Framework Based on Tetrakis-4-(4-Pyridyl)Phenylmethane. *Acta Crystallogr*. **2023**, *B79*, 432–436.

Exploring Dynamics and Interactions in Metal Organic Frameworks

Matjaž Mazaj,[1] Andraž Krajnc,[1] Tia Tajnšek,[1] Amalija Golobič,[2] Anton Meden,[2] Sebastijan Kovačič,[1,3] Erik S. Grape,[4] and Nataša Zabukovec Logar[1,5]

[1] National Institute of Chemistry, Hajdrihova 19, 1000 Ljubljana, Slovenia
[2]University of Ljubljana, Večna pot 113, 1000 Ljubljana, Slovenia
[3] University of Nova Gorica, Vipavska cesta 13, 5000 Nova Gorica, Slovenia
[4] Stockholm University, Frescativägen 8, 106 91 Stockholm, Sweden
[5] University of Maribor, Smetanova 17, 2000 Maribor, Slovenia

Metal-organic frameworks (MOFs) have emerged as one of the most structurally diverse and chemically tunable families of crystalline materials. Built from metal nodes and organic linkers, these frameworks can be tailored for a wide range of applications, from gas storage and separation to catalysis and sensing. What makes MOFs particularly intriguing from a crystallographic perspective is not only their vast structural variety, but also their inherent dynamic behavior and the complex interactions they can host within their porous architectures.

Herein, an overview of our research into the structural dynamics and functionalization strategies of MOFs, with an emphasis on how crystallographic methods can unravel their behavior under external stimuli, will be presented. Particularly MOFs response to thermal activation, humidity, and gas exposure, revealing diverse mechanisms of flexibility, phase transitions, and framework breathing. Understanding these processes is crucial for designing materials that are both stable and adaptable under operating conditions.

Beyond stability, enhancing MOF performance often requires targeted modifications to the framework itself. Our work has explored post-synthetic treatments, linker substitutions, and metal node tuning to optimize adsorption properties—particularly for CO_2 capture. These modifications are guided by structural insights and are aimed at fine-tuning host–guest interactions, pore accessibility, and adsorption selectivity.

Part of our recent efforts has also focused on the development and characterization of new MOF structures, particularly those that challenge traditional crystallographic approaches. The integration of advanced techniques such as three-dimensional electron diffraction has allowed us to solve structures from nanocrystalline samples, offering new opportunities to discover materials with unique functionalities that were previously elusive due to size or disorder.

SHORT ORAL PRESENTATIONS

The impact of supports on the Pt/SnO_2 catalytic reduction of 4-nitrophenol to 4-aminophenol

Izabela Đurasović[1], Goran Štefanić[1], Marijan Marciuš[2], Robert Peter[3], Rafael Anelić[4], Fabio Faraguna[4], Marijan Gotić[1*]

[1] Division of Materials Physics, Ruđer Bošković Institute, Zagreb, Croatia
[2] Division of Materials Chemistry, Ruđer Bošković Institute, Zagreb, Croatia
[3] Department of Physics, University of Rijeka, Rijeka, Croatia
[4] Petroleum and Petrochemical Department, Faculty of Chemical Engineering and Technology, Zagreb, Croatia

In this work, a novel synthetic route for SnO_2 supports based on an anion exchange reaction is presented and developed for the preparation of highly active Pt/SnO_2 catalysts. A strongly basic anion exchange resin was used to replace chloride ions from $SnCl_4$ solutions with hydroxide ions to obtain purer tin oxide supports with lower surface contamination and improved dispersion of platinum nanoparticles[1,2]. Three different SnO_2 supports were synthesized: (i) SnO_2 (A) obtained directly from the anion exchange reaction at room temperature; (ii) SnO_2 (B) obtained by hydrothermal treatment of as-synthesized SnO_2 at 180 °C; and (iii) SnO_2 (C) obtained by thermal annealing of hydrothermally treated SnO_2 at 600 °C. Each support was decorated with 1 mol% Pt using H_2PtCl_6 as precursor. All Pt/SnO_2 catalysts exhibited mesoporous structures with reversible type IV physisorption isotherms[3]. The Pt/SnO_2 (A) catalyst exhibited the highest specific surface area (BET area = 122.6 m^2/g) and the smallest pore diameter (d = 3.5 nm). Thermogravimetric analysis indicated that hydrothermal treatment (Pt/SnO_2 B) improved the initial crystallinity of SnO_2, while thermal annealing (Pt/SnO_2 C) further stabilized the structure by removing residual hydroxyl groups, which was explained by the slow mass loss of 8% between 20 °C and 600 °C. The catalytic performance was evaluated using the catalytic model reaction, i.e. the reduction of 4-nitrophenol (4-NP) to 4-aminophenol (4-AP) under ambient conditions. This reaction is important both for the environment and for industry. Among the catalysts tested, Pt/SnO_2 (A) exhibited the highest apparent rate constant (k = 1.27 × 10^{-2} s^{-1}) and excellent reusability, as the conversion efficiency was 84.5 % after ten consecutive cycles. These results emphasize the potential of the anion-exchange-assisted synthetic route as a simple and effective strategy to produce low-cost and high-performance nanocatalysts for the reduction of nitroaromatics.

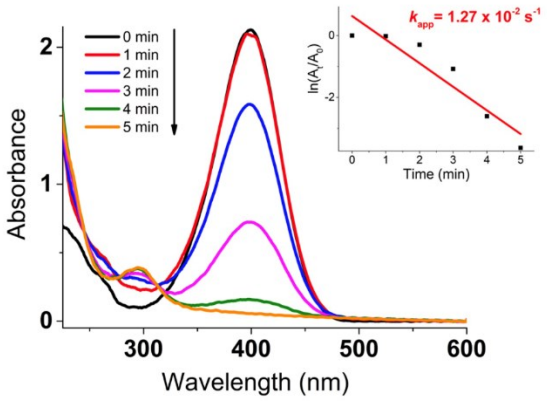

Figure 1: Catalytic reduction of 4-NP to 4-AP as a function of time using the autoclaved Pt/SnO_2 sample with 1 mol% Pt.

References:

1. Gotić, M.; Ivanda, M; Popović, S.; Musić, S., Synthesis of tungsten trioxide hydrates and their structural properties. *Mater. Sci. Eng. B* **2000**, *77*, 193-201.
2. Macera, L.; Daniele, V.; Mondelli, C.; Capron, M.; Taglieri, G., New Sustainable, Scalable and One-Step Synthesis of Iron Oxide Nanoparticles by Ion Exchange Process. *Nanomaterials* **2021**, *11*, 798.
3. Thommes, M.; Kaneko, K.; Neimark, A.V., Olivier, J.P., Physisorption of gases, with special reference to the evaluation of surface area and pore size distribution (IUPAC Technical Report). *Pure Appl. Chem.* **2015**, *87*, 1051-1069.

Funding information: This work was financially supported by Croatian Science Foundation under the project IP-2019-04-1195 "Platinum decorated iron tin oxide solid solutions for hydrogen gas sensing" (HydGasSens) and by Croatian Government and the European Union through the European Regional Development Fund - the Competitiveness and Cohesion Operational Programme (KK.01.1.1.01.0001).

Rhenium and pyrithione: the gift that keeps on giving

Uroš Rapuš*,[1] Jakob Kljun,[1] Iztok Turel[1]

[1] Faculty of Chemistry and Chemical Technology, University of Ljubljana, Večna pot 113, *SI*-1000 Ljubljana, Slovenia

Rhenium is one of the rarest elements and was the last stable element to be discovered in the periodic table. These are the main reasons why rhenium chemistry was unexplored for a long time. In recent years, however, rhenium complexes of all kinds have attracted increasing attention due to their stability, favourable spectroscopic properties and versatile biological activity. Rhenium complexes are active against various type of cancer as well as bacterial, viral and parasitic infections.[1,2]

In recent years, our research group developed metal complexes mainly with ruthenium and zinc and investigated their antitumour and antiviral activity.[3,4] Recently, we have extended our research to rhenium complexes due to the spectroscopic properties and biological activity already mentioned.

Pyrithione ligands are one of the main focus points of our research group. Pyrithione is the trivial name for 1-hydroxypyridine-2(1*H*)-thione. It is a naturally occurring compound that has been known for more than 75 years. Pyrithione has a moderate antimicrobial effect, which is significantly enhanced when used as a ligand in metal complexes.

The chemistry of rhenium and pyrithione is practically unexplored. During our studies, we were also able to obtain several interesting and unexpected products, either as by-products or as decomposition products, which we were able to characterise using X-ray diffraction on single crystals. The selected compound was further studied for its activity in biological systems, where it showed strong cytotoxicity as well as antibacterial and antiviral effects.[5]

Funding information: We are grateful for the financial support from the junior research grant for Uroš Rapuš and the program grant P1-0175 of the Slovenian Research and Innovation Agency (ARIS). The authors also acknowledge the support of the Centre for Research Infrastructure at the University of Ljubljana, Faculty of Chemistry and Chemical Technology, which is part of the Network of Research and Infrastructural Centres UL (MRIC UL) and is financially supported by the Slovenian Research and Innovation Agency (ARIS; Infrastructure programme No. I0-0022).

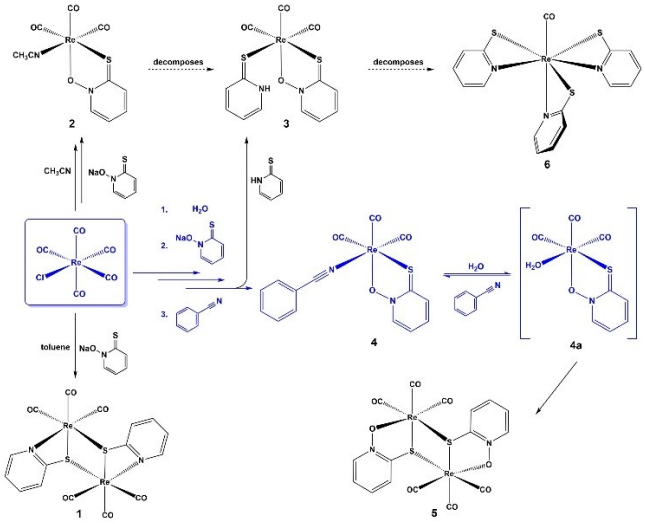

Scheme 1: Various products observed in reactions of rhenium(I) with pyrithione.

References:

1. Leonidova, A.; Gasser, G. Underestimated Potential of Organometallic Rhenium Complexes as Anticancer Agents. *ACS Chem Biol* **2014**, *9* (10), 2180–2193.
2. Schindler, K.; Zobi, F. Anticancer and Antibiotic Rhenium Tri- and Dicarbonyl Complexes: Current Research and Future Perspectives. *Molecules,* **2022**, *27* (2), 539.
3. Kladnik, J.; Kljun, J.; Burmeister, H.; Ott, I.; Romero-Canelón, I.; Turel, I. Towards Identification of Essential Structural Elements of Organoruthenium(II)-Pyrithionato Complexes for Anticancer Activity. *Chem Eur J,* **2019**, *25* (62), 14169–14182.
4. Kladnik, J.; Dolinar, A.; Kljun, J.; Perea, D.; Grau-Expósito, J.; Genescà, M.; Novinec, M.; Buzon, M. J.; Turel, I. Zinc Pyrithione Is a Potent Inhibitor of PL^{Pro} and Cathepsin L Enzymes with *Ex Vivo* Inhibition of SARS-CoV-2 Entry and Replication. *J Enzyme Inhib Med Chem* **2022**, *37* (1), 2158–2168.
5. Rapuš U.; Pivarcsik T.; Mitrović A.; Kljun J.; Bogdanov A.; Spengler G.; Meden A.; Gobec S.; Kos J.; Enyedy E. A.; Turel I. *Manuscript in preparation*.

The reversible electron transfer within supramolecular hexacyanoferrate-based charge-transfer complex

Blaženka Foretić,[1] Zoran Štefanić[2], Juraj Ovčar,[2] Dijana Žilić,[2] Jasminka Popović,[2] Igor Picek*[1]

[1] School of Medicine, University of Zagreb, Šalata 3, *HR*-10000 Zagreb, Croatia
[2] Ruđer Bošković Institute, Bijenička Cesta 54, *HR*-10000 Zagreb, Croatia

The functionality of solid supramolecular metalo-organic materials stems from the noncovalent interactions from which they assemble, endowing them with dynamic properties that can be tuned and controlled. Incorporation of quaternary pyridinium salts (QPS) as building blocks brings into focus the self-assembly of donor-acceptor charge-transfer complexes (CTCs) with distinctive hydrochromic, thermochromic and piezochromic properties[1]. These optical properties are enhanced when external stimuli cause such structural donor-acceptor reorganization through delicate adjustment of valence and conduction bands that allow charge-separation via one-electron donor-to-acceptor transfer.

Pyridinium oximes as QPS are recently recognized as promising electron-accepting and H-bond donating units for the design of 2D- and 3D-self-assemblies with hexacyanoferrate(II) as an electron donor and H-bond acceptor[2,3].

Here we present the structural and spectroscopic solid-state study of the stimuli-responsive CTC between *N*-benzylpyridinium oxime ($BPA4^+$) and hexacyanoferrate(II) (HCF^{4-})[4]. The *in-situ* PXRD was used to investigate temperature-induced dehydration of the parent, reddish-brown $(BPA4)_4HCF{\cdot}10H_2O$ (**1·10H₂O**) to anhydrous blue $(BPA4)_4HCF$ (**1**) providing evidence of a fully reversible hydrochromic behavior. The crystal structures of both phases are resolved by SCXRD[2,3] reveling the extent of structural donor-acceptor reorganization upon dehydration (Fig. 1). The crystal packing of **1**, where the hydroxyl group within oxime moiety forms a direct H-bond with cyano ligand, differs significantly from **1·10H₂O** where the HCF^{4-} core and $BPA4^+$ are bridged *via* H-bonded water molecules. The *in-situ* temperature-dependent ESR study showed that structural changes are accompanied by the intramolecular HCF^{4-}-to-$BPA4^+$ one-electron transfer, resulting in the formation of a radical BPA4• species and a small quantity of BPA4•/HCF^{3-} pair within complex **1**. To supplement these experimental results and to provide further insight into the observed hydrochromism, comparative DFT calculations of the density of states using the crystallographic data of both CTCs, **1·10H₂O** and **1** is performed.

The observed full extent of one dehydration/rehydration cycle for this redox-active CTC enables the redox-activity to be switched-on within anhydrous complex **1** and switched-off within hydrated complex **1·10H₂O**.

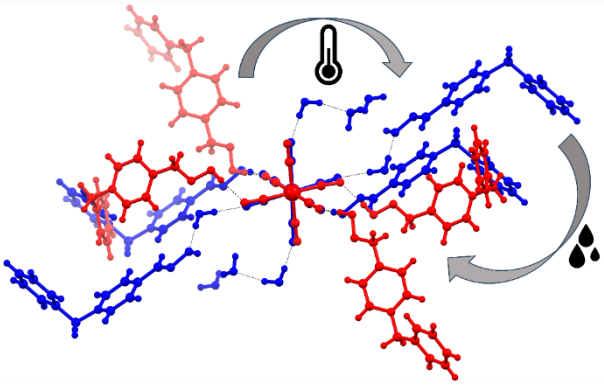

Figure 1: Reversible structural reorganization upon dehydration of **1·10H₂O** (blue) to anhydrous **1** (red).

References:

1. Yuan, T.; Xu, Y.; Zhu, C.; Jiang, Z.; Sue, H.; Fang, L.; Olson, M.A. Tunable Thermochromism of Multifunctional Charge-Transfer-Based Supramolecular Materials Assembled in Water. *Chem. Mater.* **2017**, *29*, 9937−9945.
2. Foretić, B.; Vianello, R.; Matković-Čalogović, D.; Jadreško, D.; Picek, I. Supramolecular inter-ionic charge-transfer complexes between derivatives of pyridinium-4-oxime cations and hexacyanoferrate(II) anions. *New J. Chem.* **2018**, *42*, 16115–16126.
3. Picek, I.; Matković-Čalogović, D.; Dražić, G.; Kapun, G.; Šket, P.; Popović, J.; Foretić, B. Supramolecular Solid Complexes between Bis-pyridinium-4-oxime and Distinctive Cyanoiron Platforms. *Molecules* **2024**, *29*, 1698–1713.
4. Foretić, B.; Klaser, T.; Ovčar, J.; Lončarić, I.; Žilić, D.; Šantić, A.; Štefanić, Z.; Bjelopetrović, A.; Popović, J.; Picek, I. The Reversible Electron Transfer Within Stimuli-Responsive Hydrochromic Supramolecular Material Containing Pyridinium Oxime and Hexacyanoferrate (II) Ions. Molecules 2024, 29, 5611.

Funding information: IP-2018-01-3168, Croatian Science Foundation, Croatia.

Determination of highly complex structures of zeolitic imidazolate frameworks by powder X-ray diffraction

Mihails Arhangelskis,[1]* Ivana Brekalo,[2]* Katarina Lisac,[2] Joseph R. Ramirez,[3] Petra Pongrac,[2] Yizhi Xu,[1] Michael Ferguson,[4] Joseph M. Marrett,[4] Tomislav Friščić,[4]* K. Travis Holman[5]*

[1] Faculty of Chemistry, University of Warsaw, Warsaw, Poland
[2.] Division of Physical Chemistry, Ruđer Bošković Institute, Zagreb, Croatia
[3.] Department of Chemistry, Georgetown University, Washington, D.C., USA
[4] School of Chemistry, University of Birmingham, Birmingham, UK

Zeolitic imidazolate frameworks (ZIFs) are a class of metal-organic frameworks (MOFs), renowned for structural and topological diversity.[1] The tetrahedral geometry of metal nodes, combined with angular arrangement between the metal-nitrogen coordination bonds, enforced by the imidazolate linkers, provide for geometric and topological similarity between ZIFs and zeolites.

This presentation will describe the structural characterization of two new polymorphs of zinc imidazolate (Zn(**Im**)$_2$), a highly polymorphic member of ZIF family, uncovered during a wide screening based on liquid-assisted grinding (LAG) methodology.[2] ZIF synthesis reaction with acetophenone and toluene liquid additives resulted in the formation of two previously unreported polymorphs of Zn(**Im**)$_2$, whose structures had to be determined using powder X-ray diffraction (PXRD), owing to the polycrystalline nature of the synthesized materials.

Both structure determinations proved to be highly complex, owing to the low crystallographic symmetry and presence of disordered solvent molecules within the ZIF pores. In the case of the toluene-LAG product, the asymmetric unit contained one zinc atom, three imidazolate fragments and two partially-occupied toluene molecules. The structure of the acetophenone-LAG product was even more complex, with four crystallographically-independent zinc atoms, eight imidazolate linkers and two acetophenone molecules.

Attempts to solve both structures via direct space simulated annealing methods proved to be unsuccessful, owing to the large number of molecular fragments in the asymmetric unit. Instead a combined procedure, encompassing both direct methods and simulated annealing, together with periodic density-functional theory (DFT) calculations was performed. First, direct methods, as implemented in EXPO2014,[3] were used to locate positions of zinc atoms and identify approximate locations of the imidazolate linkers. Positions of imidazolate linkers were then assigned from geometric considerations and adjusted via Rietveld refinement.[4] This was followed by the determination of guest molecule positions via simulated annealing procedure.

The multi-step structure determination process outlined above, still left some ambiguities: with the large number of symmetry-independent imidazolate linkers, 180° rotation of one linker with respect to the Zn···Zn axis would result in a vary small change in the agreement parameter, R_{wp}, making it very difficult to assign orientations of individual linkers with certainty. Reliable assignment of linker orientations was achieved by performing conformational analysis via periodic DFT calculations: configurations with different linker orientations were ranked in terms of relative lattice energy, and the lowest energy configuration was selected as the basis for the final Rietveld refinement.

Upon completion of the structure determination process, topologies of the new materials were determined. Despite clear crystallographic differences between the two structures, both were found to possess *crb* network topology. This is particularly intriguing, given that Zn(**Im**)$_2$ already possessed three reported polymorphs with *crb* topology. The addition of two new polymorphs, therefore, brings the total number of crb-Zn(**Im**)$_2$ structures to five, which is rather unprecedented in ZIF chemistry.

References:

1. Huang, X. C.; Lin, Y. Y.; Zhang, J. P.; Chen, X. M. *Angew. Chem. Int. Ed.* **2006**, *45*, 1557–1559.
2. Brekalo, I.; Lisac, K.; Ramirez, J. R.; Pongrac, P.; Xu, Y.; Ferguson, M.; Marrett, J. M.; Arhangelskis, M.; Friščić, T.; Holman, K. T. *ChemRxiv* **2025**, DOI: 10.26434/chemrxiv-2025-65t1h
3. Altomare, A.; Cuocci, C.; Giacovazzo, C.; Moliterni, A.; Rizzi, R.; Corriero, N.; Falcicchio, A. *J. Appl. Crystallogr.* **2013**, *46*, 1231–1235.
4. Rietveld, H. M. *Acta Crystallogr.* **1967**, *22*, 151–152.

High-pressure structure and phase behaviour of a naphthyl end-capped oligothiophene

Nico Giordano,*[1] Suchismita Guha,[2] Beverly Stewart,[3] Jakob Kjelstrup-Hansen,[4] and Matti Knaapila*[5]

[1] Deutsches Elektronen-Synchrotron DESY, Notkestr. 85, 22607 Hamburg, Germany
[2] Department of Physics and Astronomy, University of Missouri, Columbia, Missouri 65211, United States
[3] School of Chemistry and Bioscience, Faculty of Life Sciences, University of Bradford, Bradford, West Yorkshire, BD7 1DP, United Kingdom
[4] NanoSYD, Mads Clausen Institute, University of Southern Denmark, 6400 Sønderborg, Denmark
[5] Department of Physics, Norwegian University of Science and Technology, 7491 Trondheim Norway

Understanding macromolecular self-organisation is essential in the physics and materials science of π-conjugated molecules such as the thiophene derivatives owing to their intriguing opto-electronic properties and applications as thin film organic semiconductor materials (OSM). Fundamental principles in how charge transportation and other properties depend on intermolecular separation and relative displacements between molecules have already been well established.[1,2] Packing modifications are typically achieved by the chemical addition of bulky end-caps but another, less conventional, route is by the application of an external force. Pressure provides a clean tool to modify molecular packing and alter the physical properties without chemical interference, as has been shown for other optically active π-conjugated molecules.[3]

Here we present high-pressure single-crystal structures and molecular packing energies of the OSM, 5,5′-bis(naphth-2-yl)-2,2′-bithiophene (NaT2) which undergoes a subtle isostructural phase transition at *ca.* 3.5 GPa. The phase transition is fully reversible and is characterised by the formation of new S···H intermolecular contacts and a change in the compression pathway. The crystal undergoes a yellow to red colour change on compression that is also fully reversible. Single crystal X-ray diffraction data were collected to 7.6 GPa on beamline P02.2 at PETRA III and are supported by optical and Raman spectroscopy measurements.

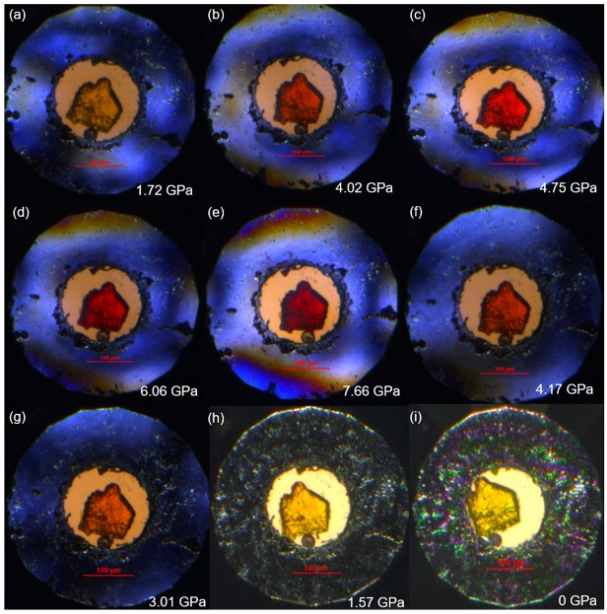

Figure 1: NaT2 undergoes a colour change from yellow to red on compression that is fully reversible on decompression.

References:

1. Brédas, J. L.; Calbert, J. P.; da Silva Filho, D. A.; Cornil, J. Organic Semiconductors: A Theoretical Characterization of the Basic Parameters Governing Charge Transport. *Proc. Natl. Acad. Sci.* **2002**, 99 (9), 5804–5809.
2. Brédas, J.-L.; Beljonne, D.; Coropceanu, V.; Cornil, J. Charge-Transfer and Energy-Transfer Processes in π-Conjugated Oligomers and Polymers: A Molecular Picture. *Chem. Rev.* **2004**, 104 (11), 4971–5004.
3. Schmidtke, J. P.; Friend, R. H.; Silva, C. Tuning Interfacial Charge-Transfer Excitons at Polymer-Polymer Heterojunctions under Hydrostatic Pressure. *Phys. Rev. Lett.* **2008**, 100 (15), 157401.

Advancing Structural Science: Innovations in Rigaku Oxford Diffraction Instrumentation

Felix Hennersdorf

Rigaku Europe SE, Hugenottenallee 167, 63263 Neu-Isenburg, Germany

Join us for an overview of the latest advancements in X-ray diffraction technology from Rigaku Oxford Diffraction, designed to meet the evolving needs of crystallographers across disciplines.

At the heart of our offering is the **XtaLAB Synergy platform**, a highly adaptable system that combines either microfocus or rotating anode X-ray sources with a range of **Hybrid Photon Counting (HPC) detectors**. This modular design allows researchers to configure their instruments to match specific experimental requirements, from routine structure determination to challenging crystallographic problems.

We'll also highlight a suite of automation and performance-enhancing tools that streamline workflows and boost productivity. These include the **XtaLAB Synergy Flow** robotic sample changer, the **Intelligent Goniometer Head (IGH3)** for automated crystal centering, and the **XtalCheck-S** plate scanning device for high-throughput screening. For specialized applications, we offer a **high-pressure unit** to expand experimental capabilities.

Finally, we'll introduce the **PhotonJetMAX-S**, our newest and brightest X-ray source, engineered to deliver superior data quality and faster acquisition times.

This presentation will showcase how Rigaku's integrated solutions can help crystallographers work more efficiently, solve more complex structures, and push the boundaries of what's possible in structural science.

Complex zoned tourmaline with darrellhenryite and fluor-rossmanite components from San Piero in Campo, Island of Elba, Italy

Andreas Ertl,[1,2]* Federico Pezzotta,[3] Hans-Peter Meyer,[4] Thomas Ludwig,[4] Gerald Giester[2]

[1] Mineralogisch-Petrographische Abt., Naturhistorisches Museum, Burgring 7, 1010 Wien, Austria
[2] Institut für Mineralogie und Kristallographie, Universität Wien, Josef-Holaubek-Platz 2, 1090 Wien, Austria
[3] MUM – Mineralogical Museum "Luigi Celleri", 57034 San Piero In Campo, Livorno, Italy
[4] Institut für Geowissenschaften, Universität Heidelberg, Im Neuenheimer Feld 234-236, 69120 Heidelberg, Germany

Pale pink tourmaline was described from the Fonte del Prete rare-element-enriched granitic pegmatite dike, located near the village of San Piero in Campo, Island of Elba, Italy. This pegmatite displays lithium-cesium-tantalum (LCT)-type geochemical features, and is genetically related to the Monte Capanne pluton[1]. The dike exhibits complex asymmetric zonation, with miarolitic pockets containing primitive to highly developed assemblages[2]. There is a notable occurrence of Nb and Ta oxides, as well as complex oxides, which occur mainly in the pockets[1]. Pale pink tourmaline crystals up to a few cm in length, also from pockets, were investigated in detail.

The sample examined originates from a large specimen containing pale pink tourmaline crystals acquired by the Museo Civico di Storia Naturale di Milano from Cap. Giuseppe Pisani in 1882 (acquisition no. 18292). This historical specimen was one of the few tourmaline specimens that survived a bombing raid during World War II in the basement of the museum.

Near the core of a crystal with 1 cm diameter and ~2 cm length the crystal chemical formula is $^{X}(Na_{0.5}\square_{0.5})$ $^{Y}(Al_{2.3}Li_{0.7})$ $^{Z}Al_6$ $(BO_3)_3$ $[Si_{5.6}B_{0.3}Al_{0.1}O_{18}]$ $^{V}(OH)_3$ $^{W}[O_{0.7}F_{0.2}(OH)_{0.1}]$, determined by microprobe and ion probe data. When using currently valid tourmaline end-members to describe this tourmaline zone, it consists essentially of darrellhenryite (35 mol%) and fluor-rossmanite (25 mol%). It contains smaller amounts of ertlite (17 mol%), alumino-oxy-rossmanite (11 mol%) and rossmanite (10 mol%).

A piece between core and rim with lattice parameters of a = 15.797(1), c = 7.086(1) Å ($R1$ = 1.32%) has the crystal chemical formula $^{X}(Na_{0.5}\square_{0.5})$ $^{Y}(Al_{2.2}Li_{0.8})$ $^{Z}Al_6$ $(BO_3)_3$ $[Si_{5.5}B_{0.3}Al_{0.2}O_{18}]$ $^{V}(OH)_3$ $^{W}[O_{0.4}F_{0.3}(OH)_{0.3}]$. The <$T$-O> distance of 1.615 Å is in agreement with small amounts of B and Al at the tetrahedral site.[3]

A rim-near part of this crystal shows the formula $^{X}(Na_{0.6}\square_{0.4})$ $^{Y}(Al_{2.0}Li_{1.0})$ $^{Z}Al_6$ $(BO_3)_3$ $[Si_{5.5}B_{0.3}Al_{0.2}O_{18}]$ $^{V}(OH)_3$ $^{W}[F_{0.5}(OH)_{0.3}O_{0.2}]$. This zone consists essentially of fluor-elbaite (35 mol%) and rossmanite (34 mol%). It also contains smaller amounts of other end-members (ertlite, fluor-liddicoatite, alumino-oxy-rossmanite, fluor-rossmanite).

Today, in addition to the type locality of darrellhenryite, six other localities of this end-member are listed in Mindat.org. Darrellhenryite is often associated with fluor-elbaite, as is the case in Fonte del Prete.

In the original description of fluor-rossmanite[4], this tourmaline was characterized as intergrown with fluor-elbaite and darrellhenryite within the same crystal. The pale pink fluor-rossmanite type material was reported to contain 46 mol% fluor-rossmanite and 32 mol% darrellhenryite.[4] The core-near zone of a pale pink tourmaline crystal from Fonte del Prete contains also both end-members as main components (35 mol% darrellhenryite, 25 mol% fluor-rossmanite).

During the final crystallization stage of the tourmaline studied, the Li, F and Na contents increased.

References:

1. Aurisicchio, C.; De Vito, C.; Ferrini, V.; Orlandi, P., Nb and Ta oxide minerals in the Fonte Del Prete granitic-pegmatite dike, island of Elba, Italy. *Can. Mineral.* **2002**, *40*, 799-814.
2. Orlandi, P.; Pezzotta, F., Minerali dell'Isola d'Elba. Edizioni Novecento Grafico, Bergamo, **1997**.
3. Ertl, A.; Henry, D.; Tillmanns, E., Tetrahedral substitutions in tourmaline: A review. *Eur. J. Mineral.* **2018**, *30*, 465-470.
4. Kasatkin, A. V.; Nestola, F.; Day, M. C.; Goreliva, L. A.; Škoda, R.; Vereshchagin, O. S.; Agakhanov, A. A.; Belakovskiy, D. I.; Pamato, M. G.; Cempírek, J.; Mikhail Yu. A., Fluor-rossmanite, $\square(Al_2Li)Al_6(Si_6O_{18})(BO_3)_3(OH)_3F$, a new tourmaline supergroup mineral from Malkhan pegmatite field, Western Siberia, Russia. *Min. Mag.* **2024**, *88*, 668-676

Funding information: This research was funded in part (AE) by the Austrian Science Fund (FWF) project P 35585.

From order to disorder or from Pnma to Pbam

Žan Zakošek*,[1,2] Evgeny Goreshnik,[1] Janez Kovač,[3]

[1] Jožef Stefan Institute, The Department of Inorganic Chemistry and Technology, Jamova cesta 39, 1000 Ljubljana, Slovenia
[2] Jožef Stefan International Postgraduate School, Jamova cesta 39, 1000 Ljubljana, Slovenia
[3] Jožef Stefan Institute, Department of Surface Engineering, Jamova cesta 39, 1000 Ljubljana, Slovenia

Due to the d^{10} electronic configuration, organic Cu(I) halides have interesting luminescent[1] and catalytic[2] properties. By using different organic ligands, we can produce compounds with different properties[3].

Our research is focussed on the search for new organic Cu(I) bromides. We have chosen hexamethylenetetramine (HMTA) as the organic ligand because it has multiple binding sites that can lead to a wide variety of arrangements of metal centres around the ligand. Currently only 3 entries from the CuBr – HBr – HMTA systems can be found in the CSD (version 5.46). At the conference 3 new compounds from the ternary system CuBr – HBr – HMTA will be presented. Two of them contain $Cu_2Br_2hmta_2$ chains with acetonitrile between the chains, but crystallise in two different space groups P*nma* and P*bam*.

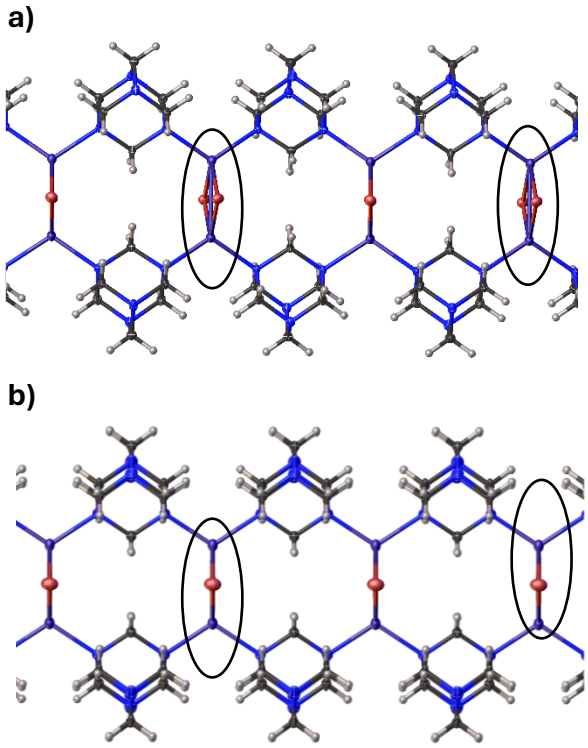

Figure 1: Slight distortion of the Br^- in the $Cu_2Br_2hmta_2$ chains in the crystal structure a) (P*nma*), while in structure b) (P*bam*) all Br^- are perfectly aligned.

In the third structure, a disorder of Cu^+ ions between two positions is observed and the presence of Cu(I) was confirmed by XPS analysis.

References:

1. Liu, W.; Lustig, W. P.; Li, J. Luminescent Inorganic-Organic Hybrid Semiconductor Materials for Energy-Saving Lighting Applications. EnergyChem 2019, 1 (2), 100008. https://doi.org/10.1016/j.enchem.2019.100008.
2. Fagan, P. J.; Hauptman, E.; Shapiro, R.; Casalnuovo, A. Using Intelligent/Random Library Screening To Design Focused Libraries for the Optimization of Homogeneous Catalysts: Ullmann Ether Formation. J Am Chem Soc 2000, 122 (21), 5043–5051. https://doi.org/10.1021/ja000094c.
3. Araki, H.; Tsuge, K.; Sasaki, Y.; Ishizaka, S.; Kitamura, N. Luminescence Ranging from Red to Blue: A Series of Copper(I)−Halide Complexes Having Rhombic {Cu 2 (μ-X) 2 } (X = Br and I) Units with N -Heteroaromatic Ligands. Inorg Chem 2005, 44 (26), 9667–9675. https://doi.org/10.1021/ic0510359.

Funding information: Authors acknowledge the financial support from the Slovenian Research Agency (research core funding No. P1–0045; Inorganic Chemistry and Technology).

Reversible single crystal-to-single crystal phase transformation and quantum crystallographic study of a charge-transfer system

Krešimir Molčanov,*[1] Petra Stanić,[1] Lidija Androš Dubraja,[1] Lidija Molčanov[1]

[1] Ruđer Bošković Institute, Bijenička 54, *HR*-10000 Zagreb, Croatia

Charge-transfer compounds comprising electron donor tetramethylphenylenediamine (TMPD, Wurster's blue) with electron acceptors tetrachloro- and tetrabromoquinone (Cl_4Q and Br_4Q, respective) comprises stacks of alternating donor and acceptor moieties[1] (Fig. 1). Both compounds have two phases, with minor differences in stacking geometry: in the high-temperature (HT) phase the rings are parallel (Fig. 1b), while in the low-temperature (LT) phase their mean planes are inclined by about 2.5° (Fig. 1a)[1].

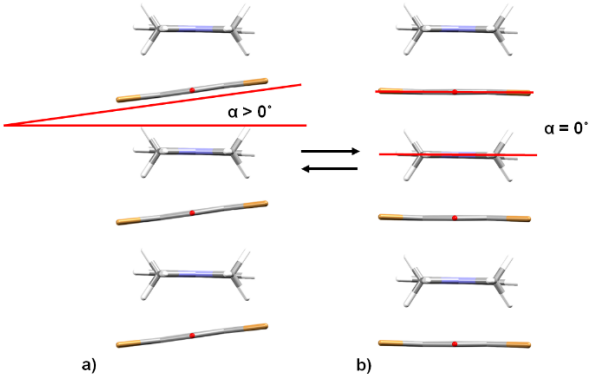

Figure 1: Stacks of alternating donor and acceptor moieties in TMPD·Br4Q: a) low-temperature phase and b) high-temperature phase. The interplanar angle α in a) is exaggerated for clarity.

The phase change was studied by variable-temperature crystallography and thermal analysis (TG/DTA and DSC). It proceeds via a single crystal-to-single crystal mechanism, similar to those observed in salts of pancake-bonded semiquinone radicals[2,3]. Very small enthalpy and poor ordering of the crystals near temperature of the phase transition indicate a gradual, second-order mechanism consistent with small re-alignment of positions of the stacked moieties.

These crystals represent a rare case of 'self-healing' crystals[4]: upon cooling single crystals of the HT phase split into twins of the LT phase. Two domains in the LT phase are rotated by 180° about crystallographic axis *c*.

Details of electron density in partially charged TMPD and Cl_4Q moieties in HT phase of TMPD·Cl_4Q are studied by X-ray charge density. Maximum electron density between the rings exceeding 0.57 e $Å^{-3}$ and presence of (3,+3) critical points (i.e. local electron density minima) are indicate existence of strong partially covalent interactions (pancake-bonds) between the rings (Fig. 2).

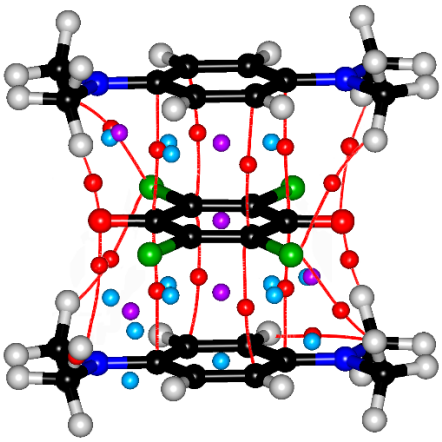

Figure 2 Critical points in a pancake-bonded contact between TMPD and Cl_4Q moieties.

References:

1. Stanić, P.; Nikšić-Franjić, I.; Pavić, L.; Molčanov, K. Two electron multicentre bonding (pancake bonding) between electron donors and acceptors in charge-transfer compounds of *N*,*N*,*N*′,*N*′-tetramethyl-*p*-phenylenediamine (TMPD) and (semi)quinoid electron acceptors. *Cryst. Growth Des.*, **2023**, *23*, 4460-4471.
2. Molčanov, K.; Kojić-Prodić, B.; Babić, D.; Pajić, D.; Novosel, N.; Zadro, K. Temperature induced reversible structural and magnetic phase transitions in a crystal of tetrachlorosemiquinone anion radical, *CrystEngComm*, **2012**, *14*, 7958-7964.
3. Stanić, P.; Poręba, T.; Androš Dubraja, L.; Krawczuk, A.; Molčanov, K. Stacks of equidistant 5,6-dichloro-2,3-dicyanosemiquinone (DDQ) radicals under variable temperature and high pressure conditions. *Cryst. Growth Des.*, **2023**, *23*, 3284-3296.
4. Vušak, D.; Naumov, P.; Jeličić, Ž.; Matković-Čalogović, D.; Prugovečki, B. Thermally Induced Reversible Martensitic Phase Transformation and Self-Healing in Nickel Glycinamide Crystals, *Angew. Chem., Int. Ed.*, **2025**, *64*, e202421769.

Funding information: This work was financed by the Croatian Science Foundation, grant IP-2024-05-8711.

Crystal structure of O-protonated 2-fluoroacetamide

Ana Siljanovska Virant*,[1] Olha Sanko,[1] Erik Uran,[1] Matic Lozinšek[1]

[1] Jožef Stefan Institute, Jamova cesta 39, *SI*-1000 Ljubljana, Slovenia

The acid-catalyzed hydrolysis of nitriles to primary amides is a well-established transformation in organic chemistry.[1] With careful control of the reaction conditions, hydrolysis can be stopped at the amide stage, thus preventing further conversion to carboxylic acids. The mechanism typically proceeds via protonation of the nitrile group, followed by nucleophilic attack by water at the electrophilic nitrile carbon atom. Subsequent proton transfer and resonance stabilization leads to the formation of an *O*-protonated amide intermediate. These species are generally unstable under ambient conditions and are rapidly stabilized by deprotonation. However, at low temperatures and in the presence of weakly coordinating anions, such transient species can be trapped and structurally characterized.[2]

The behavior of some protonated primary amides in superacidic media has been studied previously.[2] In all reported cases, protonation of the amide occurs at the carbonyl oxygen atom. However, the *in situ* hydrolysis of a nitrile, followed by amide protonation under superacidic conditions has not yet been reported. Only a few examples of protonated amides formed via hydrolysis of nitriles under mild acidic conditions have been structurally characterized.[3,4,5]

Herein the single-crystal X-ray diffraction structure of *O*-protonated 2-fluoroacetamide, formed by hydrolysis of fluoroacetonitrile in HF/AsF_5 medium, is presented. Employing AsF_6^- as stabilizing anion and performing the crystallization below −40 °C enabled the isolation and structural characterization of this reactive intermediate.

The compound forms a hydrogen-bonded network connecting the cation to four different fluorine atoms of four AsF_6^- anions via O−H···F and N−H···F hydrogen bonds (Figure 1). Notably, one of the amide hydrogens functions as a bifurcated hydrogen-bond donor, while the other amide hydrogen and the hydroxyl group each participate in a single hydrogen bond.

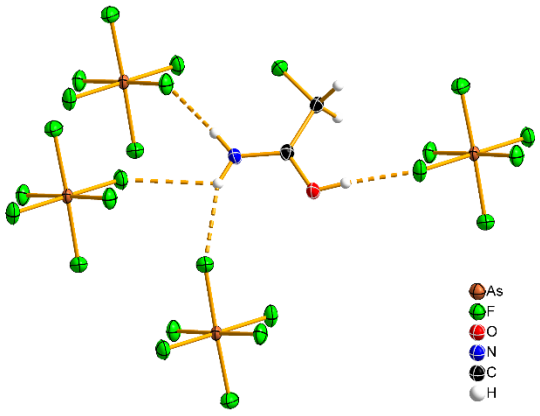

Figure 1: Hydrogen bond network in the solid-state structure of *O*-protonated 2-fluoroacetamide.

References:

1. Moorthy, J. N., Singhal, N., Facile and Highly Selective Conversion of Nitriles to Amides via Indirect Acid-Catalyzed Hydration Using TFA or AcOH–H_2SO_4. *J. Org. Chem.* **2005**, *70*, 1926–1929.
2. Axhausen, J., Ritter, C., Lux, K., Kornath, A., The Protonation of Acetamide and Thioacetamide in Superacidic Solutions: Crystal Structures of $[H_3CC(OH)NH_2]^+AsF_6^-$ and $[H_3CC(SH)NH_2]^+AsF_6^-$. *Z. Anorg. Allg. Chem.* **2013**, *639*, 65–72.
3. Shehadi, I., Abla, F., Wakefield, B. et al. Facile protic hydration of acetonitrile to protonated acetamide at oxygen mediated by chloroauric acid: insights from experimental and calculations. *Res. Chem. Intermed*. **2020**, *46*, 593–607.
4. Hasche, S., Reich, O., Beckmann, I., Krebs, B., Stabilization of Oxohalogeno and Halogenochalkogenates(IV) by Protonacceptors–Synthesis, Structure and Properties of $[C_4H_{10}NO]_2[SeOCl_4]$, $[C_4H_{10}NO]_2[Se_2Br_{10}]$ and $[(CH_3)_2CHC(NH_2)(OH)][Te_3Cl_{13}]\cdot(CH_3)_2CHCN$. *Z. Anorg. Allg. Chem.* **1997**, *623*, 724–734.
5. Liu, L.-K., Luo, F.-T., Hsieh, L.-C., Acetamide hydrochloride. *Acta Crystallogr. C* **1994**, *50*, 1333–1335.

Funding information: The Slovenian Research and Innovation Agency (ARIS) (J1-60022) and the European Research Council (ERC) under the European Union's Horizon 2020 Research and Innovation Programme (Starting Grant 950625) are gratefully acknowledged.

A new metal complex with a natural asymmetric bipyridine

Jure Jakoš,[1] Elisabeth M. Huf,[2] Jakob Kljun*[1]

[1] Faculty of Chemistry and Chemical Technology, University of Ljubljana, Večna pot 113, *SI*-1000 Ljubljana, Slovenia
[2] Institute of Inorganic Chemistry, Universität Regensburg, Universitätsstraße 31, DE-93053 Regensburg, Germany

Mankind has fought microbes for a long time with various treatments. From the use of metals such as silver or copper to disinfect water, to various silver, arsenic and mercury salts, were used until the discovery of antibiotics in the early 20th century. Their discovery saved millions of lives, but their excessive and ill-considered use led to the development of antimicrobial resistance, which the World Health Organization now considers a serious threat to public health. Rational use, modification of existing agents, unconventional approaches and treatments (such as nanoparticles, bacteriophages and metal-containing compounds such as metal complexes) are just some of the efforts being made to combat this problem[1].

A potentially interesting compound was discovered in the 1950s when researchers were investigating an extract of *Streptomyces caerules*. They came across an impurity that inhibited the growth of various filamentous fungi, yeasts and some bacteria. A more detailed study and complete characterization (CHN, IR, UV-Vis, MS, NMR…) of the extract led to the discovery of a new asymmetric 2,2'-bipyridine, which the researchers named caerulomycin. A new family of compounds was discovered and the first caerulomycin was later named caerulomycin A (CaeA) (**Figure 1**)[2].

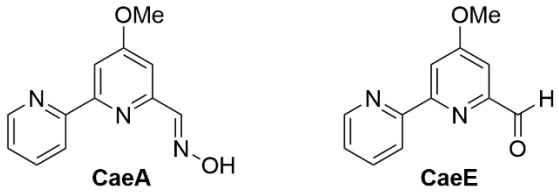

Figure 1: Structure of two Caerulomycins

Subsequent studies on biological activity have shown that these compounds are not only potential antifungal and antibacterial agents, but also have potential anticancer, immunoregulatory and other properties[2–4].

The first synthesis of CaeA was published in 1969. Later, in 1998, a synthesis of CaeE was published, which can later be converted into CaeA[5]. We have succeeded in optimizing and improving the yield of this synthesis in combination with newer published methods[6]. With the synthesized CaeE, we succeeded in producing the first rhenium complex containing CaeE as a ligand (**Figure 2**).

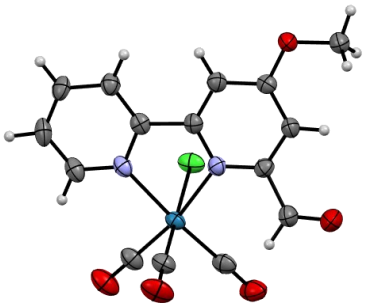

Figure 2: Crystal structure of the rhenium(I) complex with caerulomycin E.

References:

1. Salam, M. A.; Al-Amin, M. Y.; Salam, M. T.; Sigh Pawar, J.; Akhter N.; Rabaan, A. A.; Alqumber, M. A. A. Antimicrobial Resistance: A Growing Serious Threat for Global Public Health. *Healthcare* **2023**, *11*, 1946
2. Funk, A.; Divekar, P. V. Caerulomycin, a New Antibiotic from Streptomyces Caeruleus Baldacci, I. Production, Isolation, Assay. and Biological Properties. *Can. J. Microbiol.* **1959**, 5, 317–321
3. Tong, L.; Sun, W.; Wu, S.; Han, Y. Characterization of Caerulomycin A as a DualTargeting Anticancer Agent. *Eur. J. Pharmacol*. **2022**, *922*, 174914
4. Singla, A. K.; Krishna Gurram, R.; Chauhan, A.; Khatri, N.; Vohra, R. M.; Jolly, R. S.; Agrewala, J. N. Caerulomycin A Suppresses Immunity by Inhibiting T Cell Activity. *PLOS ONE* **2014**, *9*
5. Trécourt, F.; Gervais, B.; Mongin, O.; Le Gal, C.; Mongin, F.; Quéguiner, G. First Syntheses of Caerulomycin E and Collismycins A and C. A New Synthesis of Caerulomycin A. *J. Org. Chem*. **1998**, *63*, 2892–2897
6. Bobrov, D. N.; Tyvorskii V. I. Facile synthesis of caerulomycin e by the formation of 2, 2′-bipyridine core via a 2-pyridyl substituted 4H-pyran-4-one.Formal synthesis of caerulomycin A. *Tetrahedron* **2010**, *66*, 5432–5434

Funding information: We are grateful for the financial support from the junior research grant for Jure Jakoš and program grant P1-0175 of the Slovenian Research and Innovation Agency (ARIS). The authors also acknowledge the support of the Centre for Research Infrastructure at the University of Ljubljana, Faculty of Chemistry and Chemical Technology, which is part of the Network of Research and Infrastructural Centers UL (MRIC UL) and is financially supported by ARIS; Infrastructure program No. I0-0022.

Structural Characterization of XeF^+ Adducts with Fluoronitriles: $[CH_2FCN{-}XeF][AsF_6]$ and $[CHF_2CN{-}XeF][AsF_6]$

Olha Sanko*,[1,2] Matic Lozinšek[1,2]

[1] Jožef Stefan Institute, Jamova cesta 39, 1000 Ljubljana, Slovenia
[2] Jožef Stefan International Postgraduate School, Jamova cesta 39, 1000 Ljubljana, Slovenia

Compounds featuring Xe–N bonds can be formed by coordination of the highly electrophilic XeF^+ species to the lone pair of the nitrile ligands (RC≡N). The following adduct cations with (fluoro)acetonitriles have previously been characterized in solution by NMR spectroscopy:[1,2] $[CH_3CN{-}XeF]^+$, $[CH_2FCN{-}XeF]^+$ and $[CF_3CN{-}XeF]^+$. The $[CH_3CN{-}XeF]^+[AsF_6]^-{\cdot}HF$ compound is the only crystallographically characterized example to date[3].

This study extends the known series of FXe–N-bonded adduct cations by reporting solid-state structural characterization of $[CH_2FCN{-}XeF]^+[AsF_6]^-$ and $[CHF_2CN{-}XeF]^+[AsF_6]^-$ (Figure 1). These adduct cation salts were synthesized by reacting fluoroacetonitrile and difluoroacetonitrile with $[XeF]^+[AsF_6]^-$ in anhydrous HF at low temperature. The products were isolated and characterized by low-temperature single-crystal X-ray diffraction and low-temperature Raman spectroscopy.

The adduct cation salt $[CH_2FCN{-}XeF]^+[AsF_6]^-$ crystallizes in the monoclinic space group $P2_1/c$ (Z = 8), with two crystallographically distinct $[CH_2FCN{-}XeF]^+$ adduct cations and two $[AsF_6]^-$ anions per asymmetric unit. The observed Xe–N bond lengths are 2.1947(9) Å and 2.2302(10) Å, with nearly linear Xe–N≡C angles of 178.63(9)° and 172.03(10)°. The compound $[CHF_2CN{-}XeF]^+[AsF_6]^-$ crystallizes in the orthorhombic space group *Pnma* (Z = 4), with a single crystallographically unique $[CHF_2CN{-}XeF]^+$ adduct cation exhibiting a Xe–N bond length of 2.1928(16) Å and a nearly linear Xe–N≡C angle of 178.59(5)°.

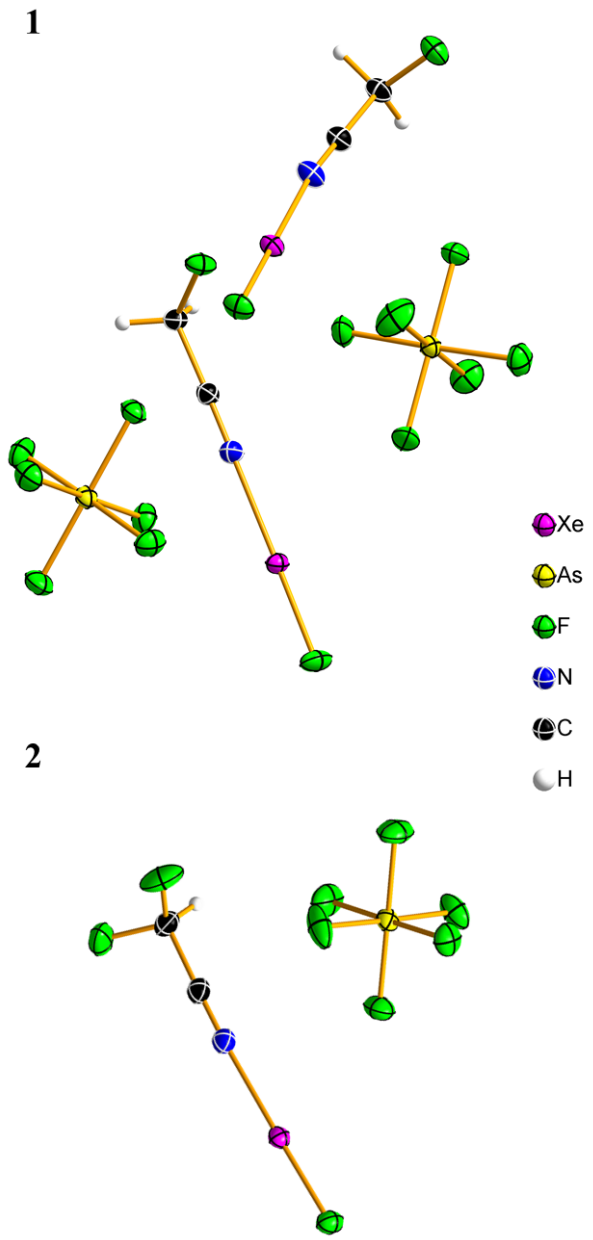

Figure 1: The crystal structure of (1) $[CH_2FCNXeF]^+[AsF_6]^-$ and (2) $[CHF_2CNXeF]^+[AsF_6]^-$. Ellipsoids are shown at the 50% probability level.

References:

1. Emara, A. A. A.; Schrobilgen, G. J., Fluoro(nitrile)xenon(II) Cations, $RC{\equiv}N{-}XeF^+AsF_6^-$ (R = H, CH_3, CH_2F, C_2H_5, C_2F_5, C_3F_7, or C_6F_5); Novel Examples of Xenon–Nitrogen Bonds and $^{129}Xe{-}^{13}C$, $^{129}Xe{-}^{1}H$, and $^{129}Xe{-}^{14}N$ Nuclear Spin-Spin Couplings. *J. Chem. Soc., Chem. Commun.* **1987**, 1644–1646.
2. Schrobilgen, G. J., The Fluoro(perfluoroalkylnitrile)-noble-gas(II) Cations, $R_FC{\equiv}N{-}NgF^+$ (Ng = Kr or Xe; R_F = CF_3, C_2F_5, *n*-C_3F_7), and the Fluoro(trifluoro-*s*-triazine)xenon(II) Cation, *s*-$C_3F_3N_2N{-}XeF^+$; Novel Noble Gas–Nitrogen Bonds. *J. Chem. Soc., Chem. Commun.* **1987**, 1506–1508.
3. Fir, B. A., *M.S. Thesis, McMaster University*, **1999**.

Funding information: This work was funded by the ERC Starting Grant (No. 950625), under the European Union's Horizon 2020 Research and Innovation Programme.

Supramolecular structures of two N-heterocyclic hybrids based on quinoline and 1,2,3-triazole moieties

Mario Cetina,[1,*] Silvija Maračić,[2] and Silvana Raić Malić[2]

[1] University of Zagreb, Faculty of Textile Technology, Department of Applied Chemistry, Prilaz baruna Filipovića 28a, *HR*-10000 Zagreb, Croatia

[2] University of Zagreb, Faculty of Chemical Engineering and Technology, Department of Organic Chemistry, Marulićev trg 20, *HR*-10000 Zagreb, Croatia

Quinoline is an important constituent of compounds with diverse applications, some of which display potent cytostatic activity through different mechanisms of action such as DNA intercalation, apoptosis, abrogation of cell migration, inhibition of angiogenesis and disregulation of nuclear receptor signalling [1,2]. Moreover, it was found that halogenated compounds have an important role in therapeutic application increasing their lipophilicity, metabolic stability and improving interactions of protein–ligand complexes [3]. Taking into consideration the aforementioned, we have synthesized 6-phenylquinoline derivatives containing a trifluoromethyl group at C-2 and a nonsubstituted (**1**) and *p*-chloro-substituted (**2**) phenyl-1,2,3-triazole moieties (Figure 1). We succeeded to obtain single crystals of both compounds, and in this contribution, we present their X-ray structures.

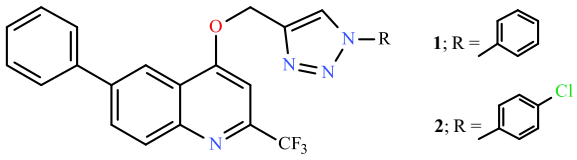

Figure 1: Molecular structures of the *N*-heterocyclic hybrids based on quinoline and 1,2,3-triazole moities

The corresponding bond lengths in these two structures are similar, as well as the conformations of the molecules. However, it should be noted that phenyl ring in **2** is almost parallel to the triazole ring to which it is attached [dihedral angle is 2.89(10)°], whereas in **1** it forms an angle of 18.39(13)°.

In both structures, two C−H···N hydrogen bonds generate a dimer motif, while their combination leads to the construction of one-dimensional chain of dimers. In **2**, one C−H···π interaction links neighbouring chains into two-dimensional network, which is further extended by one π···π interaction into a three-dimensional network (Figure 2a). In the structure of **1**, the one-dimensional chains of dimers are linked by two C–H···F hydrogen bonds, so creating three-dimensional network (Figure 2b). Two C−H···π interactions and one π···π interaction also participate in the formation of such supramolecular structure.

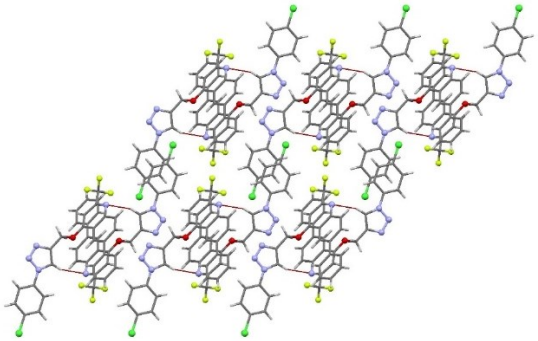

(a)

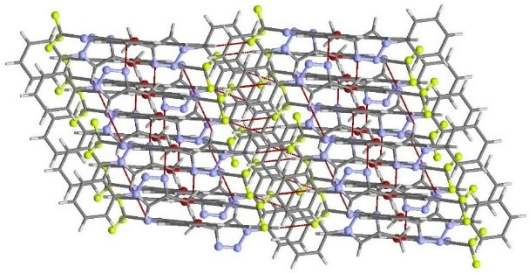

(b)

Figure 2: A part of the crystal structure of **2** (a) and **1** (b), showing three-dimensional networks formed by hydrogen bonds, C−H···π and π···π interactions.

References:

1. Cheng, G.; Hao, H.; Dai, M.; Liu, Z.; Yuan, Z. Antibacterial action of quinolones: from target to network. *Eur. J. Med. Chem.* **2013,** *66,* 555–562.
2. de O. Freitas, L. B.; Borgati, T. F.; de Freitas, R. P.; Ruiz, A. L. T. G.; Marchetti, G. M.; de Carvalho, J. E.; da Cunha, E. F. F.; Ramalho, T. C.; Alves, R. B. Synthesis and antiproliferative activity of 8-hydroxyquinoline derivatives containing a 1,2,3-triazole moiety. *Eur. J. Med. Chem.* **2014,** *84,* 595–604.
3. Auffinger, P.; Hays, F. A.; Westhof, E.; Ho, P. S. Halogen bonds in biological molecules. *Proc. Natl. Acad. Sci. U. S. A.* **2004,** *101,* 16789–16794.

Cobalt(II) complexes with 4-(hydroxymethyl)pyridine and sulfato ligands

Marta Počkaj*

[1] Faculty of Chemistry and Chemical Technology, University of Ljubljana, Večna pot 113, *SI*-1000 Ljubljana, Slovenia

Pyridine alcohols are a class of heterocyclic compounds that contain both a pyridine ring and hydroxyl group (OH). These bifunctional molecules act as ambidentate ligands capable of coordinating to metal centres through both the nitrogen atom from the ring and the oxygen atom from the alcohol group. However, the coordination behaviour of the pyridine alcohol is influenced by position of the hydroxyl group on the pyridine ring and protonation state of the hydroxyl group (neutral or deprotonated). Additionally, other substituent on the pyridine ring can also affect coordination mode with their steric and/or electronic effects. Consequently, a variety of coordination modes can be established. Pyridine alcohols are thus employed to stabilize a broad range of metal oxidation states and coordination environments, making them valuable in catalysis, bioinorganic modeling, and materials science, especially in the development of new synthetic approaches towards different materials with interesting physical properties, such as MOFs [1, 2].

As a result of simple reactions between cobalt(II) sulfate(VI) heptahydrate and 4-pyridinemethanol (4pym) using different solvents and metal:ligand ratios, several new compounds were prepared. Two of them formed single crystals that were appropriate for X-ray structure analysis. Mononuclear compound **1**, i.e. $[Co(OSO_3)(4pym)_2(H_2O)_3]$, crystallizes in orthorhombic $Pna2_1$ space group (No. 33) with four molecules in unit cell. Contrary to **1**, in which sulfato ligand is monodentate, in compound **2** sulfato ligand acts as a bridge between adjacent cobalt centres, thus forming the polynuclear chain-like structure with formula $[Co(\mu\text{-}OSO_3)(4pym)_4]_n$ which crystallizes in monoclinic $P2_1/c$ space group (No. 14). In both compounds, molecules and chains are interconnected by branched network of hydrogen bonds leading to 3D structure. To further evaluate intermolecular interactions, Hirshfeld surface analysis of both compounds was also studied using *CrystalExplorer* [3].

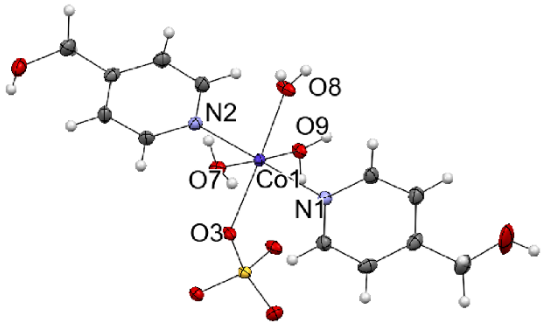

Figure 1: Coordination molecule in **1**. Ellipsoids are given at 50% probability while hydrogen atoms are shown as spheres of arbitrary radii.

References:

1. Ma, P.-P., Hao, Z.-M., Wang, P., Zhang, W.-H., Young, D. J. *trans*-$[Ni(pdm)_2]^{2+}$ (pdm = 2-pyridinemethanol) as a reliable synthon for isoreticular metal–organic frameworks of linear dicarboxylates. *J. Solid State Chem.* **2023**, B*317*, 123721.
2. Mylonas-Margaritis, I., Mayans, J., Tong, W., Farras, P., Escuer, A., McArdle, P., Papatriantafyllopoulou, C. Synthesis and characterization of new coordination compounds by the use of 2-pyridinemethanol and di- or tricarboxylic acids. *CrystEngComm* **2021**, *23*, 5489−5497.
3. Spackman, P. R., Turner, M. J., McKinnon, J. J., Wolff, S. K., Grimwood, D. J., Jayatilaka, D., Spackman, M. A. Cry*stalExplorer*: a program for Hirshfeld surface analysis, visualization and quantitative analysis of molecular crystals. *J. Appl. Cryst.* **2021**, *54*, 1006–1011.

Funding information: We are grateful for the financial support of the Slovenian Research and Innovation Agency (ARIS, program grant P1-0175) and Anja Pečkaj for synthetis optimization. The author also acknowledges the support of the Centre for Research Infrastructure at the University of Ljubljana, Faculty of Chemistry and Chemical Technology, which is part of the Network of Research and Infrastructural Centers UL (MRIC UL) and is financially supported by ARIS; Infrastructure program No. I0-0022.

Coordination of Cu(I) with guanazole and N-methyl guanazole derivatives

Andrii Hultiaiev[1], Evgeny Goreshnik[1]

[1] Department of Inorganic Chemistry and Technology, Jožef Stefan Institute, Jamova cesta 39, *SI*-1000 Ljubljana, Slovenia

Two new **copper(I)- halide - guanazole** (3,5-diamine-1,2,4-triazole, **datrz**) compounds, a new **N,N´-dimethyl-guanazole** derivative, and a compound with a **N-methyl guanazole** derivative coordinated to **Cu(I)** and **Cl** were synthesized and studied. A search in the **CSD CCDC**[1] revealed neither copper(I)-chloride compounds with guanazole nor compounds that include **N-methyl-guanazole** derivatives. However, some **copper-guanazole** compounds with bromide, iodide, hydroxide, and water ligands were found[2-4]. This was the reason for a more careful investigation of copper(I) chloride coordination compounds with **guanazole**.

The crystallographically independent unit of the compound **Cu_2ClBr(datrz)** (**1**) consists of neutral **datrz** molecules coordinated via two nitrogen atoms from the cycle with two copper centres. Each copper ion is four-fold coordinated, the **Cu1** ion has an almost regular tetrahedral environment. The Cu2 centre has a slightly distorted tetrahedral environment. Each of them also coordinates two mixed chloride-bromide centres. Due to the bridging role of the anions, infinite $(Cu_2ClBr)_n$ inorganic chains are formed that run along the 100 direction. These chains are connected to each other via the bridging **Datrz** ligand.

The **compound Cu_8Cl_6(datrz$^-$)$_2$ (2)** contains a 5-coordinated negatively charged **datrz** core. The N2 atom from the cycle is bound to the Cu1 bridge between two organic residues. Another nitrogen atoms are linked to the copper centres of the **inorganic 2D network $(Cu_7Cl_6)_n$**. In this network, the metal centres **Cu2** and **Cu3** are 3-coordinated, **Cu4** and **Cu5** are 4-coordinated with a slightly distorted tetrahedral surrounding. The inorganic fragment in the shape of folded layers extends along the a and c axes.

The **compound [N,N´-Met_2datrz]Cl (3)** contains a new organic core of N,N´-dimethyl guanazole (**N,N´-Met_2-datrz**) organic core. An isolated chloride anion **Cl1** shows us that this core carries the positive charge +1. This compound was obtained under solvothermal conditions from guanazole and methanol in a weakly-acidic (HCl) medium.

The **compound Cu_2Cl_2(N-Metdatrz) (4)** contains a new ligand - **N-Met-datrz**. It coordinates via the **N3** donor atom with the **Cu1** center from the inorganic dimer **Cu_2Cl_2**. The copper ion is three-coordinated. The 2-coordinated metal centre **Cu2** serves as a bridge between two organic ligands. Infinite **organic-inorganic hybrid chains** running along the b-axis appeared. The $CuCl_2^-$ anion containing two-coordinated **Cu3** ion equalises the charge.

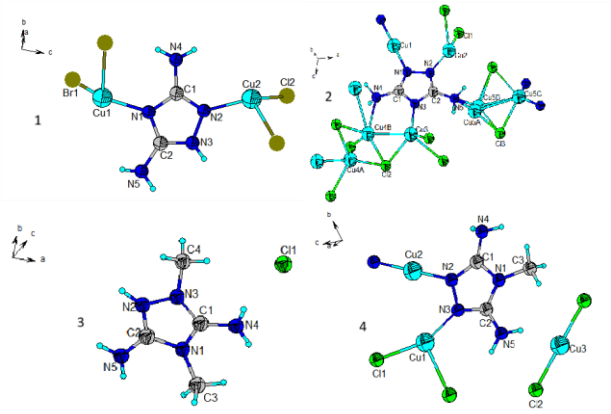

Figure 1: Chemical structures of the compounds 1, 2, 3, and 4

Table 1: Cell parameters of the compounds 1,2, 3, and 4

	1	**2**	**3**	**4**
Space group	$P2_1/c$	$P2_1/n$	P 1	P 1
a	3.8320(2)	9.1935(2)	5.5062(4)	4.0027(2)
b	13.2575(8)	3.6488(1)	8.0642(7)	7.8591(5)
c	14.8477(7)	27.9769(5)	9.6968(9)	13.9942(7)
α	90	90	65.918(8)	85.375(4)
β	95.485(6)	98.869(2)	80.369(7)	85.552(4)
γ	90	90	75.252(7)	75.374(5)
V	750.84(7)	927.27(4)	379.16(6)	423.83(4)

References:

1. *Acta Cryst*. **2016**, B72, 171-179.
2. *Cryst. Growth Des.*, **2008**, 8 (10), 3735-3744
3. *Inorg. Chem. Com.*, **2006**, 9(8), 819–822.
4. *Inorg. Chem. Com.*, **2008**, *11(10), 1256–1259.*

Funding information: research core funding No. P1–0045; Inorganic Chemistry and Technology, The Slovenian Research Agency ARIS.

Aggregation and anion formation in polyfluoridotitanates(IV): From monomers to extended frameworks

Kristian Radan*, Boris Žemva, Matic Lozinšek

Jožef Stefan Institute, Jamova cesta 39, 1000 Ljubljana, Slovenia

In this study, we investigated the reactivity of titanium tetrafluoride (TiF_4) with various Lewis bases, with a particular focus on the synthesis and structural characterization of polyfluoridotitanates(IV). These reactions give rise to a broad spectrum of anionic species, ranging from simple octahedral $[TiF_6]^{2-}$ units to extended oligomeric and polymeric frameworks such as $[TiF_5]^-$ chains, $[Ti_2F_9]^-$ ladders, $[Ti_4F_{17}]^-$ layers (Figure 1), and large polynuclear anions[1,2] like $[Ti_8F_{33}]^-$ and $[Ti_9F_{38}]^{2-}$.

The products were obtained from solutions using anhydrous hydrogen fluoride (aHF) as a solvent or via carefully controlled thermal treatments, under conditions designed to modulate fluoride mobility and coordination behaviour. The resulting structures demonstrate a remarkable sensitivity to the nature of the Lewis base and the reaction environment, revealing that subtle changes in donor strength and stoichiometry can shift the equilibrium between fluoridoanions of different dimensionalities.

Among the Lewis bases studied, xenon difluoride (XeF_2) served a dual role: as a weak fluoride donor and as a probe of fluoride abstraction processes. Similar to its behavior in the XeF_2–MnF_4 system[3], XeF_2 reacts with TiF_4[4] to yield a series of structurally diverse compounds, including $2[XeF][TiF_5]\cdot XeF_2$, $[XeF][Ti_4F_{17}]$, $[Xe_2F_3][Ti_8F_{33}]$, and $[XeF]_2[Ti_9F_{38}]$. These species illustrate a continuum of XeF_2 ionization pathway[5] and highlight how the formation of highly aggregated polyfluoridotitanate(IV) anions can promote fluoride transfer, even in systems where XeF_2 is initially only partially polarized. The resulting cations ($[XeF]^+$, $[Xe_2F_3]^+$) engage in electrostatic interactions with the complex titanium fluoride anions, stabilizing unusual structural architectures.

Reactions between xenon difluoride (XeF_2) and metal tetrafluorides represent a unique class of Lewis acid–base interactions, where fluoride transfer leads to the formation of complex fluoridometallate anions and xenon-based cations. These systems serve as valuable models for studying the controlled ionization of XeF_2 and the structural evolution of the resulting fluoridometallates under varying reaction conditions. Nevertheless, despite extensive synthetic efforts, the factors dictating aggregation and structural topology remain only partially understood. This contribution highlights the structural diversity and formation preferences of polyfluoridotitanates(IV), advancing the understanding of their coordination chemistry beyond simple stoichiometric considerations.

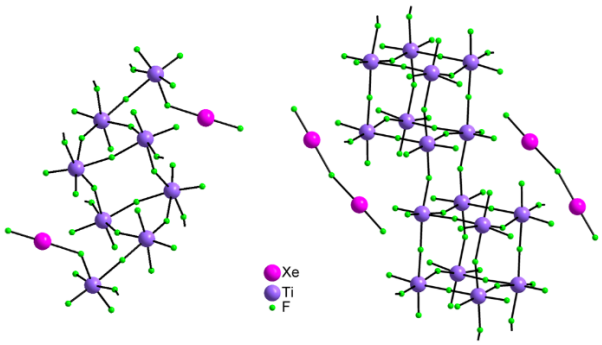

Figure 1: Constitutional isomers of the phase $XeF_2\cdot 4TiF_4$ – crystal structures of $[XeF][Ti_4F_{17}]$ (left) and $[Xe_2F_3][Ti_8F_{33}]$ (right).

References:

1. Radan, K.; Goreshnik, E.; Žemva, B., Xenon(II) Polyfluoridotitanates(IV): Synthesis and Structural Characterization of $[Xe_2F_3]^+$ and $[XeF]^+$ Salts. *Angew. Chem. Int. Ed.* **2014**, *53*, 13715–13719.
2. Radan, K., *PhD Thesis*, Jožef Stefan International Postgraduate School, **2017**.
3. Motaln, K.; Gurung, K.; Brazda, P.; Kokalj, A.; Radan, K.; Dragomir, M.; Žemva, B.; Palatinus, L.; Lozinšek, M., Reactive Noble-Gas Compounds Explored by 3D Electron Diffraction: XeF_2–MnF_4 Adducts and a Facile Sample Handling Procedure. *ACS Cent. Sci.* **2024**, *10*, 1733–1741.
4. Žemva, B.; Slivnik, J.; Bohinc, M., On the syntheses of xenon fluorotitanates(IV). *J. Inorg. Nucl Chem.* **1976**, *38*, 73–74.
5. Žemva, B.; Jesih, A.; Templeton, D. H.; Zalkin, A.; Cheetham, A. K.; Bartlett, N., Phases in the System XeF_2/XeF_5AsF_6 and Structural and Vibrational Evidence for the Following Ionization Pathway: $XeF_2 \rightarrow XeF^+ + F^-$. *J. Am. Chem. Soc.* **1987**, *109*, 7420–7427.

Funding information: European Research Council (ERC) under the European Union's Horizon 2020 Research and Innovation Programme (Starting Grant 950625)

New ternary gallide $Zr_7Ru_{6+x}Ga_{17-x}$ ($0 \le x \le 2.0$): synthesis, crystal and electronic structures

Bogdan Kotur*,[1] Volodymyr Babizhetskyy,[1] Oksana Myakush,[2] Volodymyr Smetana,[3] Anja-Verena Mudring,[3]

[1] Department of Inorganic Chemistry, Ivan Franko National University of Lviv, Kyryla & Mefodia Str. 6, 79005 Lviv, Ukraine
[2] National University of Forest and Wood Technology of Ukraine, Chuprynky Str. 103, 79057 Lviv, Ukraine
[3] Department of Biological and Chemical Engineering and iNANO, Aarhus University, 8000 Aarhus C, Denmark

A new ternary phase, $Zr_7Ru_{6+x}Ga_{17-x}$ ($0 \le x \le 2.0$) with a small homogeneity range along the isoconcentrate of 23.3 at. % Zr with the limits from 50.0 to 56.7 at. % Ga, was discovered while investigating the Zr–Ru–Ga phase diagram. The samples for investigation were synthesized by arc melting of stoichiometric amounts of the elements under an argon atmosphere, followed by annealing of ingots at 870 K for 720 h. Structural determination was performed using single-crystal X-ray techniques. The homogeneity range of the phase was analyzed using the data from powder X-ray diffraction (XRD) and energy-dispersive X-ray (EDX) analyses. The electronic structure was also calculated for an idealized ordered approximant of $Zr_7Ru_6Ga_{17}$.

$Zr_7Ru_6Ga_{17}$ crystallizes in a new cubic structure type (Pearson symbol ***cF***120, space group ***Fm*-3*m*** No. 225, ***a*** = 12.409(1) Å, ***Z*** = 4) extending the family of closely-related cubic structures described by Pearson symbols ***cF***116–120: Th_6Mn_{23}, $Mg_6Cu_{16}Si_7$, $Sc_{11}Ir_4$, $Er_3Pd_8Sb_4$, and $Ti_6Fe_7Al_{17}$. In the structure of $Zr_7Ru_6Ga_{17}$, Zr1, Zr2, and Ru atoms fully occupy the 24***e***, 4***b***, and 24***d*** Wyckoff positions, respectively (Table 1).

The crystal structure can be regarded as a deficient superstructure polyhedral variant of CaF_2 with Ga3@Ga8Zr6 rhombic dodecahedra occupying vertices and centering faces, Zr2@Ga8Zr6 centering the edges and Ga2b@Ga8Ru6 centering all octants. The refinement of the corresponding site occupancy factor (SOF) for the Ga atoms resulted in a SOF of 0.72 for Ga2a (site 32*f*), also revealing a decent level of positional disorder. Two significant peaks of 29 and 21 $e^-/Å^3$ close to the Ga2a position were detected. Simultaneous refinement of the corresponding SOFs for the neighbouring two gallium sites resulted in values of only 0.24 for Ga2b (site 8***c***) and 0.22 for Ga2c (site 32***f***), respectively. Considering the SOFs and the multiplicity for three gallium atoms, their sum gives Ga2a + Ga2b + Ga2c = 23 + 7 + 2 = 32 atoms, compensating for the partial occupancy of the position Ga2a.

Density functional theory (DFT)-based electronic structure calculations using the linear muffin tin orbital-atomic sphere approximation (LMTO-ASA) approach, performed for an ordered approximant of the crystal structure, support the metallic character and reveal peculiar features around the Fermi level, ***i.e.,*** three van Hove singularities (vHSs) at high-symmetry points of its band structure, which point to the proximity to super-conductivity. However, the temperature dependence of the electrical resistivity in the 2–300 K temperature range, ***ρ(T),*** reflects the metallic character of the compound.

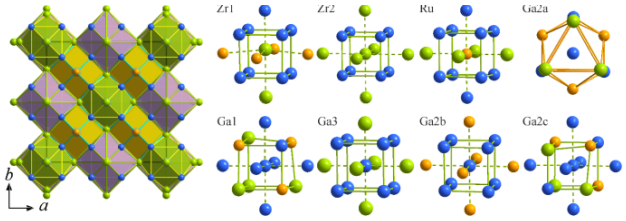

Figure 1: Projection of the crystal structure of $Zr_7Ru_6Ga_{17}$ and coordination polyhedra of the atoms. Zr, Ru, and Ga atoms are green, orange and blue, respectively. Mutually exclusive components of the Ga split disorder are not shown for clarity purposes.

Table 2: Atomic coordinates for $Zr_7Ru_6Ga_{17}$

Atom	Wyckoff position	*x*	SOF
Zr1	24*e* (*x*, 0, 0)	0.2253(2)	1
Zr2	4*b* (½, ½, ½)		1
Ru	24*d* (0, ¼, ¼)		1
Ga1	32*f* (*x*, *x*, *x*)	0.37586(7)	1
Ga2a	32*f* (*x*, *x*, *x*)	0.1562(2)	0.72(1)
Ga2c	32*f* (*x*, *x*, *x*)	0.1266(5)	0.22(2)
Ga2b	8*c* (¼, ¼, ¼)		0.24(2)
Ga3	4*a* (0, 0, 0)		1

Funding information: B.K. and V.B. thank for financial support: Grant No SFI-PD-Ukraine-00014574, The Simons Foundation International, Ltd.

Copper coordination compounds with aminopyridine derivatives of picolinic acid

Mišel Hozjan,[1*] Franc Perdih[1], Zvonko Jagličić[2]

[1] Faculty of Chemistry and Chemical Technology, University of Ljubljana, Večna pot 113, *SI*-1000 Ljubljana, Slovenia
[2] Institute of Mathematics, Physics and Mechanics & Faculty of Civil and Geodetic Engineering, University of Ljubljana, Jadranska 19, 1000 Ljubljana, Slovenia

Copper exhibits a versatile coordination chemistry, with complexes known to exist in oxidation states ranging from 0 to +4. However, the +1 and +2 states are the most prevalent, with +2 being particularly dominant[1]. The d^9 configuration of Cu(II) typically favors a tetragonal coordination environment, characterized by four short equatorial bonds and one or two longer axial bonds. Nevertheless, copper(II) complexes can adopt a variety of other geometries, including tetrahedral, square planar, and trigonal bipyramidal arrangements. The coordination chemistry of copper(II) is a subject of considerable interest due to the inherent stability of its complexes, the diverse range of geometries they exhibit, and their significant biological relevance. Copper compounds serve as catalysts in both homogeneous and heterogeneous reactions, function as fungicides, pesticides, and wood preservatives, and are employed as pigments in paints and glasses. Furthermore, copper compounds are considered as crucial components of high-temperature superconductors.

Given its borderline soft character, the d^9 Cu(II) center exhibits a strong affinity for amine ligands, such as pyridine and its derivatives. In our research, we have investigated amide derivatives of picolinic acid, primarily aminopyridine derivatives, and explored their diverse coordination capabilities with copper. These complexes were synthesized in the presence of bases like ammonia and pyridine, which were often incorporated into the metal's coordination sphere. The resulting products displayed a wide array of intriguing crystal structures. Given that some copper–picolinic acid compounds in the literature have exhibited interesting magnetic properties[2], we also tested a select few of our compounds for these properties.

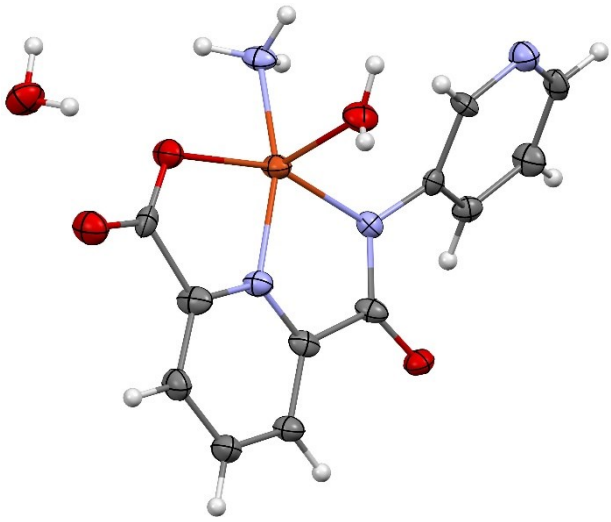

Figure 1: An example of a copper(II) coordination compound with a picolinic acid derivative.

References:

1. Rasyda, Y. A.; Rahardjo, S. B.; Marliyana, S. D. Synthesis and Structure Characterization of Copper(II) Complex with Phenylhydrazine. *J Phys Conf Ser* **2021**, *1912* (1), 012029.
2. Singh, J.; Hundal, G.; Corbella, M.; Gupta, R. Synthesis, Characterization and Structures of Copper(II) Complexes with Amide-Based Ligands: Unusual Formation of a Linear Trimer and a Zig-Zag Chain and Their Contrast Magnetic Behaviour. *Polyhedron* **2007**, *26* (14), 3893–3903.

Funding information: This work was funded by the financial support from the junior research grant for Mišel Hozjan and the program grant P1-0175 of the Slovenian Research Agency (ARRS). We also acknowledge the support of the Centre for Research Infrastructure at the University of Ljubljana, Faculty of Chemistry and Chemical Technology, which is part of the Network of Research and Infrastructural Centres UL (MRIC UL) and is financially supported by the Slovenian Research Agency (Infrastructure programme No. I0-0022).

Interaction of DNA with copper(II)–homoserine coordination polymers: structural insights and biological relevance

Ivana Kekez[1], Darko Vušak[1], David Kučera-Čavara[1], Biserka Prugovečki[1]*

[1] Department of Chemistry, Faculty of Science, University of Zagreb, Horvatovac 102a, 10000 Zagreb, Croatia

Casiopeinas are copper-based compounds with notable biological activity, demonstrating promising antineoplastic effects across various cancers[1]. Two primary mechanisms of action have been proposed based on experimental findings: the induction of reactive oxygen species (ROS) and direct binding and interaction with nucleic acids[2]. Previous research in our group revealed great potential for studying cytotoxicity of ternary Cu coordination compounds on cancer cells[3–4]. In this work, the biological properties of two compounds differing in the lack (**1** - *trans*-[Cu(μ-L-hser)(L-hser)]$_n$) or presence (**2**-{[Cu(μ-L-hser)(H_2O)(bpy)]$_2SO_4 \cdot 2H_2O$}$_n$ (L-hser = L-homoserinate, bpy = 2,2'-bipyridine)) of heterocyclic bases were investigated. Compound **2** exhibited moderate antiproliferative activity (IC_{50}) against all three tested cell lines: H460 (lung carcinoma), MCF-7 (breast carcinoma), and HCT116 (colon carcinoma), with an IC_{50} range of 15.8–19.3 μmol dm^{-3}. Antibacterial assays demonstrated moderate activity with an *MIC* value of 64 μg mL^{-1} against the Gram-negative bacterial strain *Moraxella catarrhalis* ATCC 23246. Since no biological activity was found for compound **1**, which lacks the coordinated heterocyclic base, we confirmed the necessity of a heterocyclic base for the potential biological application of Cu(II) complexes. To investigate the DNA interaction profile of ternary compound **2**, we performed UV and fluorescence spectroscopy, as well as single-crystal X-ray diffraction. Absorption and fluorescence spectra suggested a lower binding affinity of **2** to the double-stranded **DNA** dodecamer ds(CGCGAATTCGCG). Addition of compound **2** to the crystallization solution containing ds(CGCGAATTCGCG) changed the unit cell parameters of **DNA** (PDB ID:1BNA)[5] from the orthorhombic crystal system to the tetragonal. This insight provides a valuable direction for future structure-based design of more potent copper(II) antibacterial and anticancer agents to address the limitations of current therapies.

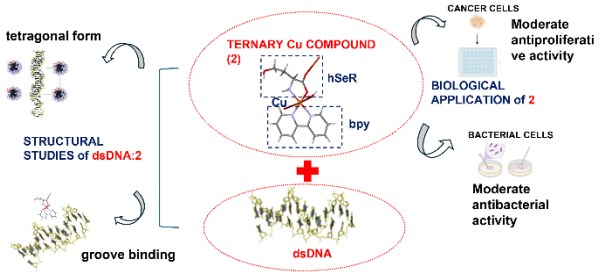

Figure 1: A schematic illustration summarizing the structural investigation of the **DNA**–compound **2** interaction and the biological activity results of compound **2**.

References:

1. González-Ballesteros, M. M., Sánchez-Sánchez, L., Espinoza-Guillén, A., Espinal-Enríquez J., Mejía, C., Hernández-Lemus, E. & Ruiz-Azuara L. Antitumoral and Antimetastatic Activity by Mixed Chelate Copper(II) Compounds (Casiopeínas®) on Triple-Negative Breast Cancer, In Vitro and In Vivo Models. *Int. J. Mol. Sci.* **2024**, *25(16)*, 8803-638.
2. Li, L., Wang, Y., Li, M., Wang, H. & Dong, X. Metal Complexes or Chelators with ROS Regulation Capacity: Promising Candidates for Cancer Treatment. *Molecules*. **2021**, *27(1)*, 148.
3. Vušak, D., Šimunović Letić, M., Tašner, M., Matković-Čalogović, D., Jurec, J., Žilić, D. & Prugovečki, B. Solvatomorphic Diversity in Coordination Compounds of Copper(II) with L-Homoserine and 1,10-Phenanthroline: Syntheses, Crystal Structures and ESR Study. *Molecules*. **2024**, *29(23)*, 5621.
4. Vušak, D., Primožić, M., & Prugovečki, B. Atmosphere-Controlled Solvatomorphic Transitions of Ternary Copper(II) Coordination Compounds in Solid State. *Crystals*. **2024**, *14(11)*, 986.
5. Drew, H. R; Wing, R. M., Takano, T., Broka, C., Tanaka, S., Itakura, K. & Dickerson, R. E. Structure of a B-DNA dodecamer: Conformation and dynamics*. *Proc. Nati. Acad. Sci. USA* **1981**, *78*, 2179-2183.

Funding information: This research was funded by an institutional project financed by the University of Zagreb entitled Synthesis and structural characterization of organic and complex compounds; protein structure.

Exploring the Chemistry of Pyrithione and Copper

Benjamin Poljanc,[1] Jakob Kljun,[1] Iztok Turel*[1]

[1] Faculty of Chemistry and Chemical Technology, University of Ljubljana, Večna pot 113, *SI*-1000 Ljubljana, Slovenia

Pyrithiones are sulfur-containing aromatic heterocycles that contain a thiohydroxamic group. They were first synthesized in the 1950s[1] and also identified as natural products.[2] Pyrithiones have attracted considerable attention due to their ability to coordinate almost any metal ion and their biological activity.[3,4] The most widely studied complex is zinc pyrithione, which is valued for its broad-spectrum antimicrobial activity and low water solubility, which enables prolonged retention on surfaces such as skin or marine coatings.[5]

Recent studies emphasize the potential of pyrithione metal complexes – especially with zinc and precious metals – as promising agents against bacterial, fungal and even viral pathogens such as SARS-CoV-2.[5] These results underline the continued relevance of pyrithione-based systems for medical and industrial applications and justify further exploration of their coordination chemistry and bioactivity. In parallel, there is a growing research interest in copper complexes, as appropriately designed ligand systems have shown promising anticancer activity.[6]

In recent years, our research group has prepared various pyrithione analogs and their metal complexes, including numerous copper(II) complexes. Due to the very poor solubility of these complexes in water and most organic solvents, obtaining single crystals of these complexes is not trivial.[7] However, with the use of uncommonly utilized crystallization techniques, we have succeeded in obtaining the crystals and determining the structure of the complex.

In this presentation I will present the synthesis procedure for preparation of copper(II) complex with 4-(trifluoromethyl)pyrithione, the method and instrument we used to obtain the single crystals and the determined crystal structure.

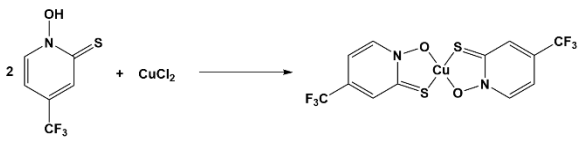

Figure 1: Reaction scheme for the preparation of copper(II) complex with 4-(trifluoromethyl)pyrithione.

References:

1. Shaw, E.; Bernstein, J.; Losee, K.; Lott, W. A.: Analogs of Aspergillic Acid. IV. Substituted 2-Bromopyridine-N-oxides and Their Converion to Cyclic Thiohydroxamic Acids[1]. *J. Am. Chem. Soc.* **1950**, *72*, 4362–4364.
2. O'Donnell, G.; Poeschl, R.; Zimhony, O.; Gunaratnam, M.; Moreira, J. B. C.; Neidle, S.; Evangelopoulos, D.; Bhakta, S.; Malkinson, J. P.; Boshoff, H. I.; Lenaerts, A.; Gibbsons S.: Bioactive pyridine-*N*-oxide disulfides from *Allium stipitatum*. *J. Nat. Prod.* **2009**, *72*, 360–365.
3. Robinson, M. A.: Complexes of 1-Hydroxy 2-Pyridinethione. *J. Inorg. Nuc. Chem.* **1964**, *26*, 1277–1281.
4. Kladnik, J.; Kljun, J.; Burnmeister, H.; Ott, I.; Romero-Canelón, I.; Turel, I.: Towards Identification of Essential Structural Elements of Organoruthenium(II)-Pyrithionato Complexes for Anticancer Activity. *Chem. Eur. J.* **2019**, *25*, 14169–14182.
5. Kladnik, J.; Dolinar, A.; Kljun, J.; Perea, D.; Grau-Expósito, J.; Genescà, M.; Novinec, M.; Buzon, M. J.; Turel, I.: Zinc pyrithione is a potent inhibitor of PLPro and cathepsin L enzymes with *ex vivo* inhibition of SARS-CoV-2 entry and replication. *J. Enzyme Inhib. Med. Chem.* **2022**, *37*, 2158–2168.
6. Krasnovskaya, O.; Naumov, A.; Guk, D.; Gorelkin, P.; Erofeev, A.; Beloglazkina, E.; Majouga, A.: Copper coordination compounds as biologically active agents. *Int. J. Mol. Sci.* **2020**, *21*, 3965.
7. Mishra, A.: Bioactivity of Substituted Copper Pyrithione Complexes; Doctoral Dissertation, Durham University, **2022**.

Funding information: We are grateful for the financial support from the junior research grant for Benjamin Poljanc and the program grant P1-0175 of the Slovenian Research and Innovation Agency (ARIS). The authors also acknowledge the support of the Centre for Research Infrastructure at the University of Ljubljana, Faculty of Chemistry and Chemical Technology, which is part of the Network of Research and Infrastructural Centres UL (MRIC UL) and is financially supported by the Slovenian Research and Innovation Agency (ARIS; Infrastructure programme No. I0-0022).

Understanding the sensitivity of high-energy materials using crystallographic data

Ivana Veljković,[1] Danijela Kretić,[2] Dragan Ninković,[3] Dušan Veljković*,[2]

[1] University of Belgrade – Institute of Chemistry, Technology and Metallurgy – National Institute of the Republic of Serbia, Njegoševa 12, Belgrade, Serbia
[2] University of Belgrade – Faculty of Chemistry, Studentski trg 12 – 16, Belgrade, Serbia
[3] Innovative Centre of the Faculty of Chemistry, Studentski trg 12 – 16, Belgrade, Serbia

Understanding and controlling the sensitivity of high-energy materials (HEMs) is crucial for the safe design and application of energetic compounds. In this study, we explore how geometrical parameters derived from crystal structures can be used to predict and potentially fine-tune the sensitivity of HEMs toward detonation. Using crystallographic data, we focus on the analysis of C–NO_2 bond lengths, the distances and angles between neighboring nitro groups, and the presence of specific substituents[1] or noncovalent interactions, such as hydrogen bonding.[2] These structural features were analyzed in the context of the results of quantum chemical calculations, particularly Bond Dissociation Energies (BDEs) of the C–NO_2 bond. This bond is often the weakest bond in molecules of nitroaromatic explosives ("trigger bond") and it`s dissociation represents the initial step in a detonation process.

Additionally, we examined Electrostatic Potential maps (MEP), with a particular focus on the distribution of positive potential above the central region of aromatic ring, which is an indicator of highly energetic properties of selected molecule. These values are shown to be sensitive to structural variations and are highly dependent on the surrounding chemical environment. Coordination compounds, in particular, offer a versatile platform for such adjustments.[3] By careful selection of transition metal centers and appropriate ligands, it is possible to fine-tune the electrostatic potential on the surface of the molecule and, consequently, its sensitivity.

Our study includes experimental and theoretical analysis of several systems, including the Co(AcAc-NO_2)$_3$ complex.[4] Initiation of this compound in an open flame, supported BDE/MEP data, confirmed its high-energy character. The introduction of chelate rings emerges as a promising strategy for modulating detonation sensitivity in coordination-based HEMs.

These insights not only deepen our understanding of structure–property relationships in energetic materials but also point toward new design principles for safer high-energy compounds with improved detonation characteristics.

References:

1. Veljković, I.; Đunović, A.; Veljković, D., Influence of halogen substituents on sensitivity towards detonation of polycyclic nitroaromatic high-energy molecules. *J. Phys. Org. Chem.,* **2024**, *37(10)*, e4649.
2. Kretić, D.; Radovanović, J.; Veljković, D Can the sensitivity of energetic materials be tuned by using hydrogen bonds? Another look at the role of hydrogen bonding in the design of high energetic compounds. *Phys. Chem. Chem. Phys.,* **2021***, 23,* 7472-7479.
3. Kretić, D.; Veljković, I.; Đunović, A.; Veljković, D., Chelate Coordination Compounds as a New Class of High-Energy Materials: The Case of Nitro-Bis(Acetylacetonato) Complexes. *Molecules*, **2021**, *26(18)*, 5438.
4. Kretić, D.; Veljković, I.; Veljković, D., Tris(3-nitropentane-2,4-dionato-κ2 O,O′) Complexes as a New Type of Highly Energetic Materials: Theoretical and Experimental Considerations. *Chemistry*, **2023**, *5(3)*, 1843-1854

Funding information: This research was supported by the Science Fund of the Republic of Serbia, PROMIS, #6066886, CD-HEM. This research has been financially supported by the Ministry of Science, Technological Development and Innovation of Republic of Serbia (Contract numbers: 451-03-136/2025-03/200026), 451-03-136/2025-03/200168 and 451-03-136/2025-03/200288), and it contributes to the achievement of Sustainable Development Goals 9 (Industry, Innovation, and Infrastructure) and 12 (Responsible Consumption and Production).

Structure of two morpholinium iodidoantimonates and one iodidobismuthate

Amalija Golobič*,[1] Filip Kóša[1] and Miha Bukleski[2]

[1] Faculty of Chemistry and Chemical Technology, University of Ljubljana, Večna pot 113, *SI*-1000 Ljubljana, Slovenia
[2] Institute of Chemistry, Faculty of Natural Sciences and Mathematics, Ss. Cyril and Methodius University, Arhimedova 5, 1000 Skopje, North Macedonia

Morpholinium iodidoantimonates and iodido bismuthates are hybrid materials which combine organic cations with inorganic iodidoantimonate or iodidobismuthate frameworks, respectively. Similarly, as halogenidoplumbates with organic cations, bismuth and antimony analogues have interesting optic and electronic properties. Their advantage is that they are less toxic, which makes them more environmentally acceptable.

Structure of three compounds: $(C_4H_{10}NO)_2SbI_5$ (**1**), $(C_4H_{10}NO)_4Sb_4I_{16}\cdot 2(CH_3CN)$ (**2**) and $(C_4H_{10}NO)_4Bi_4I_{16}\cdot 6H_2O$ (**3**) was determined by X-ray single crystal structure determination. Diffraction data were collected at 150 K by SuperNova diffractometer using MoK$_\alpha$ radiation. Crystalographic data:

(**1**) Mr=932,51, orthorhombic, $P2_12_12_1$, a=9.6609(3), b=10.8121(3), c=19.6110(7) Å, Z=4, D_x=3.024 Mg m^{-3}, μ=8.88 mm^{-1}, brown sticks, 21350 measured and 5527 independent reflections, 180 parameters, R_{int}=0.036, R=0.024, wR=0.045.

(**2**) Mr=2952.03, orthorhombic, $Pbca$, a=12.8815(2), b= 20.3941(4), c=23.0504(4) Å, Z=4, D_x=3.238 Mg m^{-3}, μ=9.95 mm^{-1}, orange prisms, 58154 measured and 8688 independent reflections, 233 parameters R_{int}=0.048, R=0.032, wR=0.067.

(**3**) Mr= 3326.93, monoclinic, $P2_1/c$, a=11,8205(16), b= 20.5779(15), c=13.5091(8) Å, β=108.198(8)°, Z=2, D_x=3.540 Mg m^{-3}, μ=19.19 mm^{-1}, red prisms, 66738 measured and 8698 independent reflections, 232 parameters, R_{int}=0.067, R=0.036, wR=0.081.

In all three structures each Bi^{3+} or Sb^{3+} is coordinated by six jodido ligands in a shape of distored octahedron. In **(1)** neighbouring octahedra are interconnected through the vertices and form one-dimensional infinite zigzag chains $[SbI_5^{2-}]_n$ with the symmetry of twofold screw axis running along the *a*-edge (Fig. 1). In **(2)** and **(3)** four octahedra are via two edges connected into four-nuclear centrosymmetric $[Sb_4I_{16}^{4-}]$ or $[Bi_4I_{16}^{4-}]$ complex anions (Figs. 2 and 3). In all three structures each morpholinium cation is in chair conformation and is a donor of two N-H hydrogen bonds accepted by iodido ligands and in **(3)** also by water molecules. **(2)** contains solvent acetonitrile.

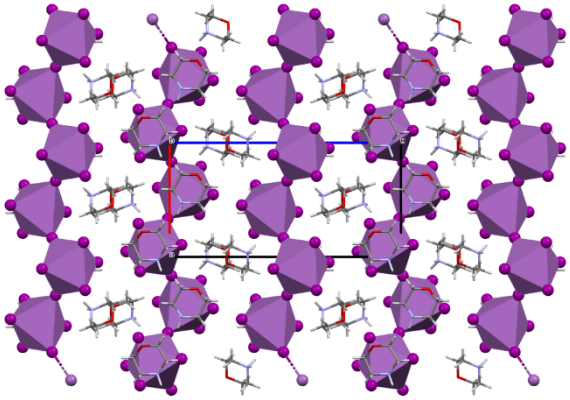

Figure 1: Structure of $(C_4H_{10}NO)_2SbI_5$

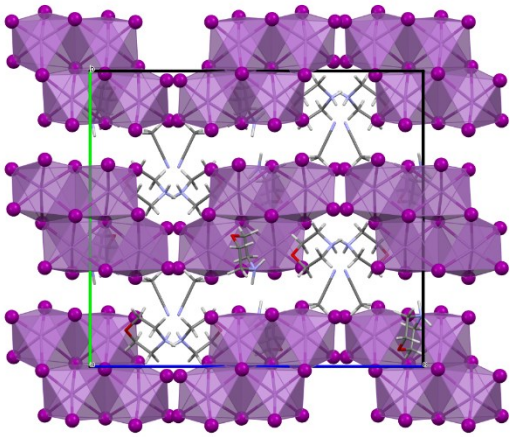

Figure 2: Structure of $(C_4H_{10}NO)_4Sb_4I_{16}\cdot 2(CH_3CN)$

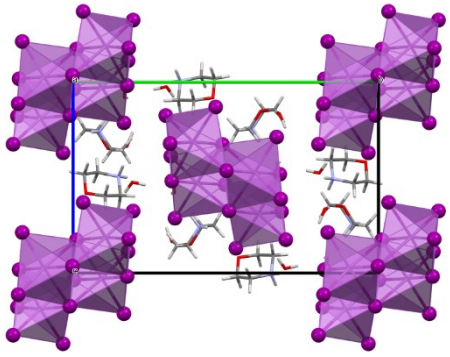

Figure 3: Structure of $(C_4H_{10}NO)_4Bi_4I_{16}\cdot 6H_2O$

Funding information: Financial support of the Slovenian Research and Innovation Agency is gratefully acknowledged (Grant P1-0175).

Crystal Dynamics of Oxitropium Bromide: Thermal Expansion Anisotropy Preceding Explosive Phase Transition

Teodoro Klaser[1,2] and Željko Skoko*[1]

[1] Department of Physics, Faculty of Science, University of Zagreb, Bijenička 32, Zagreb, Croatia
[2] Department of Physics, University of Trento, Via Sommarive 14, Trento, Italy

The thermosalient effect, a phenomenon where crystals exhibit sudden jumps during phase transitions, was investigated in oxitropium bromide (OXTB). Using variable-temperature X-ray powder diffraction, structural evolution leading to this remarkable behavior was explored, with particular emphasis on the role of anisotropic thermal expansion. The findings reveal exceptional thermal anisotropy in the low-temperature Form A, characterized by unusually high positive thermal expansion coefficients along crystallographic axes *a* and *b* - up to five times higher than typical values for molecular crystals. Notably, the significant negative thermal expansion (NTE) along the c-axis was also observed, a rare phenomenon that contributes substantially to the material's dynamic behavior. After phase transition (at approximately 45°C), the high-temperature Form B exhibits positive thermal expansion along all axes but maintains high anisotropy with the *a*-axis coefficient nearly double that observed in the low-temperature form.

Complementary density functional theory (DFT) calculations revealed that despite substantial thermal anisotropy, OXTB does not exhibit negative compressibility, indicating that NTE is driven primarily by thermal rather than mechanical properties. Elastic property analysis further demonstrated a preferential direction for energy propagation, aligned with the z-direction, facilitating rapid and collective strain release crucial for the thermosalient transition.

Sound propagation studies demonstrated a preferred pathway for energy transfer along the *z*-direction, which aligns with the direction of negative thermal expansion, facilitating rapid strain release during phase transition. These findings confirm that the thermosalient effect results from cooperative molecular motion, leading to an abrupt and energetic transformation driven primarily by the interplay of structural anisotropy and elastic properties, with anisotropic thermal expansion serving as the key prerequisite for thermosalience in molecular crystals.

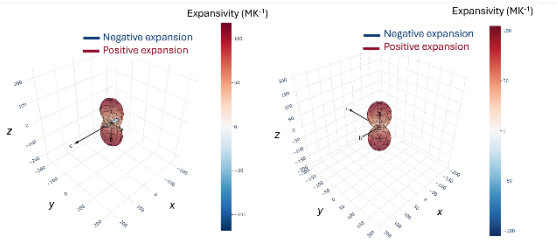

Figure 1. Thermal expansivity indicatrix of OXTB form A and B determined from *in-situ* variable-temperature powder X-ray diffraction.

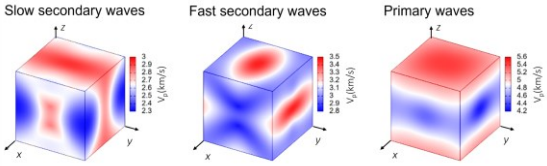

Figure 2. Phase velocity of waves through OXTB Form A.

References:

1. Klaser, T.; Popović, J.; Lončarić, I.; Skoko, Ž. Structural Evolution Leading to the Thermosalient Phase Transition of Oxitropium Bromide. *Molecules* **2025**, 30, 1107.
2. Skoko, Ž., Zamir, S., Naumov, P., Bernsten, J. The Thermosalient Phenomenon. "Jumping Crystals" and Crystal Chemistry of the Anticholinergic Agent Oxitropium Bromide. *J. Am. Chem. Soc.* **2010**, 132, 40, 14191–14202
3. Lončarić, I.; Popović, J.; Despoja, V.; Burazer, S.; Grgičević, I.; Popović, D.; Skoko, Ž. Reversible Thermosalient Effect of N′-2-Propylidene-4-hydroxybenzohydrazide Accompanied by an Immense Negative Compressibility: Structural and Theoretical Arguments Aiming toward the Elucidation of Jumping Phenomenon. *Cryst. Growth Des.* **2017**, 17, 8, 4445–4453

Presentation of SCAN d.o.o.

Jernej Žižek

SCAN, d.o.o., Preddvor, Breg ob Kokri 7, 4205 Preddvor

SCAN, d.o.o. is specialized in selling high quality laboratory instruments from the field of electron microscopy, vacuum technology and cryogenics.

We are distributor of the world best companies in these fields such as JEOL, Pfeiffer Vacuum and Cryopal.

Beside this we sell also other laboratory equipment and perform service support to our customers for all products, that we sell.

Analytical techniques that we support are as follows: Electron microscopes, EDS, WDS, SXES, XPS, AUGER, ED XRF, NMR and MS spectrometers.[1]

Vacuum program covers different oil and dry vacuum pumps, vacuum pumping systems, vacuum gauges, Quadrupole Mass Spectrometers, vacuum chambers in standard version and also as per customer's request.[2]

Cryogenic program includes different dewar containers for transport, storing liquid nitrogen (LIN) and liquid helium (LHE) and for storage of biological samples at liquid nitrogen temperature. Programmable freezing of samples from room temperature to liquid nitrogen temperature is also part of supply.[3]

Figure 1. X-ray fluorescence spectrometer.[1]

Figure 2. X-ray photoelectron spectrometer.[1]

Figure 3. Scanning electron microscope.[1]

References:

1. https://www.jeol.com/
2. www.pfeiffer-vacuum.com
3. www.cryopal.com

Application of MicroED to determining new macromolecular structures: the structure of Toll-like receptor adaptor MyD88 TIR-domain signalosome

Bostjan Kobe*[1], Max T. B. Clabbers[2], Yan Li[1], Laura C. Pacoste[2], Weixi Gu[1], Jeffrey D. Nanson[1,3], Thomas Ve[4], Hongyi Xu[2,5]

[1] School of Chemistry and Molecular Biosciences, The University of Queensland, Brisbane, QLD 4072, Australia
[2] Department of Materials and Environmental Chemistry, Stockholm University, 114 18 Stockholm, Sweden
[3] Gulbali Institute, Charles Sturt University, Wagga Wagga, NSW 2678, Australia.
[4] Institute for Biomedicine and Glycomics, Griffith University, Gold Coast, QLD 4215, Australia
[5] Research School of Chemistry, Australian National University, Canberra, ACT 2601, Australia

MyD88 and MAL are TIR (Toll/interleukin-1 receptor) domain-containing Toll-like receptor (TLR) adaptor proteins that signal downstream of TLRs to induce pro-inflammatory cytokine production. The TIR domain of MAL (MAL^{TIR}) forms filaments in vitro and induces formation of crystalline higher-order assemblies of the MyD88 TIR domain ($MyD88^{TIR}$). These crystals were too small for conventional X-ray crystallography, but were ideally suited to structure determination by microcrystal electron diffraction (MicroED), yielding a structure at 3 Å resolution. In parallel, we determined the same crystal structure using serial femtosecond crystallography (SFX) at 2.3 Å resolution, allowing a direct comparison of the MicroED and SFX techniques[1].

The structure of MAL-induced $MyD88^{TIR}$ microcrystals reveals a two-stranded higher-order assembly arrangement of TIR domains analogous to that seen previously in filaments of MAL TIR domains[2]. Mutagenesis showed that the $MyD88^{TIR}$ assembly interfaces are critical for TLR4 signalling in cells. These structures are consistent with the mechanism of signal transduction, distinctive in innate-immunity and cell-death pathways, termed SCAF (signalling by cooperative assembly formation)[3].

The TIR domain of TLR2, which is reported to signal as a heterodimer with either TLR1 or TLR6, also induces the formation of crystalline higher-order assemblies of $MyD88^{TIR}$ in vitro, whereas $TLR1^{TIR}$ and $TLR6^{TIR}$ do not. Using an improved data-collection protocol, the MicroED structure of $TLR2^{TIR}$-induced $MyD88^{TIR}$ microcrystals was determined at a higher resolution (2.85 Å) and with higher completeness (89%), compared with the structure of the MAL^{TIR}-induced $MyD88^{TIR}$ assembly. The data suggest that $TLR2^{TIR}$ and MAL^{TIR} interact with MyD88 in an analogous manner during signalling, nucleating $MyD88^{TIR}$ assemblies.

We will discuss the workflow for MicroED using macromolecular samples and the instrumentation used for MicroED work.

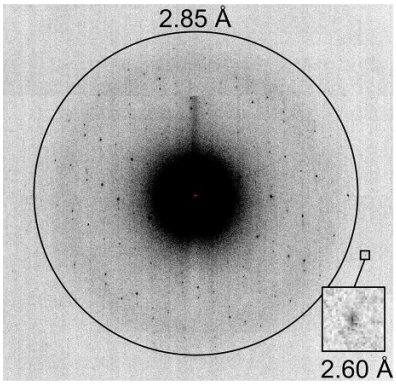

Figure 1: MicroED data collection of $TLR2^{TIR}$-induced $MyD88^{TIR}$ microcrystals. Diffraction pattern derived from a single microcrystal after exposure to a fluence of ~0.14 e/Å^2 (0º rotation), showing visual spots up to 2.6 Å resolution.

References:

1. Clabbers, M. T. B. et al, MyD88 TIR domain higher-order assembly interactions revealed by microcrystal electron diffraction and serial femtosecond crystallography. *Nat Commun* **2021**, *12*, 2578.
2. Ve, T. et al, Structural basis of TIR-domain-assembly formation in MAL- and MyD88-dependent TLR4 signaling. *Nat. Struct. Mol. Biol.* **2017**, *24*, 743-751.
3. Kobe, B. et al, Signalling by co-operative higher-order assembly formation: linking evidence at molecular and cellular levels. *Biochem J* **2025**, *482*, 275-294.
4. Li, Y et al, Microcrystal electron diffraction structure of Toll-like receptor 2 TIR-domain-nucleated MyD88 TIR-domain higher-order assembly. *Acta Crystallogr D Struct Biol* **2024**, *80*, 699-7123.

Synthesis and Characterization of Copper(I) Complexes with Chelating 2-(Methylthio)pyrimidines

Blaž Antonin,[1] Uroš Rapuš,[1] Jakob Kljun[1]

[1] Faculty of Chemistry and Chemical Technology, University of Ljubljana, Večna pot 113, *SI*-1000 Ljubljana, Slovenia

Copper(I) complexes with 2,2'-bipyridine or structurally related N,N-ligands have attracted significant attention due to their promising cytotoxicity useful in cancer treatment, as well as interesting optical and electrochemical properties[1]. As copper(I) in most cases exhibits tetrahedral geometry, stoichiometric ratio between metal and bidentate chelating ligand can be either 1:1 or 1:2. In the former case, additional co-ligands must also be present and can provide a way to improve and fine-tune certain properties. One of them is solubility. Nonpolar groups can increase lipophilicity and thus increase bioavailability of compound. Phosphine ligands are often used and can be further functionalized to change their polarity and how sterically demanding they are[2,3].

In this work, copper(I) complexes were prepared using 4-heteroaryl-2-(methylthio)pyrimidines, where heteroaryl groups were different heterocycles with nitrogen at position 2'. This provides a coordination mode analogous to 2,2'-bipyridine, as well as structural diversity.

Seven new complexes from two sets, using six bipyridine-like ligands, were synthesized and characterized by NMR, IR and UV-VIS spectroscopy, mass spectrometry and CHN elemental analysis. Crystal structures of five of them were determined by X-ray diffraction on single crystal.

To prepare the first series of compounds, cuprous chloride was reacted with the N,N-ligand and triphenylphosphine in stoichiometric ratio 1:1:1. The resulting complex was prepared and characterized with one ligand, but reaction was not as successful with other ligands. Single crystals of one additional complex were obtained but the low yield of the synthesis did not allow us a comprehensive physicochemical characterization. Synthesis of complexes with other ligands was also unsuccessfully attempted. The main issue is, except in the first case, the preferential formation of insoluble binuclear complex of cuprous chloride and triphenylphosphine. Both obtained crystal structures have typical tetrahedral geometry around copper ion with τ_4 factor close to 0,9.

In the second set of compounds ligands are bound to central ion in stochiometric ration 2:1. This can be achieved by using a salt with non-coordinating anion, such as PF_6^-. The geometry of the complexes was shown to be very deformed, to the point where it's closer to trigonal pyramidal than tetrahedral for some complexes.

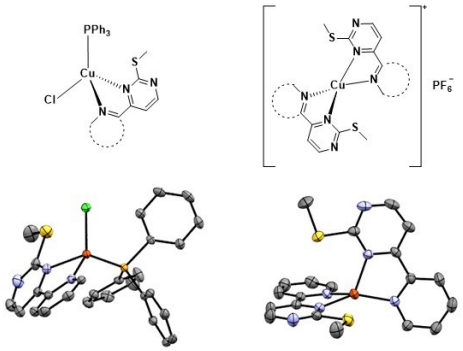

Figure 1: Schemes and example of crystal structures of prepared complexes in stoichiometric ratio 1:1 (left) and 1:2 (right). Thermal ellipsoids were drawn at 50% probability level and hydrogen atoms were omitted.

References:

1. Constable, E. C.; Housecroft, C. E. The Early Years of 2,2′-Bipyridine—A Ligand in Its Own Lifetime. *Molecules* **2019**, 24 (21).
2. Alvarez, N.; Noble, C.; Torre, M. H.; Kremer, E.; Ellena, J.; Peres de Araujo, M.; Costa-Filho, A. J.; Mendes, L. F.; Kramer, M. G.; Facchin, G. Synthesis, Structural Characterization and Cytotoxic Activity against Tumor Cells of Heteroleptic Copper(I) Complexes with Aromatic Diimines and Phosphines. *Inorg. Chim. Acta*. **2017**, 466, 559–564.
3. Babgi, B. A.; Mashat, K. H.; Abdellattif, M. H.; Arshad, M. N.; Alzahrani, K. A.; Asiri, A. M.; Du, J.; Humphrey, M. G.; Hussien, M. A. Synthesis, Structures, DNA-Binding, Cytotoxicity and Molecular Docking of $CuBr(PPh_3)$(Diimine). *Polyhedron* **2020**, 192, 114847.

Funding information: We are grateful for the financial support from the program grant P1-0175 of the Slovenian Research and Innovation Agency (ARIS). The authors also acknowledge the support of the Centre for Research Infrastructure at the University of Ljubljana, Faculty of Chemistry and Chemical Technology, which is part of the Network of Research and Infrastructural Centres UL (MRIC UL) and is financially supported by the Slovenian Research and Innovation Agency (ARIS; Infrastructure programme No. I0-0022).

Evolution of Phase Composition in Recycled Materials During Hydration and Carbonation

Vesna Zalar Serjun*,[1] Anton Meden,[2] Romana Cerc Korošec,[2] Marta Počkaj,[2] Primož Oprčkal[1]

[1] Slovenian National Building and Civil Engineering Institute, Dimičeva ulica 12, *SI*-1000 Ljubljana, Slovenia
[2] Faculty of Chemistry and Chemical Technology, University of Ljubljana, Večna pot 113, *SI*-1000 Ljubljana, Slovenia

Industrial by-products are increasingly considered valuable alternatives to primary raw materials. In the construction sector, where vast quantities of resources are consumed, their use aligns with the goals of the European Green Deal. Recycled materials that exhibit binder-like properties or can act as cement supplements are particularly important. Two key properties that support their utilization are hydraulic activity and the potential for CO_2 capture. Hydraulic activity enables their application as binders, while mineral carbonation capacity provides a pathway to reduce the carbon footprint—both by sequestering CO_2 and substituting conventional binders.

This study investigates recycled materials from combustion and steel production processes, focusing on their hydraulic reactivity and CO_2 capture potential. Various ash types from combustion and steel refining slags were hydrated under different water-to-binder ratios, and curing was monitored over time. Carbonation experiments were carried out under semi-dry conditions with varying CO_2 concentrations. Special attention was given to changes in phase composition as influenced by moisture, CO_2 levels, and curing duration.

Nearly all investigated industrial by-products exhibit hydraulic activity, with the lowest hydration activity observed in ashes not collected by electrostatic precipitation. Paper ashes, due to their high calcareous phase content, were the most reactive, while the amorphous phase content in coal and co-combustion ashes influenced their hydration mechanisms. Higher humidity improve the carbonation degree in larger extent than higher concentration of CO_2 itself. Carbonation of different hydration products was evidently identified. Figure 1 (a) show that different phases form in ash treated under varying CO_2 and moisture contents. The XRD analysis over time reveals different mechanisms in the two carbonation chambers used (Fig 1 b and c).

The results show that hydration and carbonation processes occur simultaneously and can influence each other. The interactions between these two mechanisms can be complex under curing conditions. While hydration products such as $Ca(OH)_2$ and Ettringite are susceptible to carbonation, the primary carbonation product—$CaCO_3$—can, in turn, affect both the kinetics of hydration and the composition of hydration products. Therefore, a comprehensive understanding of the overall hardening process is essential. Future work will focus on identifying and clarifying the key influencing factors.

(a)

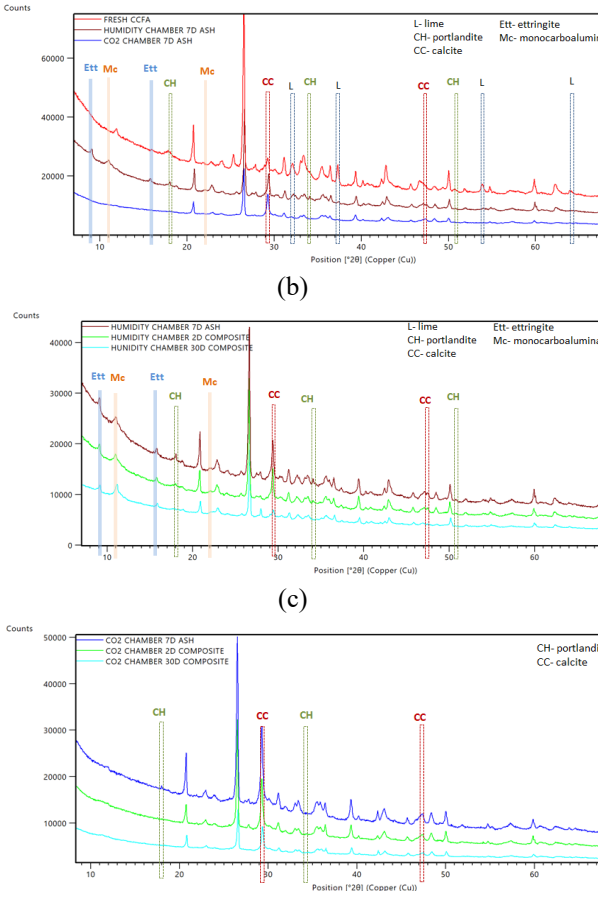

Figure 1: (a) XRD patterns showing the formation of different phases in ash treated under varying CO_2 concentrations and moisture contents. (b, c) Time-dependent XRD analysis indicating different carbonation mechanisms in the two chambers used.

Funding information: P2-027 and J1-4413, Slovenian Research and Innovation Agency (ARIS), Slovenia; JTC-2021_196, ERA-MIN3, EU.

Vaterite-calcite transformation mediated by micro- and nanoplastics addition

Jasminka Kontrec,[1] Branka Njegić Džakula,[1] Nives Matijaković Mlinarić,[1] Marijan Marciuš,[1] Nenad Tomašić[2]*

[1] Rudjer Bošković Institute, Bijenička cesta 54, HR-10000 Zagreb, Croatia
[2] Faculty of Science, University of Zagreb, Horvatovac 102a, HR-10000 Zagreb, Croatia

Occurrence of micro- and nanoplastics in natural environments is of great concern due to their influence on living organisms. Effect of various microplastics on calcium carbonate precipitation was studied using X-ray powder diffraction. Calcium carbonate samples were prepared by precipitation of vaterite in water solution, and letting it transform to calcite for 10 days. Several sample batches were prepared by addition of various microplastics in order to investigate their influence on calcium carbonate phase transition: polyethylene (PE), polystyrene (PS and PS-COOH) and polymethyl methacrylate (PMMA), with additional diversification in particle size (1.5 μm, 1 μm and 300 nm). Samples were further treated by humic acid (HA). Calcite *104* reflection parameters were used as an estimate of calcite crystallinity (*d*-value, full width at half maximum, and peak area), in order to indicate completeness of vaterite-calcite transformation.

All three types of microplastics presented an influence on vaterite-calcite transformation. This could be viewed in light of kinetics modification during vaterite-calcite transformation, which in aquatic solution has been described by dissolution-reprecipitation mechanism[1]. In general, PS microplastics exhibit the greatest influence on crystallization of calcite from starting vaterite-dominant mixture. In the case of 1.5 μm PS this effect is more pronounced if PS is treated with HA. With 300 nm untreated PS particles present in the carbonate solution, this effect is even more pronounced. In the case of PS-COOH, and particularly PS-COOH treated with HA, calcite *104* reflection parameters are approaching those of the blank calcite sample. In presence of 1.5 μm PE and PMMA, change of calcite *104* reflection parameters is less pronounced. In all the studied cases microplastics seem to affect the two-step mechanism of vaterite-calcite transition, particularly calcite reprecipitation. The change in *104* reflection parameters when compared to those of the blank sample might be a result of ordering in calcite crystal structure. The observed lowering of crystal structure order in calcite in presence of microplastics could be attributed to retardation of vaterite-calcite transformation. Also, newly precipitating calcite could have found a new crystallization substrate (microplastics) along with dissolving vaterite and freshly formed calcite crystals. Perhaps, this can be related to the splitting of *104* reflection into two discrete maxima observed in the sample containing PS microplastics treated with HA (Figure 1), which might be seen as an occurrence of two-generation calcite. To confirm this phenomenon, several experiment repetitions with precipitation parameters varied are required. It was observed that the second step of vaterite-calcite transformation, i.e. reprecipitation of calcite, is ten times slower than the first step[2], and the rate of the whole mechanism is controlled by surface area of crystallizing calcite, also suggested in calcite seeded experiments[3]. The smaller the area the smaller the rate of crystallization, so for the same time of calcite maturation (10 days) the samples obtained various degree of calcite crystallinity depending on the microplastics involved.

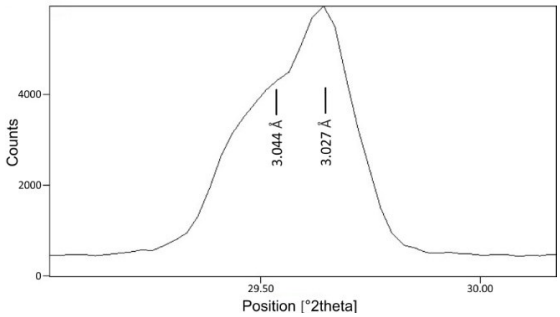

Figure 1: Splitting of *104* calcite reflection in presence of 1.5 μm PS treated with HA

References:

1. Spanos, N., Koutsoukos, P. G., The transformation of vaterite to calcite: effect of the conditions of the solutions in contact with the mineral phase. *Journal of Crystal Growth* **1998**, *191*, 783-790.
2. Rodriguez-Blanco, J. D., Shaw, S., Benning, L. G., The kinetics and mechanisms of amorphous calcium carbonate (ACC) crystallization to calcite, via vaterite. *Nanoscale* **2011**, *3*, 265-271.
3. Ogino, T., Suzuki, T., Sawada, K., The formation and transformation mechanism of calcium carbonate in water. *Journal of Crystal Growth* **1990**, *100*, 159-167.

Funding information: The Adris Foundation – program Knowledge and Discovery

Copper(II) compounds with short α,ω-dicarboxylates

Bojan Kozlevčar*,[1] Andrej Pevec,[1]

[1] Faculty of Chemistry and Chemical Technology, University of Ljubljana, Večna pot 113, *SI*-1000 Ljubljana, Slovenia

A rational design synthetic path is often used in coordination chemistry to obtain a suitable product. Thus, specific metal ions along with terminal (L) and bridging (μ-L) ligands in appropriate solvent may be selected carefully.

Often copper(II) is seen in these compounds with a pyridine type molecule as a neutral ligand besides a dianionic ligand as a potential bridge and a net-neutrality provider. Copper(II) species are namely user friendly to obtain crystalline products and such compounds may serve also as magnetic material and enzyme mimetic or catalytic purposes already in water solutions at regular room conditions.

Usually is the bridging ligand the most decisive pick to isolate a suitable compound with more than one metal center. These bridges mey be aleady water molecules, hydroxyde or chloride anions, however the additional ligands then regulate more the geometry of the coordination sphere. The oxalate dianion prooved as very useful, as being double bidentate subsequently enabling a strong antiferromagnetic coupling of both bridged copper(II) there[1]. An application of a similar dicarboxylate, having a short CH_2 spacer in $(OOC(CH_2)_nCOO)^{2-}$, n = 1-4, shows different bridges as sterical factors have their role as well[2,3].

Herein, we present several copper(II) compounds with terminal neutral pyridine type ligand (L) along with α,ω-dicarboxylate bridging dianions $(μ\text{-}L)^{2-}$ in $[Cu(μ\text{-}L)(L)_2]$ species. These compounds show bridging potential of α,ω-dicarboxylates in several, though limited options. The starting compounds at basic room temperature conditions clearly enable some controlling variations to obtain certain types of the final solid products. Isolated compounds are either dinulear (Figure 1) or polymeric (Figure 2). Their IR spectra show strong resemblance with almost no distinction due to the different type of the structure. The amino moiety plays a distinctive role connecting intramolecullarly the carboxylate group via H-bond in each of these compounds. As seen already from the simlar previously reported compounds, a shorter bridge favourize a dinuclear structure, while a longer bridge points towards a polynuclear product. Tentative temeperature dependant magnetic measurements suggest no stronger magnetic coupling is expected for these compounds, thus differently as seen for the related oxalates[1].

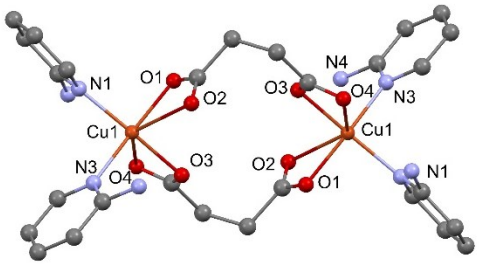

Figure 1: The dinuclear copper succinate compound with 2-aminopyridine. H-atoms are omitted for clarity.

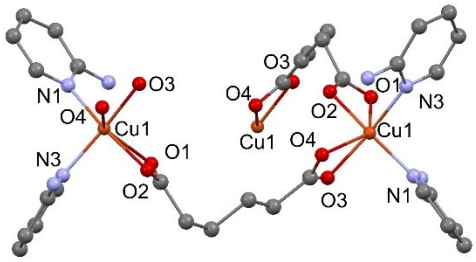

Figure 2: The polymeric copper adipato compound with 2-aminopyridine. H-atoms are omitted for clarity.

References:

1. Castro, I.; Calatayud, M.L.; Orts-Arroyo, M.; Marino, N.; De Munno, G.; Lloret, F.; Ruiz-García, R.; Julve, M.; Oxalato as polyatomic coordination center and magnetic coupler in copper(II)-polypyrazole inverse polynuclear complexes and coordination polymers. *Coord. Chem. Rev.*, **2022**, 471, 214730.
2. Lah, N.; Clérac, R.; Cu(II) coordination polymers incorporating 3-aminopyridine and flexible aliphatic dicarboxylate ligands: Synthesis, structure and magnetic properties. *Polyhedron*, **2009**, *28*, 2466-2472.
3. Ghosh, A.K.; Ghoshal, D.; Zangrando, E.; Ribas, J.; Ray Chaudhuri, N.; Syntheses, Crystal Structures, and Magnetic Properties of Metal−Organic Hybrid Materials of Cu(II): Effect of a Long Chain Dicarboxylate Backbone, and Counteranion in Their Structural Diversity. *Inorg. Chem.*, **2007**, *46*, 3057−3071.

Funding information: P1-0175, ARIS (Public agency for research activity RS), Slovenia, and The Centre for Research Infrastructure at the Faculty of Chemistry and Chemical Technology UL, Slovenia.

Characterization of the $LaTaTiO_6$–$La_{1/3}TaO_3$ tie line in the system La_2O_3–Ta_2O_5–TiO_2 by X-ray powder diffraction

Nadja Ziherl*,[1] Srečo D. Škapin,[2] Matjaž Spreitzer[2] and Amalija Golobič[1]

[1] Faculty of Chemistry and Chemical Technology, University of Ljubljana, Večna pot 113, *SI*-1000 Ljubljana, Slovenia
[2] Jožef Stefan Institute, Jamova 39, 1000 Ljubljana, Slovenia

In the search for new ceramics with improved dielectric properties, we investigate the ternary system La_2O_3–Ta_2O_5–TiO_2. Here we report characterization of several samples from $LaTaTiO_6$–$La_{1/3}TaO_3$ tie line, which was performed in order to determine the compositional range of the $La_{1/3}TaO_3$ based solid solubility and check the existence of solid solubility based on the $LaTaTiO_6$.

The samples were prepared by conventional solid-state reaction technique from the oxides (compositions given in Table 1) with firing at least two times in tube furnace at 1350°C with intermittent air quenching, crushing and homogenization. X-ray powder diffractograms were measured at room temperature by D4, Bruker (CuK_α) and by PANalytical X'Pert PRO MPD diffractometer ($CuK_{\alpha1}$), respectively.

Table 3: Initial reaction composition of **S**1 to **S7**.

Sample	La_2O_3 [mol %]	Ta_2O_5 [mol %]	TiO_2 [mol %]
S1	25	64	11
S2	25	60	15
S3	25	58	17
S4	25	40	35
S5	25	30	45
S6	25	27	48
S7	25	25	50

Samples **S1** and **S2** are solid solution of $La_{2/3}TiO_3$ and $La_{1/3}TaO_3$, with formula $La_{(1+x)/3}Ti_xTa_{1-x}O_3$ with x 0.08 and 0.11, respectively. As was confirmed by Rietveld refinement they are isostructural with $La_{1/3}TaO_3$, which has a defect perovskite structure with tetragonal *P*4/*mmm* space group. Compared to the well-known cubic perovskite structure of ABO_3, in $La_{1/3}TaO_3$ Ta^{5+} are on B sites, octahedrally coordinated by six O^{2-}, while La^{3+} are

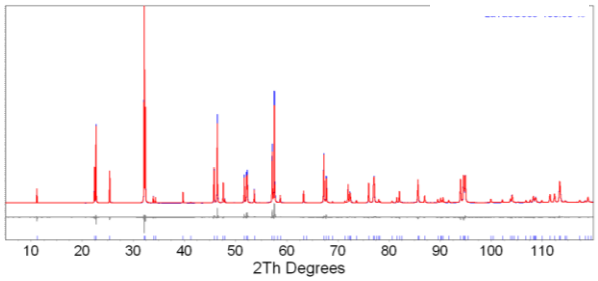

Figure 1: Final Rietveld plot for $La_{0,37}Ta_{0,89}Ti_{0,11}O_3$, **S2**.

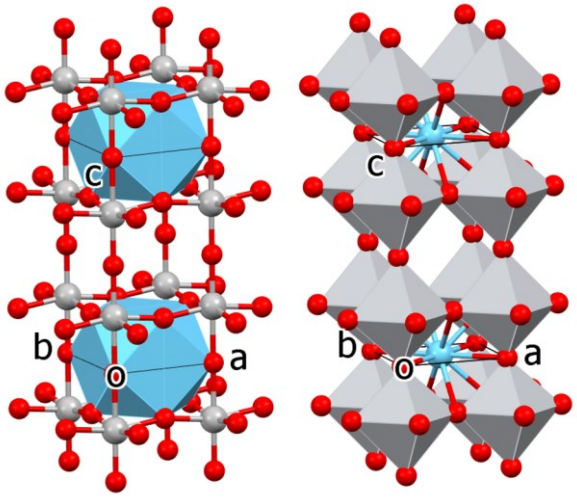

Figure 2: Structure of $La_{0,37}Ta_{0,89}Ti_{0,11}O_3$, **S2**; blue: La^{3+}, red: O^{2-} and gray Ti^{4+}/Ta^{5+}

on every second A site along the *c* axis with the occupancy of 67%, leaving the remaining half of them vacant and causing doubling of the *c* cell edge. In solid solution **S1** and **S2** O and B sites remain to be fully occupied. Ta^{5+} and Ti^{4+} are randomly distributed on B site with the occupancy of 8 and 11% of Ti^{4+} in **S1** and **S2**, respectively. The occupancy of La^{3+} site is higher: 72 and 74 % in **S1** and **S2**, respectively. In the final Rietveld refinement 17 parameters (unit cell, positional and displacement parameters, zero error, scale factor, background, crystalline size and micro-strain parameters) were refined. Final Rietveld refinement plot for **S2** with Rwp = 9,67%, is shown in Figure 1. Drawing of structure of **S2** is presented in Figure 2: La^{3+} is coordinated by twelve O^{2-} in a shape of a cuboctahedron with bond lengths 2.680-2.763 Å and Ti^{4+}/Ta^{5+} octahedrally with six O^{2-} with bond lengths 1.887-2.073 Å, respectively.

S2 is the end composition of solid solution. **S3**, **S4**, **S5** and **S6** consist of two phases: $La_{0,37}Ta_{0,89}Ti_{0,11}O_3$ and orthorhombic $LaTaTiO_6$. **S7** consists of $LaTaTiO_6$ only. This means that there is no solid solubility on the $LaTaTiO_6$ side of the $LaTaTiO_6$–$La_{1/3}TaO_3$ tie line.

Acknowledgement: Financial support of the Slovenian Research and Innovation Agency is gratefully acknowledged (Grants P2-0091 and P1-0175).

Crystal Structures and Solution Speciation Studies of Rhenium(I)-Tricarbonyl Complexes of Bipyridine Analogs

Jakob Kljun[1], Uroš Rapuš[1], Tamás Pivarcsik[2], Éva A. Enyedy[2], Iztok Turel[1]

[1] Faculty of Chemistry and Chemical Technology, University of Ljubljana, Večna pot 113, *SI*-1000 Ljubljana, Slovenia
[2] Department of Molecular and Analytical Chemistry, Interdisciplinary Excellence Centre, University of Szeged, Dóm tér 7-8., H-6720 Szeged, Hungary

Recently,[1] we reported the synthesis and characterization of twelve novel rhenium(I) complexes with the general formula *fac*-$[Re(CO)_3(NN)X]^{n+}$ where (NN) is a 2,2'-bipyridine analogue ligand, X = Cl^-, Br^- or H_2O and n = 0 or 1, focusing on their speciation in aqueous solution. The organorhenium complexes prepared are stable in a wide pH range in aqueous solution and no release of the bidentate ligands or the carbonyl ligands was observed. The stability of the complexes in various biologically relevant matrices such as the cell culture medium and real blood serum, was also demonstrated.

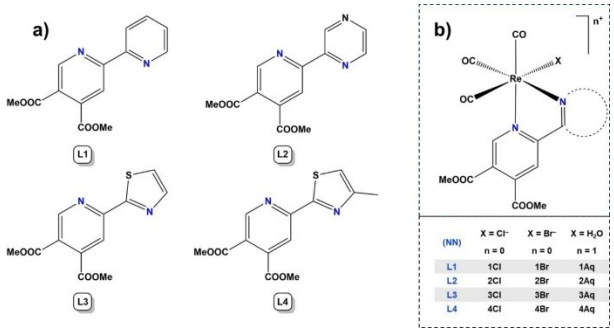

Figure 1: a) Structure of ligands and b) general structure of the twelve rhenium(I)-tricarbonyl complexes synthesized.

However, simultaneous substitution of the chlorido or bromido ligand by a water molecule and slow hydrolysis of the ester bonds in the ligands were observed, affecting both the solubility and lipophilicity of the compounds. The aqua complexes became more lipophilic in the presence of chloride ions, while the hydrophilicity was increased significantly with time due to the hydrolysis of the ester bonds, which probably contributed to their moderate biological activity. The results also showed kinetically hindered aqueous solvation of the halido complexes and low chloride ion affinity of the aqua complexes. The deprotonation of the coordinated aqua ligand in the complexes occurs in the pH = 7 – 10 range, leading to significant formation (18 – 30%) of hydroxido species at pH = 7.4. The halido complexes showed somewhat higher toxicity on human colon adenocarcinoma cancer cells Colo205 and Colo320 with IC50 values in the concentration range between 60 and 99 μM than the corresponding aqua complexes (IC_{50} > 100 μM). In all cases, no antibacterial effect was observed (MIC > 100 μM), but some of the complexes showed moderate antiviral activity (IC_{50} ~50 μM) on *Herpes simplex* virus 2.

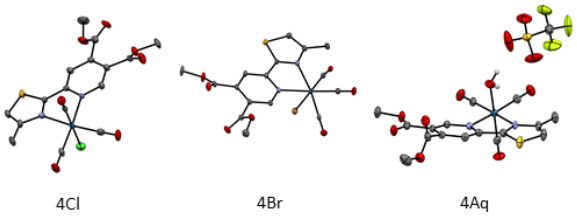

Figure 2: Crystal structures of the representative chlorido, bromido, and aqua complexes **4Cl**, **4Br**, and **4Aq**. Thermal ellipsoids are drawn at 50% probability level. All hydrogens except H_2O hydrogen atoms in aqua complexes are omitted.

References:

1. Pivarcsik, T.; Kljun, J.; Rodriguez, S. C.; Cortéz Alcaraz, D.; Rapuš, U.; Nové, M.; Várkonyi, E. F. Nyári, J.; Bogdanov, A.; Spengler, G.; Turel, I.; Enyedy, É. A.; Structural and Solution Speciation Studies on *fac*-Tricarbonylrhenium(I) Complexes of 2,2′-Bipyridine Analogues, *ACS Omega* **2024**, *9*, 44601-44615.

Funding information: We are grateful for the financial support from the program grant P1-0175 of the Slovenian Research and Innovation Agency (ARIS). The authors also acknowledge the support of the Centre for Research Infrastructure at the University of Ljubljana, Faculty of Chemistry and Chemical Technology, which is part of the Network of Research and Infrastructural Centres UL (MRIC UL) and is financially supported by the Slovenian Research and Innovation Agency (ARIS; Infrastructure programme No. I0-0022).

Xenon difluoride as a hydrogen-bond acceptor

Erik Uran*,[1,2] Matic Lozinšek[1,2]

[1] Jožef Stefan Institute, Jamova cesta 39, 1000 Ljubljana, Slovenia
[2] Jožef Stefan International Postgraduate School, Jamova cesta 39, 1000 Ljubljana, Slovenia

Xenon difluoride (XeF_2) is a linear, centrosymmetric, nonpolar molecule that is highly soluble in the polar protic solvent anhydrous HF,[1] owing to FXeF···FH hydrogen-bonding interactions. Moreover, reactions involving XeF_2 are often catalyzed by HF due to the formation of hydrogen bonds and polarization of the xenon–fluorine bond.[2]

The hydrogen-bonding ability of XeF_2 has not been systematically studied or utilized for cocrystal formation. Only a few examples of XeF_2 acting as a hydrogen bond acceptor in the solid state have been reported. These include $(H_3O)[AsF_6]\cdot 2XeF_2$,[2] $HNO_3\cdot XeF_2$[3] and $[Cd(FH)_2(XeF_2)(TaF_6)_2]$,[4] in which either OH···F(Xe) or HF···F(Xe) hydrogen bonds are observed. Another example is $(CF_3C(OH)NH_2)[AsF_6]\cdot XeF_2\cdot x$HF cocrystal,[5] where the presence of O/N−H···F(Xe) hydrogen bonds was inferred solely from Raman spectroscopy.

To explore the potential of XeF_2 as O/N−H···F(Xe) hydrogen-bond acceptor, protonated trifluoroacetamide, pentafluoropropionamide and heptafluorobutyramide were reacted with XeF_2 at low temperatures in aHF, yielding $(RC(OH)NH_2)[AsF_6]\cdot XeF_2$ cocrystals.

In the crystal structure of $(F_3CC(OH)NH_2)[AsF_6]\cdot XeF_2$ (Figure 1), both O−H···F(Xe) and N−H···F(Xe) hydrogen bonds are observed, the latter being crystallographically characterized for the first time. In contrast, the crystal structures of $(F_5C_2C(OH)NH_2)[AsF_6]\cdot XeF_2$ and $(F_7C_3C(OH)NH_2)[AsF_6]\cdot XeF_2$ exhibit only N−H···F(Xe) hydrogen bonding, whilst the $C{=}OH^+$ groups form hydrogen bonds with $[AsF_6]^-$ anions. The (O)H···F(Xe) hydrogen bond in $(F_3CC(OH)NH_2)[AsF_6]\cdot XeF_2$ (2.545(1) Å) is shorter than the corresponding hydrogen bonds in $(H_3O)[AsF_6]\cdot 2XeF_2$ (2.571(3) Å)[2] and $HNO_3\cdot XeF_2$ (2.690(1) Å).[3] By contrast, the N−H···F(Xe) hydrogen bonds in studied cocrystals are typically longer (2.667(6)–2.7875(14) Å). In all compounds, the cocrystallized XeF_2 molecules exhibit slight deviations from the symmetrical linear geometry observed in pure XeF_2, which is also corroborated by low-temperature Raman spectroscopy.

Overall, these findings demonstrate that, under suitable conditions, XeF_2 can serve as a reliable hydrogen bond acceptor, thereby opening new avenues in the crystal engineering of cocrystals based on the noble-gas compounds.

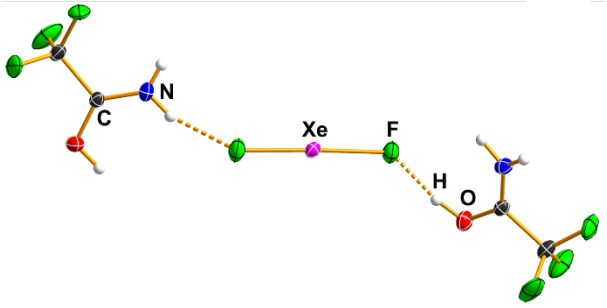

Figure 1: Hydrogen bonding of XeF_2 observed in the crystal structure of $(F_3CC(OH)NH_2)[AsF_6]\cdot XeF_2$ cocrystal. Atoms are shown with the 50% probability ellipsoids. Hydrogen atoms are represented as spheres of arbitrary radius.

References:

1. Tramšek, M.; Žemva, B., Synthesis, Properties and Chemistry of Xenon(II) Fluoride. *Acta. Chim. Slov.* **2006**, *53*, 105–116.
2. Tius, M. A., Xenon difluoride in synthesis. *Tetrahedron* **1995**, *51*, 6605–6634.
3. Gerken, M.; Moran, M. D.; Mercier, H. P. A.; Pointner, B. E.; Schrobilgen, G. J.; Hoge, B.; Christe, K. O.; Boatz, J. A., On the XeF^+/H_2O System: Synthesis and Characterization of the Xenon(II) Oxide Fluoride Cation, $FXeOXeFXeF^+$. *J. Am. Chem. Soc.* **2009**, *131*, 13474–13489.
4. Moran, M. D.; Brock, D. S.; Mercier, H. P. A.; Schrobilgen, G. J., $Xe_3OF_3^+$, a Precursor to a Noble-Gas Nitrate; Syntheses and Structural Characterizations of $FXeONO_2$, $XeF_2\cdot HNO_3$, and $XeF_2\cdot N_2O_4$. *J. Am. Chem. Soc.* **2010**, *132*, 13823–13893.
5. Lozinšek, M., *PhD Thesis*, University of Ljubljana, **2013**.
6. Schrobilgen, G. J.; Whalen, J. M., The Xenon-Oxygen-Bonded Cation $CF_3C(OXeF)NH_2^+$ and Related $CF_3C(OH)NH_2^+AsF_6^-$ and $CF_3C(OH)$-$NH_2^+AsF_6^-\cdot XeF_2\cdot x$HF Salts. Their Syntheses and Characterization by Multi-NMR and Raman Spectroscopy. *Inorg. Chem*. **1994**, *33*, 5207–5218.

Funding information: European Research Council (ERC) under the European Union's Horizon 2020 Research and Innovation Programme (Starting Grant 950625)

Crystal structure determination of reactive compounds by 3D electron diffraction

Matic Lozinšek*,[1,2] Klemen Motaln,[1,2] Kshitij Gurung,[3] Petr Brázda,[3] Erik Uran,[1,2] Kristian Radan,[1] Mirela Dragomir,[1,2] Lukaš Palatinus[3]

[1] Jožef Stefan Institute, Jamova cesta 39, 1000 Ljubljana, Slovenia
[2] Jožef Stefan International Postgraduate School, Jamova cesta 39, 1000 Ljubljana, Slovenia
[3] Institute of Physics of the Czech Academy of Sciences, Na Slovance 1999/2, Prague 8, 18221, Czechia

3D electron diffraction (3D ED) is a powerful "new" tool in the chemical crystallographer's characterization toolkit[1]. The determination of crystal and molecular structures from powder samples with nanometer-sized crystallites opens exciting new possibilities. It enables rapid structural elucidation of a sample, bypassing the often arduous crystallization step, and allows crystal structure determination of compounds for which suitably sized crystals for single-crystal X-ray diffraction (SCXRD) cannot be grown. While a broad range of compounds have been characterized by 3D ED, air-sensitive and highly reactive compounds have received considerably less attention[2].

To enable the study of highly reactive, strongly oxidizing, and moisture-sensitive noble-gas compounds by 3D ED, we developed a specialized cryotransfer sample handling and preparation method[3,4].

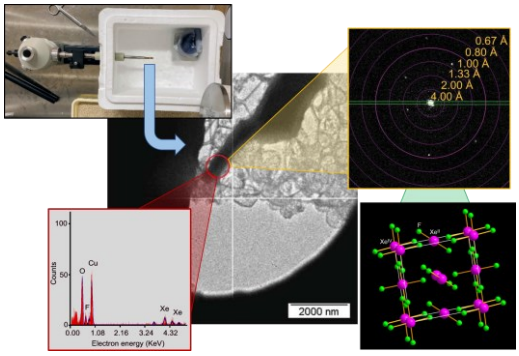

Figure 1: A developed cryotransfer method[4] was employed for the crystal structure determination of reactive, moisture-sensitive xenon fluorides using 3D ED.

This method prevents sample degradation during the transfer into a transmission electron microscope (Figure 1)[4]. We tested this technique by determining the crystal structures of several reactive xenon compounds: XeF_2, XeF_4, $XeF_2{\cdot}XeF_4$, $3XeF_2{\cdot}2MnF_4$, $XeF_2{\cdot}MnF_4$, and $XeF_2{\cdot}2MnF_4$. The 3D ED structures were cross-validated with SCXRD results, demonstrating the reliability of the methodology. Subsequently, previously unknown crystal structures of $XeF_2{\cdot}2PdF_4$ and $XeF_2{\cdot}2PtF_4$ were determined using this approach[5]. Furthermore, strongly oxidizing silver(II) compounds were also successfully studied.

The developed methodology opens new possibilities for the structural investigation of air-sensitive compounds by 3D ED.

References:

1. Gemmi, M.; Mugnaioli, E.; Gorelik, T. E.; Kolb, U.; Palatinus, L.; Boullay, P.; Hovmöller, S.; Abrahams, J. P., 3D Electron Diffraction: The Nanocrystallography Revolution. *ACS Cent. Sci.* **2019**, *5*, 1315–1329.
2. Jones, C. G.; Asay, M.; Kim, L. J.; Kleinsasser, J. F.; Saha, A.; Fulton, T. J.; Berkley, K. R.; Cascio, D.; Malyutin, A. G.; Conley, M. P.; Stoltz, B. M.; Lavallo, V.; Rodríguez, J. A.; Nelson, H. M., Characterization of Reactive Organometallic Species via MicroED. *ACS Cent. Sci.* **2019**, *5*, 1507–1513.
3. Motaln, K.; Gurung, K.; Brázda, P.; Kokalj, A.; Radan, K.; Dragomir, M.; Žemva, B.; Palatinus, L.; Lozinšek, M., Reactive Noble-Gas Compounds Explored by 3D Electron Diffraction: XeF_2–MnF_4 Adducts and a Facile Sample Handling Procedure. *ACS Cent. Sci*. **2024**, *10*, 1733–1741.
4. Gurung, K.; Uran, E.; Motaln, K.; Brázda, P.; Radan, K.; Lozinšek, M.; Palatinus, L., A simple cryotransfer method for 3D electron diffraction measurements of highly sensitive samples. *J. Appl. Cryst.* **2025**, *58*, 1079–1084.
5. Motaln, K.; Gurung, K.; Dragomir, M.; Kurzydłowski, D.; Palatinus, L.; Lozinšek, M., Crystal Structures of $XeF_2{\cdot}2PtF_4$ and $XeF_2{\cdot}2PdF_4$ Determined by 3D Electron Diffraction and Structural Models of $XePtF_6$. *Inorg. Chem.* **2025**, *64*, submitted.

Funding information: This work was funded by the Slovenian Research and Innovation Agency (N1-0189) and the Czech Science Foundation (21-06744K) in the form of a joint research project within the Central European Science Partnership and by the European Research Council (ERC Starting Grant 950625), under the European Union's Horizon 2020 Research and Innovation Programme.

Elucidation of the mechanism of elastic banding in crystalline coordination polymers with atomic-level precision

Marijana Đaković*,[1]

[1] Faculty of Science, University of Zagreb, Horvatovac 102a, *HR*-10000 Zagreb, Croatia

Mechanically adaptive crystals have garnered attention in recent years due to their ability to change in response to heat, light, and mechanical forces. These materials have numerous potential applications, including use in optical devices, electronics, wearable devices, and soft robotics. Understanding how these materials work is crucial for using them in new devices. Recently, we investigated various types of flexible crystals composed of one-dimensional coordination polymers (CPs). We found that they possess great adaptive qualities and that intermolecular interactions significantly affect their mechanical responses, resulting in flexibility and elasticity. To better understand how these materials bend, we aim to investigate the mechanisms behind their bending abilities and how intermolecular interactions influence their behaviour.

In this work, we focus on two novel one-dimensional coordination polymers, $[Cd(\mu\text{-}X)_2L_2]_n$ (where X = Cl or Br, and L = pyrazinamide), which display mechanically stimulated elastic flexibility. While various methods were employed to explore their elastic properties (such as three-point bending tests, atomic force microscopy (AFM), and computational methods), our primary focus was on understanding the atomic-level changes that occur during bending via a structural approach. By mapping the structural changes at the apex of the bent crystal using micro-focus synchrotron radiation, we identified the first mechanism of elastic bending in coordination polymer (CP) crystals. This mechanism stands apart from previously reported cases, such as flexible molecular crystals under mechanical stress or one-dimensional CP crystals that deform under quasi-hydrostatic pressure. Under mechanical stress, both the one-dimensional structural spine and the ligands adapt effectively. As the spine presents spring-like mobility upon transitioning from the interior to the exterior of the bent crystal, the ligands rotate towards linearity with the bending faces (Figure 1). Moreover, by integrating our experimental results with computational efforts, we established clear connections between structural changes along the bending faces and the strength of the weakest intermolecular bonds.

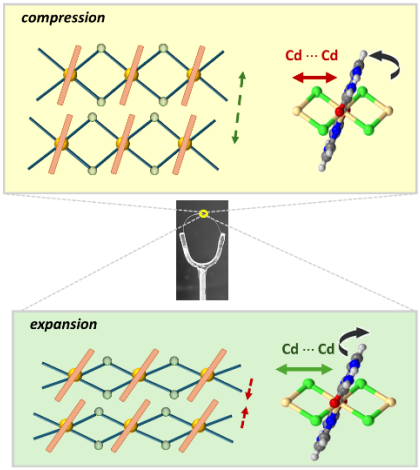

Figure 1: A schematic of the atomic-level changes at the compression and expansion side of bent crystal of $[CdCl_2(pza)_2]_n$, deduced by μ-SCXRD synchrotron mapping experiments.

References:

1. Wei, C., Li, L., Zheng, Y., Wang, L., Ma, J., Xu, M., Lin, J., Xie, L., Naumov, P., Ding, X., Feng, Q. & Huang, W. *Chem. Soc. Rev.* **2024**, *53*, 3687.
2. Đaković, M., Borovina, M., Pisačić, M., Aakeröy, C. B., Soldin, Ž., Kukovec, B.-M. & Kodrin, I. *Angew. Chem. Int. Ed*. **2018**, *57*, 14801.
3. Pisačić, M., Biljan, I., Kodrin, I., Popov, N., Soldin, Ž. & Đaković, M. *Chem. Mater*. **2021**, *33*, 3660.
4. Pisačić, M., Kodrin, I., Biljan, I., Đaković, M. *CrystEngComm* **2021**, *23*, 7072.
5. Pisačić, M., Kodrin, I., Trninić, A. Đaković, M. *Chem. Mater.* **2022**, *34*, 2439.
6. Đaković, M., Pisačić, M., Borovina, M., Kodrin, I., Kenđel, A., Frey, T., *JACS*, **2025**, *accepted.*

Funding information: This work has been fully supported by the Croatian Science Foundation under Project IP-2019-04-1242. We gratefully acknowledge the Paul Scherrer Institut, Villigen, CH, for the provision of synchrotron radiation beamtime at beamline X06SA (PXI) at the SLS.

Coordination of xenon(II) fluorides to alkali metal cations

Klemen Motaln*,[1,2] Matic Lozinšek,[1,2]

[1] Jožef Stefan Institute, Jamova cesta 39, *SI*-1000 Ljubljana, Slovenia
[2] Jožef Stefan International Postgraduate School, Jamova cesta 39, *SI*-1000 Ljubljana, Slovenia

The ability of xenon difluoride to act as a ligand to naked metal cations stand as one of the most well-explored aspects of its chemistry.[1] Since the discovery of the first XeF_2 coordination compound, which was formed following the oxidation of Xe gas by cationic Ag^{2+} in anhydrous HF (aHF) over 30 years ago,[2] more than 30 examples of these compounds have been crystallographically characterized. These compounds are typically formulated as $[M^{n+}(XeF_2)_m(AF_x^-)_n]$ where M^{n+} represents the naked metal cation and AF_x^- represents a weakly coordinating anion. The majority of known XeF_2 coordination compounds feature a divalent metal center, whereas examples of XeF_2 coordinated to a monovalent metal are much less common. This is largely due to the oxidizing power of XeF_2 dissolved in aHF, which greatly reduces the scope of monovalent metals to only those that are oxidatively resistant in such solutions.[3] From this perspective, alkali metals seem a suitable choice for preparing novel examples of XeF_2 coordination compounds featuring singly-charged metal cations. However, previous investigations only succeeded in structurally characterizing compounds with XeF_2 acting as a ligand towards Li^+, noting that such complexes are thermodynamically unstable and that those derived from the heavier alkali metals are expected to be even more so.[4]

To prepare further examples of compounds displaying XeF_2 coordination to an alkali metal center, we investigated the XeF_2–$APtF_6$ (A = Li, Na, K) systems in aHF solvent, resulting in the successful structural elucidation of $[Li(XeF_2)_3PtF_6]$, $[Na(XeF_2)PtF_6]$ and $[K(XeF_2)_2PtF_6]$ by single-crystal X-ray diffraction. The latter two compounds represent a rare case of XeF_2 ligated to Na^+ and the first example of XeF_2 coordinating K^+, respectively. Moreover, in the course of our investigations of XeF_2 in systems containing both Lewis-acidic metal tetra- and pentafluorides we have synthesized and structurally characterized $[K(Xe_2F_3)_4(AsF_6)_4][Xe_2F_3]_2[PtF_3(XeF_2)_3]_7[AsF_6]_{10}$ (**1**). The structure of this intriguing compound features two crystallographically independent K^+ cations, which are coordinated by four $[Xe_2F_3]^+$ cations, rendering it an unprecedented example of a cationic xenon(II) fluoride species acting as a ligand toward a metal center. All the aforementioned compounds were also characterized by low-temperature Raman spectroscopy.

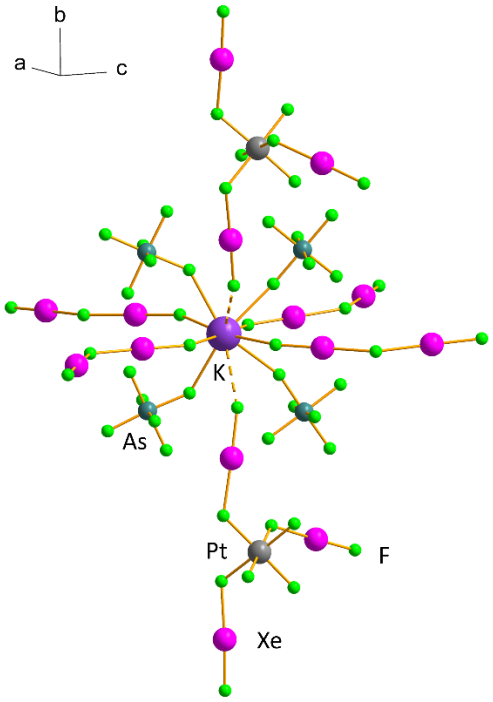

Figure 1: Section of the crystal structure of **1**, displaying the coordination environment surrounding the K^+ cation

References:

1. Tavčar, G.; Tramšek, M., XeF_2 as a Ligand to a Metal Center, an Interesting Field of Noble Gas Chemistry. *J. Fluorine Chem.* **2015**, *174*, 14–21.
2. Hagiwara, R.; Hollander, F.; Maines, C.; Bartlett, N., The Crystal Structure of $[Ag(XeF_2)_2]AsF_6$ Formed in the Oxidation of Xe by $AgFAsF_6$. *Eur. J. Solid State Inorg. Chem.* **1991**, *28*, 855–866.
3. Tramšek, M.; Žemva, B., Synthesis, Properties and Chemistry of Xenon(II) Fluoride. *Acta Chim. Slov.* **2006**, *53*, 105–116.
4. Tavčar, G.; Žemva, B., $[Li(XeF_2)_n](AF_6)$ (A = P, As, Ru, Ir), the First Xenon(II) Compounds of Lithium. Synthesis, Raman Spectrum, and Crystal Structure of $[Li(XeF_2)_3](AsF_6)$. *Inorg. Chem.* **2013**, *52* (8), 4319–4323.

Funding information: The authors gratefully acknowledge the financial support from ARIS (N1-0189) and the ERC (Starting Grant 950625) under the European Union's Horizon 2020 Research and Innovation Programme.

Fine-Tuning of Adsorption Properties of Three-Component MOFs: From Synthesis to Structure-Activity Relationship

Darko Vušak,[1] Suzana Mal,[2] Zvonimira Lemaić,[1] Marija Zora Mišković,[1] Nataša Zabukovec Logar,[2] Biserka Prugovečki[1,*]

[1] Department of Chemistry, Faculty of Science, University of Zagreb, Horvatovac 102a, *HR*-10000 Zagreb, Croatia
[2] National Institute of Chemistry, Hajdrihova ulica 19, *SI*-1000 Ljubljana, Slovenia

Due to climate changes and growth of human population, clean air and water supply become increasingly important. For example, in 2022 World Health Organization estimated that more than 2 billion people live in water-stressed countries without safe drinking water sources.[1] Metal-organic frameworks (MOFs) are a promising material for selective adsorption of gases or water harvesting. It was shown that water harvesting MOFs should have a good balance between hydrophilic and hydrophobic inner surface of pores to bind and release water at certain conditions (temperature, relative humidity) with low energy cost.[2] MOFs with amino acids as ligands have some advantages for application. They tend to form isoreticular compounds by forming similar chelate rings, while the side chains interact with molecules in the pores, enabling fine-tuning of desired properties.[3]

In this work we are presenting synthesis, crystal structures and adsorption properties of four three-component MOFs incorporating copper(II), amino acids (L-serine, HSer; L-threonine, HThr; and L-homoserine, HHser) and 1,2-di(4-pyridyl)ethylene (bpe): three isoretictural {[Cu(μ-Ser)(μ-bpe)]NO_3·solvents}$_n$ (**1**), {[Cu(μ-Thr)(μ-bpe)]NO_3·solvents}$_n$ (**2**) and {[Cu(μ-Hser)(μ-bpe)]NO_3·solvents}$_n$ (**3**) with topological type *uki*, and {[Cu(μ-Thr)(μ-bpe)]NO_3·solvents}$_n$ (**4**) with topological type *irl*. We used different approaches of synthesis at mild synthetic conditions (solution-based and mechanochemical synthesis) to produce and isolate pure materials. Crystal structures revealed the topology of the framework and the size and shape of pores (Figure 1). We investigated the thermal stability of prepared compounds and their stability under different relative humidities at 20 °C. CO_2 adsorption capacity varies depending on the amino acid side chain and the framework topology of compounds **1**–**4**. On the other hand, water adsorption is less dependent on the side chain, with all compounds displaying moderate water adsorption capacity.

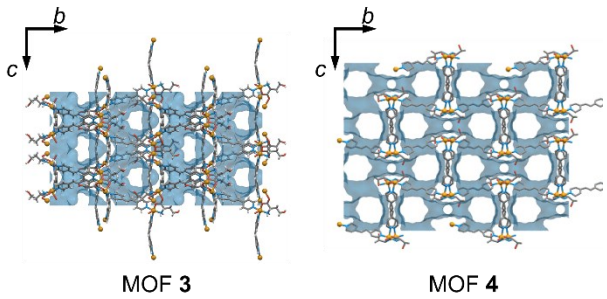

Figure 1: Crystal packing of MOF **3** (topological type *uki*) with 2D channels of solvent molecules and MOF **4** (topological type *irl*) with 3D channels of solvent molecules.

References:

1. https://www.who.int/news-room/fact-sheets/detail/drinking-water (accessed 28 May 2025)
2. Xu, W.; Yaghi, O. M., Metal–Organic Frameworks for Water Harvesting from Air, Anywhere, Anytime. *ACS Cent. Sci.* **2020**, *6*, 1348–1354.
3. Ren, C.-X.; Ji, M.; Yao, Q.-X.; Cai, L.-X.; Tan, B.; Zhang, J., Targeted Functionalization of Porous Materials for Separation of Alcohol/Water Mixtures by Modular Assembly. *Chem. Eur. J.* **2014**, *20*, 14846–14852.

Funding information: This research was funded by the project CIuK co-financed by the Croatian Government and the European Union through the European Regional Development Fund-Competitiveness and Cohesion Operational Programme (Grant KK.01.1.1.02.0016) and by an institutional project financed by the University of Zagreb entitled *Synthesis and structural characterization of organic and complex compounds; protein structure*.

Crystal growth and magnetic properties of the quantum spin liquid candidate $NdTa_7O_{19}$ and other rare-earth heptatantalates

Mirela Dragomir*,[1,2] Lia Šibav,[1,2] Matic Lozinšek,[1,2] Andrej Zorko[1,3]

[1] Jožef Stefan Institute, Jamova cesta 39, *SI*-1000 Ljubljana, Slovenia
[2] Jožef Stefan International Postgraduate School, Jamova cesta 39, *SI*-1000 Ljubljana, Slovenia
[3] Faculty of Mathematics and Physics, University of Ljubljana, Jadranska cesta 19, *SI*-1000 Ljubljana, Slovenia

Neodymium heptatantalate, $NdTa_7O_{19}$, a member of the rare earth (RE) heptatantalate series, $RETa_7O_{19}$, has recently been identified as the first quantum spin liquid (QSL) candidate on a triangular spin lattice with dominant Ising-like spin correlations[1]. QSLs are a fascinating state of matter where spins remain disordered and strongly entangled down to the lowest temperatures[2]. Evidence for a QSL ground state in $NdTa_7O_{19}$ includes the absence of magnetic Bragg peaks in the neutron powder diffraction down to 40 mK, magnetic diffuse scattering, and persistent spin dynamics previously observed by muon spectroscopy[1]. Crystal electric field analysis and bulk magnetic measurements also indicated significant magnetic anisotropy[1]. However, these studies were carried out on polycrystalline samples and single crystals are required for precise determination of anisotropy and advanced magnetic studies.

Here, we report the successful flux growth of $NdTa_7O_{19}$ single crystals using a $K_2Mo_3O_{10}$–B_2O_3 system, yielding high-quality, purple hexagonal crystals up to 3.5 mm in size[3] (Figure 1c). Moreover, we also extended this method to the Er and Gd members. Chemical composition of the grown single crystals was confirmed by SEM-EDS analysis, while their structure was analyzed by powder and single-crystal X-ray diffraction[3]. The structures of $NdTa_7O_{19}$, $ErTa_7O_{19}$ and $GdTa_7O_{19}$ were solved and refined in the $P\bar{6}c2$ space group with the RE ions forming a perfect triangular lattice (Figure 1a,b)[3]. Each RE ion is coordinated by eight oxygen ions, forming distorted REO_8 polyhedra that share edges with neighboring TaO_6 octahedra. The magnetic layers are separated by two nonmagnetic Ta-layers composed of TaO_7 polyhedra.

Magnetic susceptibility measured on $NdTa_7O_{19}$ single crystals revealed strong easy-axis anisotropy and no long-range order down to 2 K, providing clear proof of the anisotropy[3]. $ErTa_7O_{19}$ exhibited a pronounced magnetic anisotropy of the same type with no magnetic ordering down to 2 K, also suggesting a possible exotic magnetic ground state[3]. In contrast, $GdTa_7O_{19}$ showed a paramagnetic behavior[3], in agreement with literature reported measurements on powders[4].

The obtained single crystals will enable new investigations of these frustrated systems. Moreover, this flux method will be applied for the growth of other members of the $RETa_7O_{19}$ series.

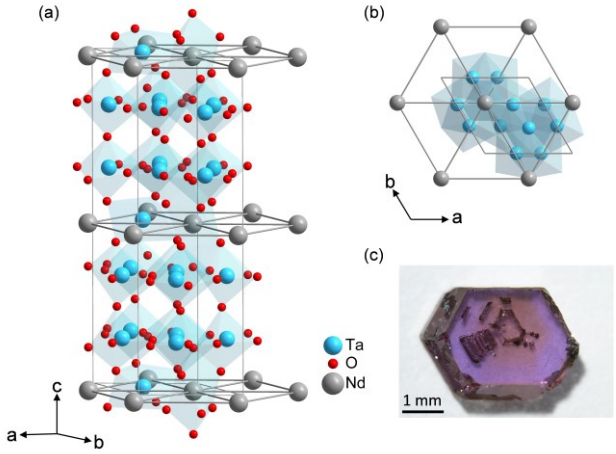

Figure 1: (a) Crystal structure of $NdTa_7O_{19}$ (b). View of the *ab*-plane showing the perfect triangular lattice. (c) Optical image of an as-grown $NdTa_7O_{19}$ crystal[3].

References:

1. Arh, T.; Sana, B.; Pregelj, M.; Khuntia, P.; Jagličić, Z.; Le, M. D.; Biswas, P. K.; Manuel, P.; Mangin-Thro, L.; Ozarowski, A.; Zorko, A. The Ising triangular-lattice antiferromagnet neodymium heptatantalate as a quantum spin liquid candidate. *Nat. Mater.* **2022**, *21*, 416–422.
2 Broholm, C.; Cava, R. J.; Kivelson, S. A.; Nocera, D. G.; Norman, M. R.; Senthil, T. Quantum spin liquids. *Science* **2020**, *367*, eaay0668.
3. Šibav, L.; Lozinšek, M.; Jagličić, Z.; Arh, T.; Khuntia, P.; Zorko, A.; Dragomir, M. *Cryst. Growth Des.* **2025**. doi.org/10.1021/acs.cgd.5c00624.
4 Wang, L.; Ouyang, Z.; Xiao, T.; Li, Z.; Tian, Z. Synthesis, Structure and Magnetism of RTa_7O_{19} (R = Pr, Sm, Eu, Gd, Dy, Ho) with Perfect Triangular Lattice. *J. Alloys Compd.* **2023**, *973*, 168390–168397.

Funding information: P2-0105 and J1-50008, Slovenian Research and Innovation Agency, Slovenia.

Crystal structures of three dyes determined by electron diffraction

Anton Meden*[1]

[1] Faculty of Chemistry and Chemical Technology, University of Ljubljana, Večna pot 113, *SI*-1000 Ljubljana, Slovenia

While preparing a project application with the "Zavod za gradbeništvo - ZAG" for the colorimetric detection of macromolecules, we were surprised to discover that none of the three common dyes (pH indicators) to be used (thymol blue - TB, cresol red – CR and bromocresol green - BCG) has a crystal structure published in the CSD.

All three dyes have similar molecular structures, based on triarylmethane with a sulfonic group attached to one of the aromatic rings. The mechanism of color change as a function of pH is well known.1 It is illustrated for TB in Figure 1.

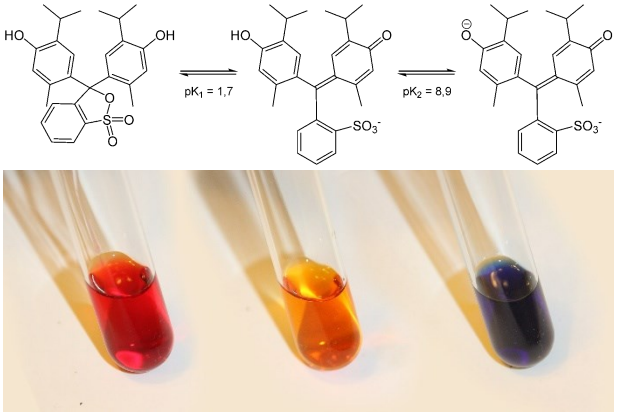

Figure1: Molecular mechanism of color change and the corresponding colors of thymol blue.[1]

The samples purchased (all from Sigma-Aldich) were in the form of fine powders. We used the Rigaku XtaLAB Synergy-ED electron diffractometer and the CrysAlisPro[2] and Olex2[3] programs to successfully solve all three structures at room temperature.

It is interesting to note that the substances are present in different forms. Only one substance (BCG) has a closed 5-membered ring with S and O. This is the form that can be found in the declarations of the purchased products (top left in Fig. 1). The other two (CR and TB) have a free sulfonic group. The molecular structures are shown in Figures 2-4.

One aim of this study was also to explore the possibilities of our new 3D ED system. The crystallographic information on the three solved/refined structures will be reported and discussed in terms of the crystallographic standards used for X-ray diffraction.

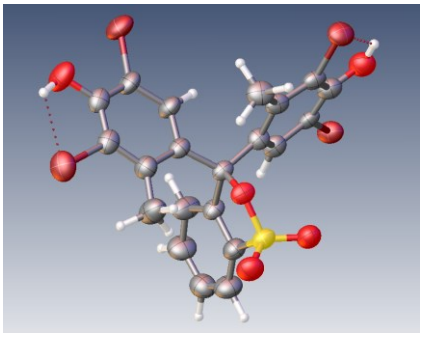

Figure 2: Molecular structure of BCG.

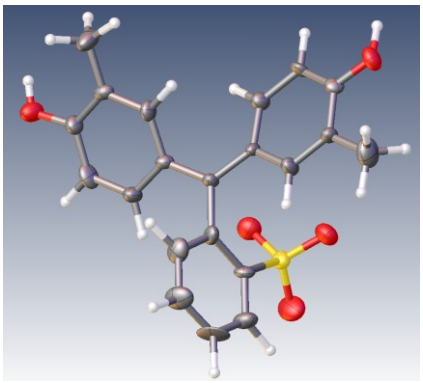

Figure 3: Molecular structure of CR.

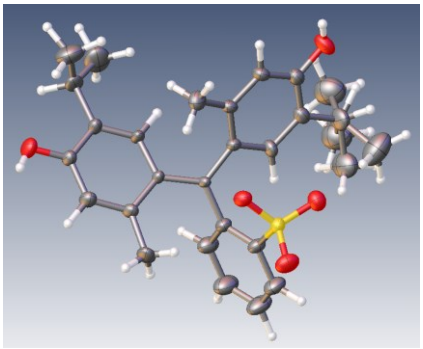

Figure 4: Molecular structure of TB.

References:

1. https://commons.wikimedia.org/w/index.php?curid=18648878.
2. CrysAlis^{Pro} V171.44.101a, Rigaku Oxford Diffraction, Copyright **1995-2025**.
3. O.V. Dolomanov & al, refinement and analysis program. *J. Appl. Cryst*. **2009**, *42*, 339-341.

Funding information: P1-0175, ARIS, Slovenia.

Software for automatic processing of high-pressure ruby fluorescence spectra

Miha Virant*,[1] Matic Lozinšek,[1]

[1] Jožef Stefan Institute, Jamova cesta 39, *SI*-1000 Ljubljana, Slovenia

High-pressure crystallography provides critical insights into the structural behaviour of materials under extreme conditions, reaching pressures comparable to those deep within planetary interiors. The methods allow for the discovery of new phases, tracking of phase transitions, and investigation of changes in bonding and electronic structure[1]. The diamond anvil cell (DAC) is the primary device for achieving static pressures in the laboratory, and owing to diamond's optical transparency, a wide range of instrumental techniques can be employed to monitor the pressure-induced changes. Among these, single crystal X-ray diffraction (SCXRD) and Raman spectroscopy are standard tools.

Accurate pressure measurement is central to meaningful high-pressure research. The ruby fluorescence method[2], based on the pressure-induced redshift of the R_1 fluorescence line of Cr^{3+}-doped Al_2O_3, has been established as a reliable calibration standard. The latest calibration model, known as the IPPS-Ruby2020 scale[3], was endorsed by the International Association for the Advancement of HP Science and Technology (AIRAPT).

To facilitate precise and reproducible pressure determination using ruby fluorescence measurements, we have developed an open-source graphical software package designed to process ruby fluorescence spectra. It supports processing of spectra directly from clipboard as well as batch processing of spectral data in various file formats. A robust algorithm composed of baseline correction and pseudo-Voigt function fitting is employed to extract the precise peak positions, which are then used to calculate pressure based on the Ruby2020 scale[3].

The user-friendly interface enables the creation of high-quality output plots and machine-readable results, simplifying documentation and analysis workflows. In addition to ruby fluorescence, the software includes auxiliary tools for calculation of DAC pressures based on the diamond Raman edge, estimating DAC pressure limits based on the culet size, and calculating gasket thickness from interferometry fringes. These features make the developed software a versatile addition to high-pressure laboratories, enhancing the reliability and efficiency of pressure determination from ruby fluorescence spectra.

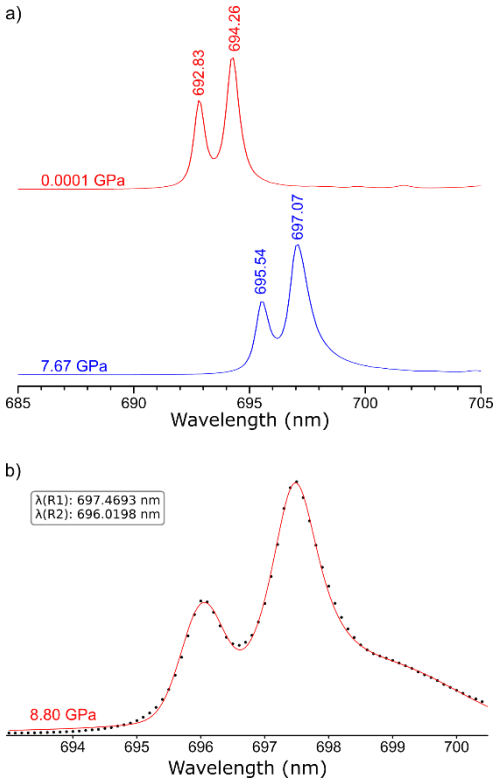

Figure: **a** Ruby fluorescence spectra measured under ambient conditions (red) and under high pressure (blue). **b** Peak position extraction in case of nonhydrostatic conditions using the implemented algorithm.

References:

1. Katrusiak, A. High-pressure crystallography. *Acta Crystallogr., Sect. A* **2008**, *64*, 135–148.
2. Forman, R. A.; Piermarini, G. J.; Barnett, J. D.; Block, S. Pressure Measurement Made by the Utilization of Ruby Sharp-Line Luminescence. *Science* **1972**, *176*, 284–285.
3. Shen, G.; Wang, Y.; Dewaele, A.; Wu, C.; Fratanduono, D. E.; Eggert, J.; Klotz, S.; Dziubek, K. F.; Loubeyre, P.; Fat'yanov, O. V.; Asimow, P. D.; Mashimo, T.; Wentzcovitch, R. M. M.; and other members of the IPPS task group. Toward an international practical pressure scale: A proposal for an IPPS ruby gauge (IPPS-Ruby2020). *High Press. Res.* **2020**, *40*, 299–314.

Funding information: European Research Council Starting Grant under the European Union's Horizon 2020 Research and Innovation Programme (950625).

Alan Lindsay Mackay, and the (Pre)-History of Quasicrystals

Vladimir Stilinović[1]

[1] Department of Chemistry, Faculty of Science, University of Zagreb, Horvatovac 102a, *HR*-10000 Zagreb, Croatia

In 2011 the Nobel Prize in Chemistry was awarded to Dan Shechtman for the discovery of quasicrystals.[1] The prize came almost three decades after Shechtman's original discovery of a rapidly quenched aluminium-manganese alloy which exhibited electron diffraction patterns of crystallographically *"forbidden"* 10-fold symmetry[2] – symmetry which is not possible in periodic assemblies (at least in three-dimensional space). This discovery was so shocking that it took Shetchtman almost wo years to finally manage to publish an account of it, and well over a decade for the most vociferous critics to fall silent, either by being convinced by the growing body of evidence of the reality of the existence of aperiodic crystals, or else by passing away. The Shechtman's discovery of quasicrystals, as well as their description as quasiperiodic structures has led to a considerable change in what was considered to be a 'crystal' (including a change of the IUCr definition of the term 'crystal' in 1992[3]), and has repeatedly been described as a (or even 'the') *paradigm shift* in crystallography.

However, while the majority of the crystallographic world "was completely unprepared for the discovery of Dan Shechtman that such aperiodic beasts could actually exist also in solid matter",[4] some crystallographers had by that time already had their 'paradigm shifted'. In June (5.-7.) 1975. on a Conference of the Yugoslav Centre of Crystallography (a direct predecessor of the Slo-Cro/Cro-Slo Crystallographic Meetings), Alan Lindsay Mackay gave a lecture titled "Generalised crystallography"[5] in which he called for crystallographers not to be limited by the International Tables – concentrating at the time strictly on periodic structures – but rather that they should set their objectives on researching and understanding understanding organised matter, regardless of its periodicity. Furthermore, he explicitly mentioned a possibility of organized matter adopting an (aperiodic) configuration exhibiting five-fold symmetry. A paper based on this lecture was published as a part of the Proceedings of the Yugoslav Centre of Crystallography, making it, to the best of my knowledge, the first paper to announce the possibility of fivefold symmetry in solids to be published. This did not end Mackay's interest on the subject – having learned of the two approaches for a quasiperiodic tiling of a plane developed by Roger Penrose, he demonstrated that a quasiperiodic pattern has a discrete diffraction pattern, and in the case of the Penrose tiling (which averagely has approximate fivefold symmetry), the diffraction pattern will exhibit 10-fold symmetry. Thus Mackay quite accurately predicted not only the existence, but also the structure of quasicrystals (as we understand them today) considerably before their discovery.

Allan Mackay passed away in the February of this year, aged 98. This presentation is dedicated to his memory, as a tribute to one of the true crystallographic *legends*, as well as a celebration of the 50th anniversary of his presentation on (a predecessor of) this conference, which has presaged one of the greatest revolutions in the history of crystallography.

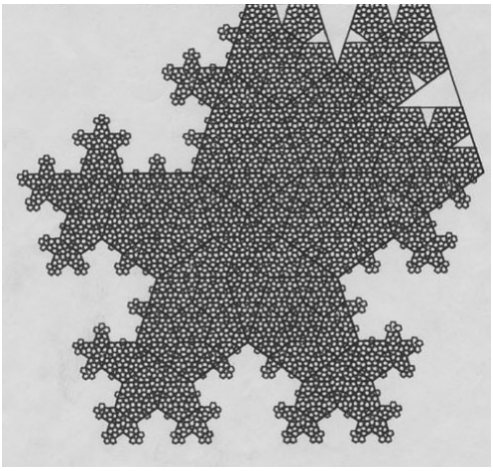

Figure 1: The 'pentagonal snowflake' – 1981 computer rendering of Penrose (quasiperiodic) tiling made by Robert Mackay and used Alan Mackay to demonstrate its diffraction pattern.[7]

References:

1. Lidin, S. *Scientific Background on the Nobel Prize in Chemistry 2011, The Discovery of Quasicrystals*, The Royal Swedish Academy of Sciences, Stockholm, Sweden, **2011**.
2. Shechtman, D.; Blech, I.; Gratias, D.; Cahn, J.W. (1984). Phys. Rev.Lett. **1984**, 53 1951.
3. UCr: Report of the Executive Committee for 1991. *Acta Cryst*., **1992**, A48, 928.
4. *Nobel Prize in Chemistry 2011, Prize announcement* https://www.nobelprize.org/prizes/chemistry/2011/prize-announcement/ (accessed May 2025)
5. Mackay A.L. *Izv. Jugosl. Centr. Krist* , 1975, 10, 15.

Can the robustness of the L-carnosine copper(II) dimer be utilized as a versatile building block?

Ivica Đilović*,[1] Draginja Mrvoš-Sermek,[1] Marina Tašner, Darko Vušak,[1] Dubravka Matković-Čalogović,[1]

[1] Faculty of Science, University of Zagreb, Horvatovac 102a, *HR*-10000 Zagreb, Croatia

Carnosine (β-alanyl-L-histidine, H_2**car**) participates in numerous physiological processes involving the coordination of metal ions. Coordination compounds of L-carnosine have garnered significant research interest due to their intriguing properties.[1] Recently, we analyzed the coordination abilities of L-carnosine in reactions with copper(II) under various conditions. We prepared three solvates of copper(II) coordination compounds with **car** ligands, determined their molecular and crystal structures, and described the conditions for their interconversion.[2-4]

In all three cases, the copper(II) ion coordination polyhedron is square-pyramidal, with solvent molecules in apical positions. All crystal structures consist of discrete dimers in which two **car** ligands coordinate two copper(II) ions. A comprehensive analysis of the structural and spectroscopic properties of activated dimers is being conducted to investigate their stability and reactivity in the absence of coordinated solvent molecules. Preliminary results indicate that generating these dimers requires heating, after which different linkers can be introduced using extended liquid-assisted milling. These findings suggest new possibilities for utilizing activated dimers in the development of novel compounds (Figure 1).

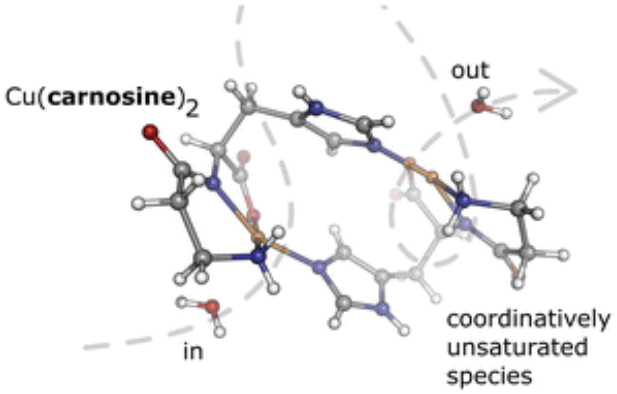

Figure 1

References:

1. Boldyrev, A. A., Aldini, G., Derave, W., *Physiol. Rev.* **2013**, *93*, 1803 -1845.
2. Mrvoš-Sermek, D., Tašner, M., Vušak, D., Judaš, N., Wzgarda-Raj, K., Đilović, I., Matković-Čalogović, D., *CrystEngComm* **2025**, *27*, 356-365.
3. Freeman, H. C., Szymanski, J. T., *Chem. Commun.* **1965**, 598–599.
4. Freeman, H. C., Szymanski, J. T., *Acta Crystallogr.* **1967**, *22*, 406–417.

Funding information: Croatian Science Foundation (grant no. IP-2014-09-4274); University of Zagreb grants for 2022-2024; CIuK project, co-financed by the Croatian Government and the European Union KK.01.1.1.02.0016.

PREVIOUS MEETINGS

Venues of Slovenian-Croatian Crystallographic Meetings

1st Otočec, Slovenia, 1992
2nd Stubičke Toplice, Croatia, 1993
3rd Kranjska Gora, Slovenia, 1994
4th Trakošćan, Croatia, 1995
5th Zreče, Slovenia, 1996
6th Umag, Croatia, 1997
7th Radenci, Slovenia, 1998
8th Rovinj, Croatia, 1999
9th Gozd Martuljek, Slovenia, 2000
10th Lovran, Croatia, 2001
11th Bohinj, Slovenia, 2002
12th Plitvice, Croatia, 2003
13th Bovec, Slovenia, 2004
14th Vrsar, Croatia, 2005
15th Jezersko, Slovenia, 2006
16th Petrčane, Croatia, 2007
17th Ptuj, Slovenia, 2008
18th Varaždin, Croatia, 2009
19th Strunjan, Slovenia, 2010
20th Baška, Croatia, 2011
21st Pokljuka, Slovenia, 2012
22nd Biograd na Moru, Croatia, 2013
23rd Logar Valley, Slovenia, 2014
24th Bol, Croatia, 2016
25th Ljubljana, Slovenia, 2017
26th Poreč, Croatia, 2018
27th Rogaška Slatina, Slovenia, 2019
28th Poreč, Croatia, 2022
29th Topolšica, Slovenia, 2023
30th Veli Lošinj, Croatia, 2024

1st Slovenian-Croatian Crystallographic Meeting, Otočec ob Krki, Slovenia.
October 1–2, 1992.

A. Kalman (Budapest, Hungary)
On the nature of hypervalent S-O bonds in sulfuranes
B. Kojić-Prodić et al. (Zagreb Croatia)
The biological significance of conformational changes of beta-D-glucopyranose moiety in peptidoglycans
C. Kratky (Graz, Austria)
Crystallography of B12-coenzymes
V. Kraševec (Ljubljana, Slovenia)
Crystallography of 2D precipitates caused by a minor phase additions in some ceramic systems

2nd Croatian-Slovenian Crystallographic Meeting, Stubičke Toplice, Croatia.
September 30–October 1, 1993.

L. Randaccio (Trieste, Italy)
Structural and solution properties of rhodoximes: the Rh analogues of cobaloximes, a vitamin B12 model
V. Kaučič (Ljubljana, Slovenia)
The structure of zeolite and aluminophosphate molecular sieves
K. Huml (Prague, Czech Republic)
Crystallography in drug design
B. Gržeta and H. Toraya (Zagreb, Croatia)
Powder-pattern-fitting methods in structure determination

3rd Slovenian-Croatian Crystallographic Meeting, Kranjska gora, Slovenia.
September 29–30, 1994.

W. Fuller, A. Mahendrasingam, and V. T. Forsyth (Keele, UK)
Structural studies of biological and industrial fibres using X-ray synchrotron radiation sources and neutron beams
A. Rečnik and D. Kolar (Ljubljana, Slovenia)
Local structure of planar faults in oxide ceramics
T. Schirmer (Basel, Switzerland)
Crystal structures of porins: proteins that form transmembrane pores
M. Luić and N. Brničević (Zagreb, Croatia)
Stereochemistry of hexanuclear niobium clusters with the [Nb6Cl12]2+ unit

4th Croatian-Slovenian Crystallographic Meeting, Trakoščan, Croatia.
September 28–30, 1995.

I. Hargittai and M. Hargittai (Budapest, Hungary)
Structure of molecules and assemblies
V. Marinkovič (Ljubljana, Slovenia)
Scanning tunneling microscopy of surface structures
H. Fuess (Darmstadt, Germany)
Contributions of crystallography to material science
D. Balzar (Zagreb, Croatia)
Diffraction line broadening - nuisance or lattice-imperfections fingerprints

5th Slovenian-Croatian Crystallographic Meeting, Zreče, Slovenia.
June 13–15, 1996
H. D. Flack (Geneve, Switzerland)
Mastering least-squares refinement
J. V. Brenčič (Ljubljana, Slovenia)
Structural studies of the halopyridine complexes of trivalent elements
P. Panjan (Ljubljana, Slovenia)
Interfacial reaction in multilayer structures studied with XTEM and XRD
H. Follner (Lienz, Austria)
Correspondence between structure and morfology and twin formation
Z. Blažina (Zagreb, Croatia)
The rare earth based intermetallics - a scientist's paradise

6th Croatian-Slovenian Crystallographic Meeting, Umag, Croatia.
June 19–21, 1997
A. Meden (Ljubljana, Slovenia)
Crystal structure solution from powder diffraction data - state of the art and perspectives
B. Ya. Kotur (Lviv, Ukrayina)
Scandium binary and ternary alloy systems and intermetallic compounds
P. Orioli (Firenze, Italy)
Structural studies on the interactions between metal ions and biological macromolecules
M. Vinković (Zagreb, Croatia)
Synergy between crystallography and computational chemistry

7th Slovenian-Croatian Crystallographic Meeting, Spa Radenci, Slovenia.
June 18–20, 1998
M. Kaftory (Haifa, Izrael)
Three decades of chemical reactions in the solid state from photodimerization to methyl transfer
A. M. Tonejc (Zagreb, Croatia)
High-resolution electron microscopy (HREM): image processing analysis of defects and grain boundaries in nanocrystalline materials
E. Tillmanns (Vienna, Austria)
How to avoid unnecessarily low symmetry in crystal structure determinations
K. Djinović Carugo (Ljubljana, Slovenia)
Protein function through crystallography

8th Croatian-Slovenian Crystallographic Meeting, Rovinj, Croatia.
June 17–19, 1999
D. Yu. Pushcharovsky (Moscow, Russia)
Recent contribution and modern perspectives in XRD studies of minerals
G. Jovanovski (Skopje, Macedonia)
Metal sacharinates and their complexes with N-donor ligands
M. Bolognesi et al. (Pavia, Italy)
The high resolution structure of GDP-4-keto-6-deoxy-D-mannose epimerase/reductase
G. G. Dodson (York, UK)
The chemistry and evolution of the catalytic structures in serine hydrolases
A. Demšar (Ljubljana, Slovenia)
The inclusion of the ionic fluorides in soluble organometallics

9th Slovenian-Croatian Crystallographic Meeting , Gozd Martuljek, Slovenia, June 17–19, 2000

C. Giacovazzo (Bari, Italia)
Phasing: from powders to proteins
Ch. Baerlocher (Zuerich, Switzerland)
The texture approach to structure solution from powder data
A. Tonejc (Zagreb, Croatia)
Crystallographic features of mechanically milled and alloyed nano-sized crystalline and amorphous materials
I. Turel (Ljubljana, Slovenia)
The crystal structures of quinolones and their metal compounds

10th Croatian-Slovenian Crystallographic Meeting, Lovran, Croatia. June 21–24, 2001

K. Prout (Oxford, UK)
Molecules in motion
G. Zanotti (Padova, Italy)
The transport of vitamin A in mammals: a crystallographer's view
B. Kobe (Brisbane, Australia):
Protein-peptide binding and its regulation
O. Milat (Zagreb, Croatia) and G. Calestani (Parma, Italy):
Crystallography of composite crystals

11th Slovenian-Croatian Crystallographic Meeting, Bohinj Lake, Slovenia. June 27–30, 2002

H. Boehm (Mainz, Germany)
Phase transitions in modulated structures
G. Giester (Vienna, Austria)
Five years of CCD X-ray data collection at Vienna University
E. R. T. Tiekink (Singapore, Singapore)
Adventures in engineering molecular solids
D. Matković-Čalogović (Zagreb, Croatia)
Some protein crystallography examples - a small molecule crystallographers view
B. Modec (Ljubljana, Slovenia)
Oxomolybdenum(V) clusters built of dinuclear metal-metal bonded units

12th Croatian - Slovenian Crystallographic Meeting, Plitvice Lakes, Croatia. June 19–22, 2003

B. Kojić-Prodić (Zagreb, Croatia)
Hydrogen bonding and supramolecular architecture
G. Vlaic (Trieste, Italy)
XFAS spectroscopies and chemistry: some selected results
J. P. Abrahams, N. Ban (Zuerich, Switzerland)
X-ray crystallographic structure determination of large asymmetric macromolecular assemblies
A. Golobič (Ljubljana, Slovenia)
Solving structural problems of ceramic materials
A. Danilovski (Zagreb, Croatia)
Biological and pharmaceutical solids in the crystallographic arena

13th Slovenian-Croatian Crystallographic Meeting, Bovec, Slovenia.
June 16–20, 2004
R. Loris (Brussel, Belgium)
Structural basis of plasmid addiction and programmed cell death in bacteria
D. Turk (Ljubljana, Slovenia)
Roles of papain-like cathepsins in immune system response: exclusive interactions as the other face of selectivity
K. Domasevitch, J. Sieler (Leipzig, Germany)
Architecture and design of new porous networks
A. Moguš-Milanković (Zagreb, Croatia)
Structure and properties of phosphate glass

14th Croatian-Slovenian Crystallographic Meeting, Vrsar, Croatia.
June 15–17, 2005
N. Lah (Ljubljana, Slovenia)
Structural diversity of copper carboxylate complexes
L. R. MacGillivray (Iowa, USA)
Molecular crystals as media for constructing molecules
R. Cerny (Geneva, Switzerland)
Crystal structures of inorganic compounds from powder diffraction
M. Milun (Zagreb, Croatia)
Atomic structure of surfaces and thin films
E. Libowitzky (Vienna, Austria)
Dynamics of crystal structures: results between diffraction and spectroscopy

15th Slovenian-Croatian Crystallographic Meeting, Jezersko, Slovenia.
June 14–18, 2006.
W. L. Duax (Buffalo, USA)
The genes and amino acid sequences and crystal structures of short chain oxireductase enzymes
R. E. Dinnebier (Stuttgart, Germany)
Powder diffraction at non-ambient conditions using 2D-detectors
G. Štefanić (Zagreb, Croatia)
Formation of high-temperature ZrO2 polymorphs at room temperature
M. Kosec (Ljubljana, Slovenia)
Ferroelectrics: from bulk to nano

16th Croatian-Slovenian Crystallographic Meeting, Petrčane, Croatia.
June 13–17, 2007.
C. Giacovazzo et al. (Bari, Italy)
EXPO2007: A tool for crystal structure solution and refinement from powder data
N. Tomašić (Zagreb, Croatia)
Metamict minerals: Insight into relic crystal structuires
R. Kužel et al. (Prague, Czech Republic)
Structural studies of submicrocrystalline materials obtaind by severe plastic deformation
B. Kozlevčar (Ljubljana, Slovenia)
Structural analysis of copper(II) coordination compounds and correlation with their magnetic properties

17th Slovenian-Croatian Crystallographic Meeting, Ptuj, Slovenia.
June 19–22, 2008.
M. Jaskolski, K. Michalska (Poznan, Poland)
L-Asparaginases, their friends and relations
G. Pavlović (Zagreb, Croatia)
Mercury(II) coordination chemistry in the environment
B. Kobe et al. (Brisbane, Australia)
Two hotdogs are better than one: The structure of acy-coa thioesterase and the complementarity of structural methods
P. Strauch (Potsdam, Germany)
Solid state EPR: a structure-spectroscopy relationship
B. Orel et al. (Ljubljana, Slovenia)
Synthesis of polyhedral oligomeric silsesquioxane (POSS) hybrids and their applications as surface modifiers

18th Croatian-Slovenian Crystallographic Meeting, Varaždin, Croatia.
June 17–21, 2009.
K. Rissanen (Jyvaeskylae, Finland)
Weak intermolecular interactions in the solid state, the supramolecular chemistry perspective
S. Petriček (Ljubljana, Slovenia)
Complexes with ethers and polyethers
P. Naumov
Direct observations of dynamic processes in crystals: from the topochemical postulate to ultrafast time-resolved diffraction
F. Antson et al. (York, England)
How viruses fill their capsids with DNA: crystallography of a DNA-translocating molecular motor
P. Dubček (Zagreb, Croatia)
Small angle probe into thin film

19th Slovenian-Croatian Crystallographic Meeting, Strunjan, Slovenia.
June 16–20, 2010.
A. L. Spek (Utrecht, The Netherlands)
Why Crystal Structure Validation?
Z. Dauter (Argonne National Lab., USA)
Nobel Prizes Related to Crystallography
A. Višnjevac (Zagreb, Croatia)
Single Crystal X-ray Crystallography as a Method of Choice in Biomimetic Modelling
I. Arčon (Nova Gorica, Slovenia)
Structural Analysis of Ordered and Disordered Materials with X-ray Absorption Spectroscopy

20th Croatian-Slovenian Crystallographic Meeting, Baška, Island Krk, Croatia. June 15–19, 2011.

V. Holy (Prague, Czech Republic)
Synchrotron-related methods of investigatio of nanostructures
A. Šantić (Zagreb, Croatia)
Charge carrier transport in materials with disordered structures
T. Friščić (Cambridge, UK)
How to be efficient and environmentally-friendly at the same time: solid-state routes to materials and molecules
A. Pevec (Ljubljana, Slovenia)
Structural studies of some organotitanium(IV) complexes
M. Cetina (Zagreb, Croatia)
From self-inclusion and host-guest complexes to channel structures

21st Slovenian-Croatian Crystallographic Meeting, Pokljuka, Slovenia. June 14–17, 2012.

L. B. McCusker (ETH Zürich, Switzerland)
Powder diffraction, electron microscopy and microdiffraction - meeting the challenge of zeolite structure analysis
K. R. Koch (Univ. of Stellenbosch, South Africa)
Deceptively simple, rich platinum(II/IV) and rhodium(III) chemistry viewed through new eyes: What secrets can the $^{195}Pt/^{103}Rh$ nuclei reveal about their molecular disguise in the solution and solid-state?
Z. Popović (Zagreb, Croatia)
Correlation between supramolecular interactions and structural characteristics of Ag(I) complexes
F. Perdih (Ljubljana, Slovenia)
Structural aspects of organotitanium fluorides

22nd Croatian-Slovenian Crystallographic Meeting, Biograd na Moru, Croatia. June June 12–16, 2013.

C. B. Aakeröy (Kansas State University, USA)
From molecular sociology to functional materials
A. Altomare (Bari, Italy)
The challenge of the ab-initio crystal structure solution by powder diffraction data: the EXPO software
V. Bermanec (Zagreb, Croatia)
The importance of collecting and investigation of mineral samples from ore deposits - example of Stari Trg (Trepča) mine
M. Jeršek (Ljubljana, Slovenia)
Inclusions in gemstones - origin, identification and valuation
J. Popović (Zagreb, Croatia)
Nanocrystalline metal oxides: synthesis, structure and properties

23rd Slovenian-Croatian Crystallographic Meeting, Logar Valley, Slovenia.
June 19–22, 2014.

I. R. Evans (Durham, UK)
Structural chemistry of functional materials: mobility in the solid state
J. S. O. Evans (Durham, UK)
Functional inorganic materials: synthesis, structure, properties and methods development
M. Đaković (Zagreb, Croatia)
From molecular structure to crystalline solids: non-covalent interactions as a structure directing force in supramolecular assemblies
T. Balić-Žunić (Copenhagen, Denmark)
Crystallography in mineralogy in the XXI century
G. Gunčar (Ljubljana, Slovenia)
A structural view of nanobodies

24th Croatian-Slovenian Crystallographic Meeting, Bol, Croatia.
September 21–25, 2016.

L. Brammer (Sheffield, UK)
Flexibility, Dynamics and Chemical Reactions in Solids: Molecular Crystals to Framework Materials
G. Dražić (Ljubljana, Slovenia)
Direct imaging and quantification of crystal structures at the atomic level using Cs corrected scanning transmission electron microscope
M. Jaskolski (Poznan, Poland)
Handling crystal pathologies in macromolecular crystallography
Ž. Skoko (Zagreb, Croatia)
Thermosalient crystals – acrobatics on the nanoscale
M. Zema (Pavia, Italy)
Crystallography and Society: outcomes of IYCr2014

25th Slovenian-Croatian Crystallographic Meeting, Ljubljana, Slovenia.
June 14–17, 2017.

D. Stalke, (Göttingen, Germany)
100 years of Lewis diagram – still valid in the light of charge density?
E. V. Boldyreva (Novosibirsk, Russia)
High-pressure studies of organic and coordination compounds
M. Marinšek (Ljubljana, Slovenia)
3D microstructure reconstruction from stack of 2D images demonstrated in Ni-SDC cermets
J. K. Cockcroft (London, UK)
Powder diffraction: an essential complementary tool for those skilled in the art but one with pitfalls for the unwary
K. Molčanov (Zagreb, Croatia)
Stacking of planar conjugated rings – beyond aromatics

26th Croatian-Slovenian Crystallographic Meeting, Poreč, Croatia.
June 13–17, 2018.
A. Katrusiak (Poznan, Poland)
High-pressure effects in hydrogen-bonded crystals
P. Scardi (Trento, Italy)
SRXRD of metal nanocrystals: learning from mistakes
S. C. Tarantino (Pavia, Italy)
Crystals' warm-up, stretching and ... workout!
Z. Štefanić (Zagreb, Croatia)
Purine nucleoside phosphorylases: a quest for enzyme mechanism and allosteric pathways
N. Zabukovec Logar (Ljubljana, Slovenia)
Crystallography in Microporous Materials Research

27th Slovenian-Croatian Crystallographic Meeting, Rogaška Slatina, Slovenia.
June 19–23, 2019.
P. Bombicz (Budapest, Hungary)
Synthon/property-engineering of calixarenes (supramolecular interactions, shape and symmetries)
M. Vrankić (Zagreb, Croatia)
Ambient and non-ambient driven X-ray powder diffraction: Insights into the structure-property relationship in powders
P. Macchi (Bern, Switzerland)
Are there molecules in crystals?
M. Lozinšek (Ljubljana, Slovenia)
Noble-gas chemistry in 21st century

28th Croatian-Slovenian Crystallographic Meeting, Poreč, Croatia.
September 7–11, 2022.
A. Bacchi (Parma, Italy)
Smart materials for the release of liquid ingredients
A. Moliterni (Bari, Italy)
Crystallography, a powerful lens for Materials Science
M. Klementová (Prague, Czech Republic)
Structure determination of nanomaterials from electron diffraction data
J. Kljun (Ljubljana, Slovenia)
Development of bioactive metal compounds: structural insights into design and molecular modes of action

29th Slovenian-Croatian Crystallographic Meeting, Topolšica, Slovenia.
June 14–18, 2023.
D. Cinčić (Zagreb, Croatia)
Crystal engineering of organic and metal-organic multicomponent halogen-bonded solids
K. Djinović Carugo (Grenoble, France)
Order from Disorder: Towards molecular architecture of the muscle Z-disk assembly
A. Kokalj (Ljubljana, Slovenia)
DFT modeling of materials and crystal structures using periodic-boundary conditions
S. Parsons (Edinburgh, UK)
High pressure phase transitions in molecular crystals

30th Croatian-Slovenian Crystallographic Meeting, Veli Lošinj, Croatia.
June 12–16, 2024.

I. Halasz (Zagreb, Croatia)
In situ powder X-ray diffraction and Raman spectroscopy for monitoring of ball-milling mechanochemistry

L. Cendron (Padua, Italy)
A structural view of SOS response in bacteria: how it works and how to block it

D. Pelc (Zagreb, Croatia)
Diffuse scattering and nanoscale correlations in quantum materials

C. Esterhuysen (Stellenbosch, South Africa)
The role of intermolecular interactions in chemical processes

M. Dragomir (Ljubljana, Slovenia)
Synthesis and structure-property relationships of selected quantum materials

LIST OF PARTICIPANTS

Blaž ANTONIN
Faculty of Chemistry and Chemical Technology, University of Ljubljana, Slovenia

Mihails ARHANGELSKIS
Faculty of Chemistry, University of Warsaw, Poland

Reinhard BOEHLER
University of Tennessee, Tennessee, USA

Mario CETINA
Faculty of Textile Technology, University of Zagreb, Croatia

Andrea ČOBIĆ
University of Zagreb, Faculty of Science, Department of Geology, Croatia

Mirela DRAGOMIR
Jožef Stefan Institute, Ljubljana, Slovenia

Marijana ĐAKOVIĆ
University of Zagreb, Faculty of Science, Department of Chemistry, Croatia

Ivica ĐILOVIĆ
University of Zagreb, Faculty of Science, Department of Chemistry, Croatia

Izabela ĐURASOVIĆ
Ruđer Bošković Institute, Zagreb, Croatia

Andreas ERTL
University of Vienna, Austria

Mauro GEMMI
Istituto Italiano di Tecnologia, Pontedera, Italy

Gerald GIESTER
University of Vienna, Austria

Nico GIORDANO
Deutsches Elektronen-Synchrotron DESY, Hamburg, Germany

Amalija GOLOBIČ
Faculty of Chemistry and Chemical Technology, University of Ljubljana, Slovenia

Marijan GOTIĆ
Ruđer Bošković Institute, Zagreb, Croatia

Felix HENNERSDORF
Rigaku Europe SE, Germany

Mišel HOZJAN
Faculty of Chemistry and Chemical Technology, University of Ljubljana, Slovenia

Andrii HULTIAIEV
Jožef Stefan Institute, Ljubljana, Slovenia

Jure JAKOŠ
Faculty of Chemistry and Chemical Technology, University of Ljubljana, Slovenia

Ivana KEKEZ
University of Zagreb, Faculty of Science, Department of Chemistry, Croatia

Jakob KLJUN
Faculty of Chemistry and Chemical Technology, University of Ljubljana, Slovenia

Boštjan KOBE
School of Chemistry, University of Queensland, Brisbane, Australia

Bogdan KOTUR
Department of Inorganic Chemistry, Ivan Franko National University of Lviv, Ukraine

Bojan KOZLEVČAR
Faculty of Chemistry and Chemical Technology, University of Ljubljana, Slovenia

Ivan LEBAN
Faculty of Chemistry and Chemical Technology, University of Ljubljana, Slovenia

Matic LOZINŠEK
Jožef Stefan Institute, Ljubljana, Slovenia

Dubravka MATKOVIĆ-ČALOGOVIĆ
University of Zagreb, Faculty of Science, Department of Chemistry, Croatia

Matjaž MAZAJ
National Institute of Chemistry, Ljubljana, Slovenia

Emma E. McCABE
Durham University, Department of Physics, United Kingdom

Anton MEDEN
Faculty of Chemistry and Chemical Technology, University of Ljubljana, Slovenia

Valentina MILAŠINOVIĆ
Ruđer Bošković Institute, Zagreb, Croatia

Krešimir MOLČANOV
Ruđer Bošković Institute, Zagreb, Croatia

Lidija MOLČANOV
Ruđer Bošković Institute, Zagreb, Croatia

Klemen MOTALN
Jožef Stefan Institute, Ljubljana, Slovenia

Igor PICEK
School of Medicine, University of Zagreb, Croatia

Marta POČKAJ
Faculty of Chemistry and Chemical Technology, University of Ljubljana, Slovenia

Benjamin POLJANC
Faculty of Chemistry and Chemical Technology, University of Ljubljana, Slovenia

Kristian RADAN
Jožef Stefan Institute, Ljubljana, Slovenia

Uroš RAPUŠ
Faculty of Chemistry and Chemical Technology, University of Ljubljana, Slovenia

Olha SANKO
Jožef Stefan Institute, Ljubljana, Slovenia

Ana SILJANOVSKA VIRANT
Jožef Stefan Institute, Ljubljana, Slovenia

Željko SKOKO
University of Zagreb, Faculty of Science, Department of Physics, Croatia

Vladimir STILINOVIĆ
University of Zagreb, Faculty of Science, Department of Chemistry, Croatia

Goran ŠTEFANIĆ
Ruđer Bošković Institute, Zagreb, Croatia

Nenad TOMAŠIĆ
Ruđer Bošković Institute, Zagreb, Croatia

Erik URAN
Jožef Stefan Institute, Ljubljana, Slovenia

Ivana VELJKOVIĆ
Institute of Chemistry, Technology and Metallurgy University of Belgrade, Serbia

Miha VIRANT
Jožef Stefan Institute, Ljubljana, Slovenia

Darko VUŠAK
University of Zagreb, Faculty of Science,
Department of Chemistry, Croatia

Žan ZAKOŠEK
Jožef Stefan Institute, Ljubljana, Slovenia

Vesna ZALAR SERJUN
Slovenian National Building and Civil
Engineering Institute, Ljubljana, Slovenia

Nadja ZIHERL
Faculty of Chemistry and Chemical
Technology, University of Ljubljana, Slovenia

Jernej ŽIŽEK
SCAN d.o.o., Preddvor, Slovenia

Representing authors are given in **bold**.

A
Androš Dubraja, Lidija 28
Anelić, Rafael 20
Antonin, Blaž **45**
Arhangelskis, Mihails **23**
B
Babizhetskyy, Volodymyr 36
Boehler, Reinhards **16**
Brázda, Petr 52
Brekalo, Ivana 23
Bukleski, Miha 41
C
Cerc Korošec, Romana 46
Cetina, Mario **32**
Clabbers, Max T. B. 44
Č
Čobić, Andrea **14**
D
Dragomir, Mirela 52, **56**
Đ
Đaković, Marijana **53**
Đilović, Ivica **60**
Đurasović, Izabela **20**
E
Enyedi, Éva A. 50
Ertl, Andreas **26**
F
Faraguna, Fabio 20
Ferguson, Michael 23
Foretić, Blaženka 22
Friščić, Tomislav 23
G
Gemmi, Mauro **17**
Giester, Gerald 26
Giordano, Nico **24**
Golobič, Amalija 18, **41**, 49
Goreshnik, Evgeny 27, 34
Gotić, Marijan 20
Grape, Erik S. 18
Gu, Weixi 44
Guha, Suchismita 24
Gurung, Kshitij 52
H
Hennersdorf, Felix **25**
Hozjan, Mišel **37**
Huf, Elisabeth M. 30
Hultiaiev, Andrii **34**
J
Jagličić, Zvonko 37
Jakoš, Jure **30**
K
Kekez, Ivana **38**
Kjelstrup-Hansen, Jakob 24

Klaser, Teodoro 42
Kljun, Jakob 21, 30, 39, 45, **50**
Knaapila, Matti 24
Kobe, Boštjan **44**
Kontrec, Jasminka 47
Kóša, Filip 41
Kotur, Bogdan **36**
Kovač, Janez 27
Kovačič, Sebastjan 18
Kozlevčar, Bojan **48**
Krajnc, Andraž 18
Kretić, Danijela 40
Kučera-Čavara, David 38
L
Lemaić, Zvonimira 55
Li, Yan 44
Lisac, Katarina 23
Lozinšek, Matic 29, 31, 35, 51, **52**, 54, 56, 58
Ludwig, Thomas 26
M
Mal, Suzana 55
Maračić, Silvija 32
Marciuš, Marijan 20, 47
Marrett, Joseph M. 23
Matijaković Mlinarič, Nives 47
Matković-Čalogović, Dubravka 60
Mazaj, Matjaž **18**
McCabe, Emma E. **15**
Meden, Anton 18, 46, **57**
Meyer, Hans-Peter 26
Mišković, Marija Zora 55
Molčanov, Krešimir **28**
Molčanov, Lidija 28
Motaln, Klemen 52, **54**
Mrvoš-Sermek, Draginja 60
Mudring, Anja-Verena 36
Myakush, Oksana 36
N
Nanson, Jeffrey D. 44
Ninković, Dragan 40
Njegić Džakula, Branka 47
O
Oprčkal, Primož 46
Ovčar, Juraj 22
P
Pacoste, Laura C. 44
Palatinus, Lukaš 52
Perdih, Franc 37
Peter, Robert 20
Pevec, Andrej 48
Pezzotta, Federico 26
Picek, Igor **22**
Pivarcsik, Tamás 50
Počkaj, Marta **33**, 46
Poljanc, Benjamin **39**

Pongrac, Petra 23
Popović, Jasminka 22
Prugovečki, Biserka 38, 55
R
Radan, Kristian **35**, 52
Raić Malić, Silvana 32
Ramirez, Joseph R. 23
Rapuš, Uroš **21**, 45, 50
S
Sanko, Olha 29, **31**
Siljanovska Virant, Ana **29**
Skoko, Željko **42**
Smetana, Volodymyr 36
Spreitzer, Matjaž 49
Stanić, Petra 28
Stewart, Beverly 24
Stilinović, Vladimir **59**
Š
Šibav, Lia 56
Škapin, Srečo D. 49
Štefanić, Goran 20
Štefanić, Zoran 22
T
Tajnšek, Tia 18
Tašner, Marina 60
Tomašić, Nenad **47**
Travis Holman, K. 23
Turel, Iztok 21, 39, 50
U
Uran, Erik 29, **51**, 52
V
Ve, Thomas 44
Veljković, Dušan 40
Veljković, Ivana **40**
Virant, Miha **58**
Vušak, Darko 38, **55**, 60
X
Xu, Hongyi 44
Xu, Yizhi 23
Z
Zabukovec Logar, Nataša 18, 55
Zakošek, Žan **27**
Zalar Serjun, Vesna **46**
Ziherl, Nadja **49**
Zorko, Andrej 56
Ž
Žemva, Boris 35
Žilić, Dijana 22
Žižek, Jernej **43**

SPONSORS' PAGES

ELECTRON MICROSCOPY

Thermo Scientific™ Helios™ 5 Laser PFIB

Fastest high-quality subsurface and 3D characterization at millimeter scale with nanometer resolution.

Phenom XL G2 Desktop SEM

The next-generation Thermo Scientific Phenom XL G2 Desktop Scanning Electron Microscope (SEM) automates your quality control process, providing accurate, reproducible results while freeing up time for value-added work.

ThermoFisher SCIENTIFIC

OPTIKA ITALY

Professional Stereo Microscopes

SLX SERIES - Stereomicroscopes For Higher Education & Laboratory
SZ SERIES - Stereozoom Microscopes For Laboratory & Industry
CL SERIES - Cold Light Illuminators
GEM SERIES - Stereozoom Microscopes For Gemology

Industrial Microscopes

MET SERIES - Metallurgical Microscopes
IS SERIES - Inspection Video Microscopes

WWW.ITR-LAB.SI

ALL YOU NEED FOR ELECTRON MICROSCOPY

ULTIMATE EQUIPMENT SOLUTIONS • CUSTOM SERVICE • HIGH QUALITY FOR OUR CUSTOMERS
PERSONAL PROFESSIONAL APPROACH • COMMITMENT TO YOUR SUCCESS

ITRLAB

Aparatura d.o.o.

Podjetje Aparatura d. o. o. je bilo ustanovljeno leta 2016 kot rezultat izkušenj na trgu laboratorijske, analitične in procesne opreme. Smo ekskluzivni distributerji podjetja BRUKER Corporation, vodilnega svetovnega proizvajalca analitične opreme. Sodelovanje temelji na medsebojnem zaupanju in kakovosti storitev; ekskluzivni dogovori o distribuciji pa vam zagotavljajo edinstveno ceno izdelka in pravočasno poprodajno podporo.

Podjetje Aparatura d. o. o. sestavlja skupina vrhunskih strokovnjakov, ki so predani podpori sedanjim in bodočim uporabnikom analitične opreme. Nenehno vlagamo v izobraževanje zaposlenih, da zagotovimo napredek naših prodajnih, aplikativnih in servisnih storitev.

Za zaposlene v podjetju so napisana skupna pravila obnašanja in vrednot. Le tako lahko zagotovimo, da se zaposleni in vodstvo zavedajo pričakovanj in da se aktivnosti izvajajo skladno z našimi temeljnimi vrednotami in etičnimi načeli.

Naši končni uporabniki so v akademskem okolju raziskovalci v laboratorijih in raziskovalnih centrih univerz, fakultet in inštitutov. V industrijskem okolju so to razvojni kader in raziskovalci v razvojnih laboratorijih ter analitiki v laboratorijih za zagotavljanje kvalitete v živilski, farmacevtski, naftni in kemični industriji, metalurgi, cementarne in mnogi drugi.

Naš cilj je stranki ponuditi najboljšo možno rešitev in izgraditi partnerski odnos, kar zagotavlja osnovo, ki je potrebna, da lahko svoje delo opravljamo uspešno in kvalitetno. Verjamemo, da uspeh pri prodaji dosežemo s temeljitim poznavanjem portfelja izdelkov, razumevanjem trga in potreb strank.

Naša misija je strankam zagotoviti opremo, sisteme, rešitve, aplikacije in storitve, ki so natančno prilagojene njihovim potrebam. Prizadevamo si ustvariti kar najvišjo stopnjo razmerja med ceno in kvaliteto in s tem največjo dodano vrednost za končnega uporabnika. Servisna in aplikativna podpora je temeljni steber pri zagotavljanju kvalitete storitve in kot takšna nosi levji delež pri zadovoljstvu strank.

Naša vizija je nenehno izboljševanje storitev, ki jih ponujamo na trgu. Verjamemo, da lahko le z nenehno samorefleksijo, prepoznavanjem potencialov za izboljšave, skrbnim planiranjem in implementacijo rešitev, standardizacijo le teh ter s ponovno evaluacijo sledimo viziji, ki smo si jo zadali.

Stranke, ki nam zaupajo:

SALONIT ANHOVO D. D. Slovenija, KNAUF INSULATION D. O. O. Slovenija, Znanstveno-raziskovalno središče SAZU, ZRC SAZU Slovenija, Geološki zavod Slovenije, Kemijski inštitut Slovenije, Institut Jožef Stefan Slovenija, CIPKeBiP – Center odličnosti za integrirane pristope v kemiji in biologiji proteinov, Saubermacher Slovenija storitve pri varstvu okolja, trgovina in transport d.o.o., i SILKEM d.o.o.,

31. SLOVENSKO-HRVAŠKO KRISTALOGRAFSKO SREČANJE

31st SLOVENIAN-CROATIAN CRYSTALLOGRAPHIC MEETING

Rogla, Slovenia
18–22 June, 2025

BOOK OF ABSTRACTS and PROGRAMME

Published by:

Chair of Inorganic Chemistry,
Faculty of Chemistry and Chemical Technology,
University of Ljubljana,
Večna pot 113,
1000 Ljubljana, Slovenia

Edited and prepared by:

Marta Počkaj
Nina Podjed

Ljubljana, June 2025